

CERN 78-11
10 November 1978

ORGANISATION EUROPÉENNE POUR LA RECHERCHE NUCLÉAIRE
CERN EUROPEAN ORGANIZATION FOR NUCLEAR RESEARCH

A GENERAL TREATMENT OF RESONANCES
IN ACCELERATORS

G. Guignard

Lectures given in the
Academic Training Programme of CERN
1977-1978

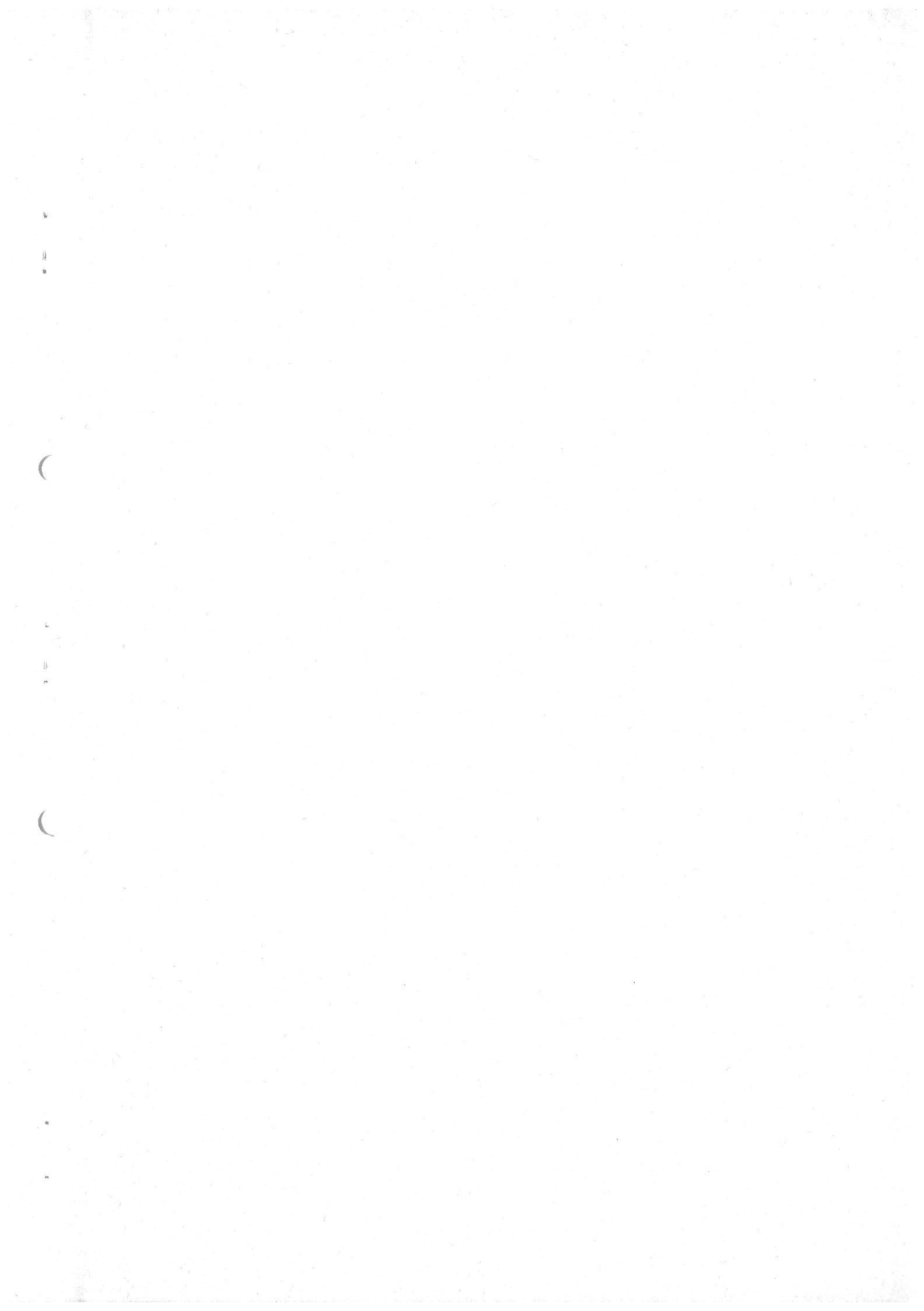
GENEVA

1978

ABSTRACT

A perturbation treatment in classical dynamics is developed for the motion of the particles in a synchrotron. This is done using the Hamiltonians of the unperturbed and perturbed motions arising from the action of the electromagnetic fields on the accelerated particle. Since the accelerator is circular, the Hamiltonians are periodic and therefore the concept of resonances can be introduced. Characteristics of the resonances such as the excitation coefficient, the stabilizing coefficients, and the bandwidth, can then be defined and resonance curves can be used for discussing the limitations of the amplitude growth or beating.

Different applications of this general theory are also given. These applications are associated with different sources of perturbation, such as transverse magnetic fields, electromagnetic fields of a coasting or bunched particle beam, and longitudinal fields. Practical examples are taken from the CERN Intersecting Storage Rings (ISR).



CONTENTS

	<u>Page</u>
LIST OF SYMBOLS	vii
1. INTRODUCTION	1
2. CHOICE OF THE FORMALISM	3
2.1 Definition of the symplectic geometry	3
2.2 Comparison of different formalisms	3
3. NOTIONS OF ANALYTICAL MECHANICS	4
3.1 Lagrangian formalism	4
3.2 Hamiltonian formalism	6
3.3 Symplectic conditions in the Hamiltonian formalism	7
3.4 Treatment of the perturbation in the Hamiltonian formalism	8
4. APPLICATION OF THE HAMILTONIAN FORMALISM TO A PARTICLE IN AN ELECTROMAGNETIC FIELD	11
4.1 Lagrangian and Hamiltonian functions in a Galilean frame	11
4.2 Lagrangian and Hamiltonian functions in relativistic conditions	12
4.3 Hamiltonian function for transverse motions in a synchrotron	13
5. PERTURBATION TREATMENT OF THE TRANSVERSE MOTIONS IN ACCELERATORS	15
5.1 Unperturbed motion and the Hamiltonian	15
5.2 Perturbed motion and the Hamiltonian	18
5.3 Equations of the perturbed motion	22
5.4 Invariants of the perturbed motion	25
6. DISCUSSION OF RESONANCE CHARACTERISTICS	28
6.1 Detailed discussion of the invariants	28
6.2 Resonance curves and bandwidths for sum resonances	34
6.3 Resonance curves and bandwidths for difference resonances	38
6.4 Criterion concerning the distance of the working point from the resonance line	40

7.	AMPLITUDE VARIATIONS IN SYSTEMS WITH CHANGING PARAMETERS	40
7.1	Non-adiabatic change of the parameters	41
7.2	Adiabatic change of the parameters	42
7.3	Change of the parameters and of the perturbation	45
8.	APPLICATIONS TO DIFFERENT SOURCES OF PERTURBATION	47
8.1	Magnetic defects in the machine hardware	48
8.2	Electromagnetic fields due to coasting beams crossing horizontally	52
8.3	Two-beam overlap knock-out	59
8.4	Linear coupling in three-dimensional fields	64
9.	CONCLUSION	70
	REFERENCES	71

LIST OF SYMBOLS FREQUENTLY USED IN THE TEXT
AND THEIR MEANING

a_2	complex amplitudes of the transverse envelope oscillations
A_s	longitudinal component of the magnetic potential vector (also noted A_θ)
A_y	general transverse component of the magnetic potential vector
B_s	longitudinal component of the magnetic induction (also noted B_θ)
B_y	general transverse component of the magnetic induction
$ B\rho $	magnetic rigidity
c	velocity of the light
$c_2(r_1)$	resonance curves which restrict the transverse amplitudes of the oscillation
e	electronic charge
e	distance from the resonance line
E_y	general transverse emittance
ξ	electric field
δ_z	vertical component of the electric field
H	Hamiltonian function
$h_{qqss0}^{(2v)}$	stabilizing coefficients of the resonance
I	beam current
L	Lagrangian function
m	mass of the particle
N	order of the resonance
n_y	general integer defining the resonance of interest
p	harmonic number of the resonance
p_s	longitudinal momentum component
p_y	general transverse momentum component, either horizontal or vertical
Q_y	number of betatron oscillations per revolution in plane (y,s)
R	average machine radius
r_2	real amplitudes of the transverse envelope oscillations
s	distance along beam axis

T	kinetic energy
t	time
\vec{v}	velocity of the particle
x	horizontal transverse coordinate
y	general transverse coordinate, either horizontal or vertical
z	vertical transverse coordinate
β	ratio of particle velocity to that of light
β_y	general transverse betatron amplitude function in plane (y,s)
γ	ratio of the total energy of the particle to its rest energy
Δe	bandwidth of the resonance
θ	azimuthal angle ($= s/R$)
κ	excitation coefficient of the resonance
μ_y	general transverse phase of the betatron oscillation
ρ	bending radius
Φ	electric potential

* * *

Note: The indices 1 and 2 are associated with the coordinates x and z, respectively. The letter i stands for the square root of -1. A point and a prime denote differentiation with respect to t and θ , respectively. The sign - on top of a variable indicates its complex conjugate, while the sign ~ on top of a matrix symbol indicates its transposition. The notation $|Z|$ stands for the modulus of Z if Z is complex, and for the absolute value of Z if Z is real. Finally, the abbreviation r.m.s. is used for root mean square.

1. INTRODUCTION

The particle motions treated in these lectures are the transverse motions in a synchrotron (circular accelerator). The longitudinal motion, whose instabilities have been described in preceding lectures, is not considered at all.

The transverse motions are commonly referred to the average circle of the accelerator. Therefore, the natural system of coordinates is the one given in Fig. 1, where

x and z are the transverse coordinates, horizontal and vertical, respectively,

s is the distance along the beam axis,

R is the average radius of the accelerator,

ρ is the bending radius,

$\theta = s/R$ is the angle at the accelerator centre.

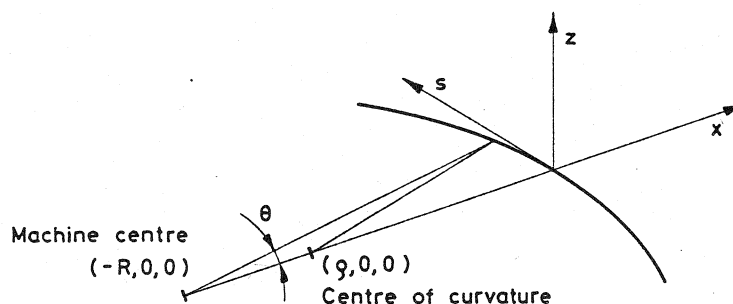


Fig. 1 Coordinate system for transverse motions in a synchrotron

The basic circular trajectory of the particles is maintained by a constant vertical magnetic field B_z , which verifies

$$p_s = eB_z \rho \quad (1.1)$$

where

p_s is the longitudinal component of the momentum \vec{p} ,

e is the electron charge.

This situation is only stable for particles moving on the average circle, i.e. for particles with a momentum \vec{p} which is tangent to this circle. For particles with slightly different initial conditions, i.e. $p_x \neq 0$ and $p_z \neq 0$, the trajectories deviate from this circle. This means that such particles are unstable.

In order to have stable conditions for all particles, a force which is proportional to the distances x and z from the circle has to be added. This is realized by including a gradient G in the guiding field, and the consequent equations of motion have the following form

$$\frac{d}{dt} p_y + \frac{e}{m} p_s G y = 0 \quad (1.2)$$

with

$$G = \frac{\partial B_z}{\partial x} = \frac{\partial B_x}{\partial z} .$$

In Eq. (1.2), m is the mass of the circulating particle and y stands either for x or z .

This is the equation of a harmonic oscillator and the solution is sinusoidal, i.e. the motion is stable.

In practice, however, the field B_z and the gradient G are not perfect. Other components exist, which induce non-linear forces, which are proportional to some power of x and z , i.e. $x^m z^n$, and forces which are proportional to the transverse speed components \dot{x} and \dot{z} .

Electric forces may also be present if the considered particles interact with an intense beam, as is the case for instance in the storage rings.

All these forces will appear on the right-hand side of the equations of motion (1.2) as perturbations. Since the accelerator is circular, these perturbations will always be periodic. Thus, we are in the situation of an anharmonic oscillator, where the forces are functions of the coordinates and of their derivatives. These forces are often treated as a perturbation of the system. In a first approximation, the solution of (1.2) can be used in the expression of the forces, so that the equations of the perturbed motion correspond to forced oscillations

$$\ddot{p}_y + kGy = F(t) \quad (1.3)$$

with $k = e p_s / m$. $F(t)$ is a sum of simple periodic functions:

$$F(t) = \sum_i f_i \cos (\gamma_i t + c_i) . \quad (1.4)$$

Particular solutions of Eq. (1.3) have the well-known form¹⁾

$$y = \frac{f_i}{(kG - my_i^2)} \cos (\gamma_i t + c_i) . \quad (1.5)$$

The amplitude is unlimited only if the resonance condition

$$kG = my_i^2 \quad (1.6)$$

is verified. On the resonance, the amplitude grows rapidly and particles are again unstable.

This was a qualitative and approximate description of resonance phenomena as they may appear in circular accelerators. My intention in these lectures is to describe a general treatment of these resonances, which are due to perturbing electromagnetic fields and which appear in the amplitudes of the transverse oscillations of the particles. This treatment gives the excitation terms, which characterize the perturbation, as functions of the parameters of the unperturbed machine and shows the way for compensating unacceptable resonances. It also gives appropriate explanations for the observed beam loss and beam blow-up, when particles are crossing such resonances or diffusing into them.

2. CHOICE OF THE FORMALISM

2.1 Definition of the symplectic geometry²⁾

Considering a space of $2n$ variables, let E be a simple domain of this space, like the generalization for $2n$ dimensions of the unit-circle or of the complete plane.

The conformal mappings of the domain E onto itself form a group Ω of linear transformations. These linear transformations can be written in the form of $2n \times 2n$ matrices M .

Then, the *symplectic group* Ω_0 consists of all real matrices M satisfying the condition

$$\tilde{M}SM = S \quad (2.1)$$

where

$$S = S^{(2n)} = \begin{pmatrix} S^{(2)} & 0 & \dots & 0 \\ 0 & S^{(2)} & & 0 \\ \vdots & \vdots & \ddots & \vdots \\ 0 & 0 & \dots & S^{(2)} \end{pmatrix}$$

$$S^{(2)} = \begin{pmatrix} 0 & 1 \\ -1 & 0 \end{pmatrix}.$$

An important theorem²⁾ states that every analytic mapping of the generalized plane onto itself is symplectic.

Going back to the linear equations of the transverse motion in an accelerator, it is well known that they define a linear transformation of the phase space (x, x', z, z') at $s = s_1$ into the phase space at $s = s_2$, i.e. an analytic mapping of the space. Therefore, by virtue of the above-mentioned theorem, the transfer matrices have to be symplectic and to satisfy Eq. (2.1).

2.2 Comparison of different formalisms

For the study of resonances, three basic formalisms can be used:

- i) A method which employs transfer matrices.
- ii) A method which directly substitutes the solutions of the unperturbed motion in the differential equations and then deduces the equations for the constants.
- iii) A Hamiltonian formalism with a perturbation theory.

The first method has the evident disadvantage of applying to linear motions and hence it is not well adapted to resonances which are due to non-linear forces. Since this method does not give differential equations and explicit solutions, it is better for numerical simulations than for theoretical predictions.

The first two methods encounter the same difficulty, i.e. to satisfy the *symplectic* conditions (Section 2.1).

When using a matrix formalism the choice of the parameters has to be made in agreement with Eq. (2.1). In the considered case of a two-dimensional motion (x, z) , the condition (2.1) gives $n(2n-1) = 6$ relations among the $(2n)^2 = 16$ elements of the transfer matrix, so the number of independent parameters cannot exceed $n(2n+1) = 10$.

In the second method, which tries to deduce the equations for the constants of the unperturbed motion, the symplectic conditions, which are implicitly contained in the differential equations, must be preserved throughout the analytical calculation in spite of any assumptions which may be required. This is *not trivial* and some published theories on linear coupling -- which were based on this method -- are wrong, since the symplectic conditions are not satisfied.

The Hamiltonian formalism has many advantages

- i) It gives the possibility of treating *non-linear* forces as well as linear ones.
- ii) It gives a technique to solve a perturbation problem, *without* making any *approximation*, based on the smallness of the perturbation.
- iii) When using a complete set of canonical variables, the transformation of the phase space at s_1 into the phase space at s_2 is always *symplectic*.
- iv) It gives explicit solutions if wanted, but also, in a simple way, the invariants of the motion.

Since neither of the other two methods has all these advantages simultaneously, the method based on the Hamiltonian formalism will be used throughout these lectures.

3. NOTIONS OF ANALYTICAL MECHANICS³⁻⁶)

3.1 Lagrangian formalism

Let us introduce the following definitions:

\vec{r} is the position-vector of a point in a space of n dimensions.

q_i ($i = 1, \dots, n$) are the independent position parameters of this point.

$T = \frac{1}{2}(\vec{dr}/dt)^2 m$ and is the kinetic energy of this point which has mass m .

t is the time.

The following intermediate variables are also useful

$$P_i = \frac{d}{dt} \left(\frac{\partial T}{\partial \dot{q}_i} \right) - \frac{\partial T}{\partial q_i} . \quad (3.1)$$

Using the definition of T , with

$$\frac{d\vec{r}}{dt} = \sum_i \frac{\partial \vec{r}}{\partial q_i} \dot{q}_i$$

and putting it into the P_i 's, we get

$$P_i = \frac{d^2 \vec{r}}{dt^2} \frac{\partial \vec{r}}{\partial q_i} m = \vec{a} \frac{\partial \vec{r}}{\partial q_i} m , \quad (3.2)$$

where \vec{a} is the acceleration vector.

Considering a set of virtual displacements δq_i -- in agreement with the restraints -- we can write

$$\sum_i P_i \delta q_i = \vec{a} \cdot \vec{\delta r} m . \quad (3.3)$$

Newton's equation gives $\vec{F} = m\vec{a}$, \vec{F} being the total force acting on m . This gives

$$\vec{a} \cdot \vec{\delta r} m = \vec{F} \cdot \vec{\delta r} \quad (3.4)$$

and, if the force can be derived from a potential V

$$\vec{F} \cdot \vec{\delta r} = - \sum_i \frac{\partial V}{\partial q_i} \delta q_i . \quad (3.5)$$

Thus Eq. (3.3) becomes

$$\sum_i \left(P_i + \frac{\partial V}{\partial q_i} \right) \delta q_i = 0 . \quad (3.6)$$

Since the parameters q_i are independent, the consequence of Eq. (3.6) is

$$P_i = \frac{d}{dt} \left(\frac{\partial T}{\partial \dot{q}_i} \right) - \frac{\partial T}{\partial q_i} = - \frac{\partial V}{\partial q_i} . \quad (3.7)$$

Equations (3.7) are the equations of Lagrange.

The definition of the *Lagrangian* function is

$$L = T - V \quad (3.8)$$

and the second equality (3.7) becomes

$$\frac{d}{dt} \left(\frac{\partial L}{\partial \dot{q}_i} \right) = \frac{\partial L}{\partial q_i} . \quad (3.9)$$

The equations (3.9) are identical to the equations of Euler-Lagrange in the variation calculation, which is expressed as follows:

To find the functions $q_i(t)$ which satisfy the conditions $q_i(t_0) = q_i^0$ and $q_i(t_1) = q_i^1$ and which are such that the action integral

$$S^* = \int_{t_0}^{t_1} L(q_i, \dot{q}_i, t) dt \quad (3.10)$$

has a maximum or minimum.

Looking for a stationary value of S^* is identical to solving the equations of motion. In fact, every mechanical system will follow a course such that the action is a minimum. This is named the *principle of least action*.

3.2 Hamiltonian formalism

Let us introduce the following new variables:

p_i ($i = 1, \dots, n$) are the conjugate momenta.

H is the Hamiltonian function of the system.

Let us put by definition

$$p_i = \frac{\partial T}{\partial \dot{q}_i} = \frac{\partial L}{\partial \dot{q}_i} \quad (3.11)$$

and

$$H = \sum_i p_i \dot{q}_i - L, \quad (3.12)$$

with $L = L(q_i, \dot{q}_i, t)$ and $H = H(q_i, p_i, t)$. The relation (3.9) gives

$$\dot{p}_i = \frac{\partial L}{\partial q_i} \quad (3.13)$$

After differentiating Eq. (3.12) we have

$$\begin{aligned} dH &= \sum_i \left[\frac{\partial H}{\partial q_i} dq_i + \frac{\partial H}{\partial p_i} dp_i \right] + \frac{\partial H}{\partial t} dt = \\ &= \sum_i \left[\dot{q}_i dp_i + p_i d\dot{q}_i - \frac{\partial L}{\partial q_i} dq_i - \frac{\partial L}{\partial \dot{q}_i} d\dot{q}_i \right] - \frac{\partial L}{\partial t} dt. \end{aligned} \quad (3.14)$$

Identifying the coefficients and using relations (3.11) and (3.13) gives the *canonical equations*

$$\begin{aligned} \dot{q}_i &= \frac{\partial H}{\partial p_i} \\ \dot{p}_i &= - \frac{\partial H}{\partial q_i} \\ \frac{\partial H}{\partial t} &= - \frac{\partial L}{\partial t}. \end{aligned}$$

(3.15)

In the case where a potential V exists and is independent of time, H becomes

$$\begin{aligned} H &= \sum_i p_i \dot{q}_i - L = \sum_i \frac{\partial L}{\partial \dot{q}_i} \dot{q}_i - L = \sum_i \frac{\partial T}{\partial \dot{q}_i} \dot{q}_i - L = \\ &= 2T - L = 2T - (T - V) \equiv T + V. \end{aligned} \quad (3.16)$$

In this development, Euler's theorem has been used. This theorem states that the following relation is valid if T has a quadratic form in \dot{q}_i

$$2T = \sum_i m\dot{q}_i^2 = \sum_i \frac{\partial T}{\partial \dot{q}_i} \dot{q}_i . \quad (3.17)$$

It is important to emphasize that the equations (3.14) and (3.15) imply

$$\boxed{\frac{dH}{dt} = \frac{\partial H}{\partial t}} , \quad (3.18)$$

which means that $H = \text{const.}$ in a conservative system.

Hence to solve the equations of motion for a system it is necessary to find L and/or H and then to derive the $2n$ first-order differential equations (3.15), where n is the number of degrees of freedom of the system.

3.3 Symplectic conditions in the Hamiltonian formalism

The Hamiltonian function can be expanded as a power series in q_i, p_i . Using a common symbol u for q and p and then summing over $2n$ parameters, we get for H

$$H = \sum_i \sum_{j \geq i} g_{ij} u_i u_j + \sum_i \sum_j \sum_k h_{ijk} u_i u_j u_k + \dots , \quad (3.19)$$

where the quadratic function corresponds to linear motions. This quadratic part G^* can be written as follows

$$G^* = \frac{1}{2} \tilde{U} G U , \quad (3.20)$$

where \tilde{U} is the line vector $(q_1, p_1, q_2, p_2, \dots, q_n, p_n)$ and G is the symmetric matrix

$$G = \begin{pmatrix} 2g_{11} & g_{12} & g_{13} & \dots \\ g_{12} & 2g_{22} & g_{23} & \dots \\ \vdots & \vdots & \vdots & \ddots \\ \vdots & \vdots & \vdots & \ddots \end{pmatrix} .$$

The linear motion associated with the quadratic part of H [Eq. (3.20)] can then be described with the matrices which transform the phase space between t_1 and t_2 :

$$U(t_2) = M U(t_1) . \quad (3.21)$$

The canonical equations (3.15) can be written in a matrix form

$$\dot{U} = S G U , \quad (3.22)$$

where S is the matrix $S^{(2n)}$ defined after Eq. (2.1).

For any two solutions U_1 and U_2 of Eq. (3.22), we have

$$\frac{d}{dt} (\tilde{U}_2 S U_1) = \dot{\tilde{U}}_2 S U_1 + \tilde{U}_2 S \dot{U}_1 = 0 \quad (3.23)$$

i.e.

$$\tilde{U}_2 S U_1 = \text{const.}$$

by virtue of Eq. (3.22) and of the equalities $\tilde{S} = -S$ and $S S = -I$, I being the unit matrix. If the transformation (3.21) is used, the invariance property (3.23) gives

$$\tilde{U}_2(t_2) S U_1(t_2) = \tilde{U}_2(t_1) \tilde{M} S M U_1(t_1) = \tilde{U}_2(t_1) S U_1(t_1) . \quad (3.24)$$

The last relation implies that M must satisfy

$$\boxed{\tilde{M} S M = S ,} \quad (3.25)$$

which means that M is symplectic.

Thus the symplectic conditions are always satisfied by the canonical set of variables used in the Hamiltonian formalism.

3.4 Treatment of the perturbation in the Hamiltonian formalism

Without making any approximations based on the smallness of the perturbing Hamiltonian H_1 , the general perturbation problem may be stated as follows. Given the general solution of the canonical equations

$$\begin{aligned} \dot{q}_i &= \frac{\partial H_0}{\partial p_i} \\ \dot{p}_i &= - \frac{\partial H_0}{\partial q_i} \end{aligned} \quad (3.26)$$

of unperturbed motion, it is required to set up a technique to find the motion for the total Hamiltonian

$$H = H_0(q_i, p_i, t) + H_1(q_i, p_i, t) . \quad (3.27)$$

Let the solution of Eqs. (3.26) be

$$\begin{aligned} q_i &= q_i(c, t) \\ p_i &= p_i(c, t) , \end{aligned} \quad (3.28)$$

where c stands for $2n$ arbitrary constants c_k ($k = 1, \dots, 2n$). These quantities are constant along each unperturbed trajectory. Solving Eqs. (3.28) gives

$$c_k = c_k(q_i, p_i, t), \quad (3.29)$$

these functions being determined by the form of H_0 .

The perturbation can be viewed in the q - t - p space (Fig. 2), where

Σ_{2n} is the surface $t = 0$,

B is any point in q - t - p ,

Γ_0 is the unperturbed trajectory through B , cutting Σ_{2n} at B^* , which is defined by

$$\begin{aligned} q_i^* &= q_i(c, 0) \\ p_i^* &= p_i(c, 0). \end{aligned} \quad (3.30)$$

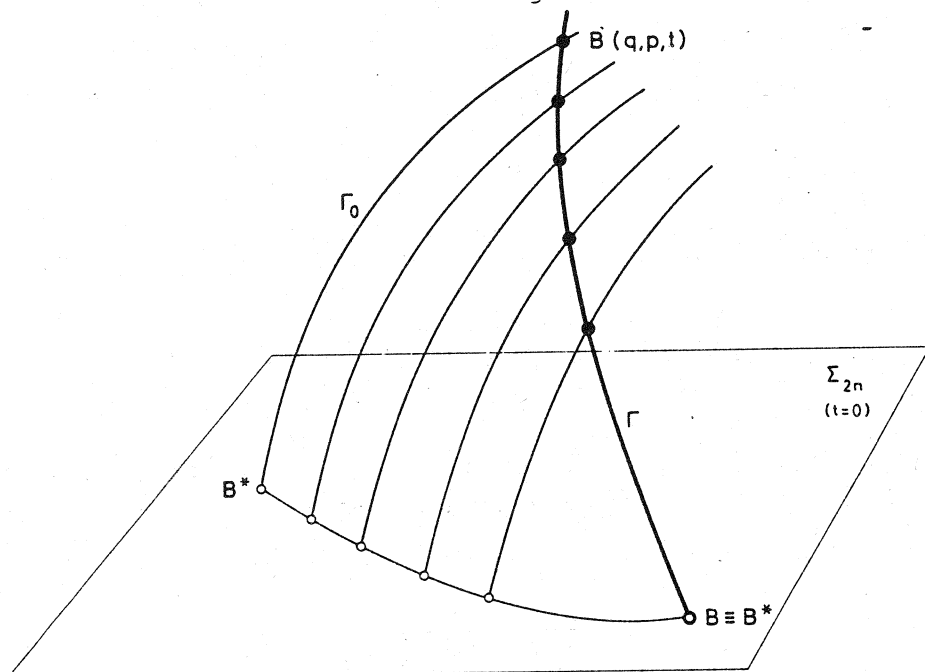


Fig. 2 View of the perturbation in the q - t - p space

The constants c_k form a system of coordinates on Σ_{2n} [Eqs. (3.30) and Fig. 2]. The trajectories Γ_0 form a system of projection lines, by which a point B is projected onto B^* .

Γ is a perturbed trajectory. At B , its direction differs from that of Γ_0 . As the representative point traverses Γ , its projection B^* moves on Σ_{2n} . Consequently, the method is called the method of variation of constants, since c_k are constant for Γ_0 but not for Γ . The problem is reduced to the study of the variation of the c_k 's with t as the point B traverses Γ .

If we knew the form of the equations $c_k = f_k(t)$, we would know the curve Γ in the q-t-p system.

The definition of the Poisson bracket is

$$[u, v] = \sum_i \left[\frac{\partial u}{\partial q_i} \frac{\partial v}{\partial p_i} - \frac{\partial v}{\partial q_i} \frac{\partial u}{\partial p_i} \right]. \quad (3.31)$$

Using this definition when the representative point moves along a trajectory, the rate of change of any function $f(q_i, p_i, t)$ is

$$\frac{df}{dt} = \frac{\partial f}{\partial t} + \sum_i \left(\frac{\partial f}{\partial q_i} \dot{q}_i + \frac{\partial f}{\partial p_i} \dot{p}_i \right) = \frac{\partial f}{\partial t} + [f, H]. \quad (3.32)$$

In Eq. (3.32), the canonical equations (3.15) have been used.

Applying Eq. (3.32) to the coefficients c_k gives on Γ (Fig. 2)

$$\dot{c}_k = \frac{\partial c_k}{\partial t} + [c_k, H_0 + H_1] \quad (3.33)$$

and on Γ_0 (Fig. 2)

$$0 = \frac{\partial c_k}{\partial t} + [c_k, H_0]. \quad (3.34)$$

By subtraction, we have on Γ

$$\boxed{\dot{c}_k = [c_k, H_1].} \quad (3.35)$$

By virtue of Eqs. (3.28), the right-hand side of Eq. (3.35) is a function of (c_k, t) and so we have a set of $2n$ equations to determine the functions $c_k = f_k(t)$.

Expressing H_1 as a function of (c_k, t) , it is possible to rewrite Eq. (3.35) as:

$$\boxed{H_1(q_i, p_i, t) = U(c_k, t)} \\ \dot{c}_k = \sum_j [c_k, c_j] \frac{\partial U}{\partial c_j}. \quad (3.36)$$

So far everything is exact. But if the derivatives of H_1 are small, then the right-hand side of the second Eq. (3.36) is small and there may be a possibility of approximating the perturbed motion by keeping only the dominant terms of U .

Hence to solve the perturbed motion, knowing the solution of the unperturbed motion, it is necessary to find H , i.e. H_1 , to express it as a function of the constants c_k , and to derive the $2n$ first-order equations (3.36).

4. APPLICATION OF THE HAMILTONIAN FORMALISM TO A PARTICLE IN AN ELECTROMAGNETIC FIELD

4.1 Lagrangian and Hamiltonian functions in a Galilean frame⁷⁾

With respect to the Galilean frame of reference, the space is homogeneous and isotropic, and time is uniform.

The Lagrangian function of a *free* point in such a system cannot depend on the position vector, nor on time, nor on the direction of the speed. It depends only on its absolute value, i.e. on $\vec{v}^2 = v^2$. In other words, L is just the kinetic energy for a *free* point, $L = (m/2)v^2$, as expected from Eq. (3.8).

If this point or particle undergoes forces which come from a potential, we know from Eq. (3.8) that

$$L = T - V = \frac{m}{2}v^2 - V . \quad (4.1)$$

Let us find V for a particle in an electromagnetic field. The Lorentz force of such a field is known to be given by

$$\vec{F} = e \left[- \vec{\text{grad}} \phi - \frac{1}{c} \frac{\partial \vec{A}}{\partial t} + \frac{1}{c} \vec{v} \times \vec{\text{rot}} \vec{A} \right] . \quad (4.2)$$

where ϕ and \vec{A} are the electric and magnetic potentials, respectively.

It is obvious from Eq. (4.2) that only the electrical potential ϕ satisfies Eq. (3.5). Nevertheless, it is still possible to define a "generalized" potential $V^*(q_i, \dot{q}_i, t)$ such that

$$\frac{d}{dt} \left(\frac{\partial V^*}{\partial q_i} \right) - \frac{\partial V^*}{\partial q_i} = F_i . \quad (4.3)$$

In this case, Eqs. (3.8) and (3.9) are still valid. Developing the cross product $\vec{v} \times \vec{\text{rot}} \vec{A}$, we get for the x -component

$$(\vec{v} \times \vec{\text{rot}} \vec{A})_x = \frac{\partial}{\partial x} (\vec{v} \cdot \vec{A}) - \left(\frac{dA_x}{dt} - \frac{\partial A_x}{\partial t} \right) . \quad (4.4)$$

Putting Eq. (4.4) in Eq. (4.2) and using $(\partial/\partial v_x) (\vec{v} \cdot \vec{A}) = A_x$, the first component of the force becomes

$$F_x = e \left[- \frac{\partial}{\partial x} \left(\phi - \frac{1}{c} \vec{v} \cdot \vec{A} \right) - \frac{1}{c} \frac{d}{dt} \frac{\partial}{\partial v_x} (\vec{v} \cdot \vec{A}) \right] . \quad (4.5)$$

Similar expressions may be written for the other components of \vec{F} . Comparing Eq. (4.5) with the expression (4.3) gives the generalized potential

$$V^* = e\phi - \frac{e}{c} \vec{v} \cdot \vec{A} \quad (4.6)$$

and the Lagrangian

$$L = T - V^* = \frac{m}{2} v^2 - e \left(\Phi - \frac{1}{c} \vec{v} \cdot \vec{A} \right) . \quad (4.7)$$

By virtue of the definitions (3.11) and (3.12), the conjugate momenta and the Hamiltonian associated with Eq. (4.7) are, respectively,

$$\begin{aligned} p_i &= mv_i + \frac{e}{c} A_i \\ H &= \frac{m}{2} v^2 + e\Phi . \end{aligned} \quad (4.8)$$

The first equation (4.8) may be solved with respect to the speed components and the obtained expressions for v_i may be put in the second equation, which then becomes

$$H = \frac{1}{2m} \left(\vec{p} - \frac{e}{c} \vec{A} \right)^2 + e\Phi . \quad (4.9)$$

This is the Hamiltonian for a single particle in the presence of an electromagnetic field in a Galilean frame.

4.2 Lagrangian and Hamiltonian functions in relativistic conditions⁷⁾

Considering the integral (3.10) for a free particle, this integral cannot depend on the reference system, i.e. it has to be invariant for Lorentz transformations. Thus it is necessarily the integral of a scalar. Only first-order differentials may appear in the integral. Hence, the only possible scalar of this form which can be created for a free particle is $-\alpha ds^*$, where α is a constant factor and ds^* the four-dimensional relativistic interval

$$ds^* = \sqrt{c^2 dt^2 - dx^2 - dz^2 - ds^2} = c \sqrt{1 - \frac{v^2}{c^2}} dt . \quad (4.10)$$

The action integral (3.10) then becomes

$$S^* = -\alpha \int_a^b ds^* . \quad (4.11)$$

and the Lagrangian for a *free* particle is

$$L = -\alpha c \sqrt{1 - \frac{v^2}{c^2}} . \quad (4.12)$$

The condition that $L = mv^2/2$ for $c \rightarrow \infty$ gives the constant, i.e. $\alpha = mc$. Hence

$$L = -mc^2 \sqrt{1 - \frac{v^2}{c^2}} . \quad (4.13)$$

In the presence of an electromagnetic field, the Lagrangian function is equal to the expression (4.13) minus the "generalized" potential V^* [Eq. (4.6)], as seen in the previous section.

$$L = -mc^2 \sqrt{1 - \frac{v^2}{c^2} - e\Phi + \frac{e}{c} \vec{v} \cdot \vec{A}} . \quad (4.14)$$

By virtue of Eqs. (3.11) and (3.12), the conjugate momenta and the Hamiltonian associated with Eq. (4.14) are, respectively

$$\begin{aligned} p_i &= \frac{mv_i}{\sqrt{1 - \frac{v^2}{c^2}}} + \frac{e}{c} A_i \\ H &= \frac{mv^2}{\sqrt{1 - \frac{v^2}{c^2}}} + mc^2 \sqrt{1 - \frac{v^2}{c^2} + e\Phi} = \frac{mc^2}{\sqrt{1 - \frac{v^2}{c^2}}} + e\Phi \end{aligned} \quad (4.15)$$

Combining the two equations (4.15) as in Section 4.1, we get for the Hamiltonian

$$H = c \sqrt{\left(\vec{p} - \frac{e}{c} \vec{A}\right)^2 + m^2 c^2} + e\Phi . \quad (4.16)$$

This is the Hamiltonian for a single relativistic particle in the presence of an electromagnetic field.

4.3 Hamiltonian function for transverse motions in a synchrotron⁸⁾

The motion of the particles in a synchrotron is relativistic longitudinally, which means that $p_s \gg p_x$ and $p_s \gg p_z$. By virtue of this, it is the expression (4.16) for the Hamiltonian which applies. This expression implies that the time t is the independent variable. However, in circular accelerators, the physics of the problem singles out the longitudinal coordinate s . It is then convenient to take either s or the angle θ (Fig. 1) as the new independent variable, both possibilities being equivalent since

$$ds = v_s dt = R d\theta . \quad (4.17)$$

The action integral (3.10) can be re-expressed by introducing the identity (3.12)

$$S^* = \int_{t_0}^{t_1} \left[\sum_i p_i \dot{q}_i - H \right] dt . \quad (4.18)$$

Taking into account the general symmetry, inherent in Hamiltonian mechanics⁶⁾, between the four canonically conjugate pairs (x, p_x) , (z, p_z) , (s, p_s) and $(t, -H)$, the integral S^* , after the change of independent variable from t to s , becomes

$$S^* = \int_a^b \left[p_x \frac{dx}{ds} + p_z \frac{dz}{ds} - H \frac{dt}{ds} + p_s \right] ds . \quad (4.19)$$

The new Hamiltonian to be considered comes from Eq. (4.19) and is equal to $-p_s$. Solving the expression (4.16) with respect to the longitudinal component of the momentum gives

$$-p_s = -\frac{e}{c} A_s - \left[\left(\frac{H - e\Phi}{c} \right)^2 - \left(p_x - \frac{e}{c} A_x \right)^2 - \left(p_z - \frac{e}{c} A_z \right)^2 - m^2 c^2 \right]^{1/2}. \quad (4.20)$$

Since H does not depend explicitly on time ($H = 0$), the quantity $(H/c)^2 - (mc)^2$ is a constant which is numerically given by

$$\left(\frac{H}{c} \right)^2 - (mc)^2 = (mc\gamma + \frac{e\Phi}{c})^2 - (mc)^2 = (mc\beta\gamma)^2 + 2mc\gamma\frac{e\Phi}{c} + (\frac{e\Phi}{c})^2 = |\vec{p}|^2 + 2|\vec{p}| \frac{e\Phi}{\beta c} + \frac{e^2\Phi^2}{c^2}. \quad (4.21)$$

By virtue of the geometry and of the characteristics of the motion in an accelerator, two assumptions may be introduced:

First assumption: since the bending radius ρ is large, the effect of curvature can be $x/\rho \ll 1$. neglected and the Hamiltonian is given by the Eq. (4.20), derived in a cartesian system.

Second assumption: since p_s is very large (hence \vec{p} is also large), it is possible to take the constant (4.21) as being numerically equal to p_s^2 , to divide the argument of the square root in Eq. (4.20) by p_s^2 , to develop the square root and to keep the first term only.

With these two assumptions, the Hamiltonian, whose independent variable is s instead of t , is [Eq. (4.20)]

$$H = -\frac{e}{c} A_s - p_s \left\{ 1 - \frac{e\Phi}{\beta c p_s} \right\} \neq \frac{1}{2} \left(\frac{e\Phi}{c p_s} \right)^2 - \frac{1}{2 p_s^2} \left[\left(p_x - \frac{e}{c} A_x \right)^2 + \left(p_z - \frac{e}{c} A_z \right)^2 \right]. \quad (4.22)$$

The Hamiltonian in the variables x , z , s , p_x/p_s and p_z/p_s is obtained by dividing Eq. (4.22) by p_s and by disregarding the constant 1. The Hamiltonian in the independent variable θ can then be obtained by multiplying by R^2 . Using the magnetic rigidity $|B_0| = p_s/e$ [Eq. (1.1)], finally we get the Hamiltonian in the variables x , z and θ :

$$H = \frac{R^2}{c|B_0|} \left(\frac{\Phi}{\beta} - A_\theta \right) + \frac{1}{2} \left[\left(\frac{R\Phi}{c|B_0|} \right)^2 + \left(p_x - \frac{RA_x}{c|B_0|} \right)^2 + \left(p_z - \frac{RA_z}{c|B_0|} \right)^2 \right], \quad (4.23)$$

where p_x, p_z are new conjugate momenta.

H is here associated with two-dimensional motions in the presence of an electromagnetic field and the whole theory of Section 3 applies with $n = 2$ and

$$\begin{aligned} q_1 &= x \\ q_2 &= z \\ p_1 = p_x &= x' + \frac{RA_x}{|B\rho|c} \\ p_2 = p_z &= z' + \frac{RA_z}{|B\rho|c}. \end{aligned} \tag{4.24}$$

In what follows, the notation (q_i, p_i) of Section 3 will be abandoned and the variables x, z, p_x , and p_z will be used.

5. PERTURBATION TREATMENT OF THE TRANSVERSE MOTIONS IN ACCELERATORS

5.1 Unperturbed motion and the Hamiltonian⁸⁻¹⁰⁾

As mentioned in the Introduction the unperturbed motion is the motion of particles, which are in the presence of magnetic fields linearly varying with x and z , and which are therefore stable. Linear fields require a quadratic potential vector \vec{A} . Since these fields have to be transverse, the longitudinal component is the only one different from zero

$$\begin{aligned} A_x = A_z &= 0 \\ A_\theta &= -\frac{c}{2} (G_1 x^2 + G_2 z^2) \end{aligned} \tag{5.1}$$

where G_1 and G_2 are gradients which are functions of θ .

Since the electric field is assumed to be equal to zero, the unperturbed Hamiltonian derived from Eq. (4.23) is

$$H_0 = + \frac{R^2}{2|B\rho|} (G_1 x^2 + G_2 z^2) + \frac{p_x^2 + p_z^2}{2} \tag{5.2}$$

and by using the definition

$$K_1 = \frac{\frac{R^2 G_1}{2}}{|B\rho|},$$

$$H_0 = \frac{1}{2} (K_1 x^2 + K_2 z^2 + p_x^2 + p_z^2). \tag{5.3}$$

The canonical equations (3.26) are in this case:

$$\begin{cases} x' = p_x \\ p_x' + K_1 x = 0 \end{cases} \quad (5.4)$$

$$\begin{cases} z' = p_z \\ p_z' + K_2 z = 0 \end{cases}$$

with

$$K_1 = K_1(\theta) = K_1(\theta + 2\pi) .$$

Expressions (5.4) are Hill's equations. If K was independent of θ , the solution of Eqs. (5.4) would be of the form $y = A \exp(i\sqrt{K}\theta)$. This form may be maintained when the force K varies with θ , but the amplitude A becomes modulated as a function of θ and the phase varies nonlinearly with θ .

The theorem of Floquet⁹⁾ states that such equations (5.4) always have two particular integrals of the form

$$y(\theta) = \frac{a_1}{2} e^{iQ_y \theta} w(\theta) \quad (5.5)$$

$$\bar{y}(\theta) = \frac{\bar{a}_1}{2} e^{-iQ_y \theta} \bar{w}(\theta) ,$$

where w is a periodic function, $w(\theta) = w(\theta + 2\pi)$, giving the amplitude and phase modulations mentioned above. Q_y is the tune and gives the linear variation of the phase.

On the other hand, it has been shown by Courant and Snyder¹⁰⁾ that solutions of Eqs. (5.4) may be written as follows

$$y(\theta) = \frac{a_1}{\sqrt{2R}} \sqrt{\beta_y(\theta)} \exp \left[+i \int_0^\theta \frac{R d\zeta}{\beta_y(\zeta)} \right] , \quad (5.6)$$

$\bar{y}(\theta) = \text{complex conjugate}$

where $\beta_y(\theta)$ is the transverse betatron amplitude. The betatron amplitude satisfies the following equation in which the force K appears

$$(\sqrt{\beta_y})'' + K_1(\theta) \sqrt{\beta_y} - \frac{R^2}{\beta_y^{3/2}} = 0 . \quad (5.7)$$

The wave number or the tune Q_y as well as the so-called phase advance μ_y are deduced from the β_y functions according to the integrals,

$$\begin{aligned}\mu_y &= \int_0^\theta \frac{R}{\beta_y(\zeta)} d\zeta \\ Q_y &= \frac{1}{2\pi} \int_0^{2\pi} \frac{R}{\beta_y(\zeta)} d\zeta,\end{aligned}\tag{5.8}$$

ζ being a variable of integration.

Comparing Eqs. (5.5) and (5.6), we get Floquet's function w (and its complex conjugate \bar{w})

$$w = \sqrt{\frac{\beta_y}{2R}} \exp \left[i \int_0^\theta \left(\frac{R}{\beta_y(\zeta)} - Q_y \right) d\zeta \right].\tag{5.9}$$

Let us denote by u the horizontal Floquet function and by v the vertical Floquet function, which are both given by Eq. (5.9) with y equal to x or z , respectively. Thus the general solutions of Eqs. (5.4) are

$$\begin{aligned}x &= a_1 u e^{iQ_x \theta} + \bar{a}_1 \bar{u} e^{-iQ_x \theta} \\ z &= a_2 v e^{iQ_z \theta} + \bar{a}_2 \bar{v} e^{-iQ_z \theta}.\end{aligned}\tag{5.10a}$$

a_1 and a_2 are complex constants of the motion.

In order to get the equivalent of Eqs. (3.28), Eqs. (5.10a) must be differentiated, keeping in mind that $y' = p_y$ for the unperturbed motion

$$\begin{aligned}p_x &= a_1(u' + iQ_x u) e^{iQ_x \theta} + \bar{a}_1(\bar{u}' - iQ_x \bar{u}) e^{-iQ_x \theta} \\ p_z &= a_2(v' + iQ_z v) e^{iQ_z \theta} + \bar{a}_2(\bar{v}' - iQ_z \bar{v}) e^{-iQ_z \theta}.\end{aligned}\tag{5.10b}$$

Solving Eqs. (5.10) with respect to the constants a_1, \bar{a}_1 , and a_2, \bar{a}_2 , we have the equivalent of Eq. (3.29)

$$\begin{aligned}a_1 &= \frac{1}{W(u)} \left[(\bar{u}' - iQ_x \bar{u})_x - \bar{u} p_x \right] e^{-iQ_x \theta} \\ \bar{a}_1 &= - \frac{1}{W(u)} \left[(u' + iQ_x u)_x - u p_x \right] e^{iQ_x \theta}\end{aligned}\tag{5.11}$$

with

$$W(u) = u(\bar{u}' - iQ_x \bar{u}) - (u' + iQ_x u)\bar{u} = -i .$$

a_2 and \bar{a}_2 satisfy similar expressions, in which v , z , p_z , and Q_z take the place of u , x , p_x , and Q_x , respectively.

5.2 Perturbed motion and the Hamiltonian^{8,11)}

At first, let us find the analytical form of the perturbing Hamiltonian H_1 [Eq. (3.27)]. The total Hamiltonian H is given in Eq. (4.23) and the unperturbed Hamiltonian H_0 in Eq. (5.3). Subtracting H_0 from H , we obtain H_1

$$\begin{aligned} H_1 = & \frac{1}{2} \left[-\frac{2R^2}{|B\rho|c} A_\theta - \frac{2R}{|B\rho|c} (p_x A_x + p_z A_z) + \frac{2R^2 \Phi}{|B\rho|c} \right. \\ & \left. + \left(\frac{RA_x}{|B\rho|c} \right)^2 + \left(\frac{RA_z}{|B\rho|c} \right)^2 + \left(\frac{R\Phi}{|B\rho|c} \right)^2 \right], \end{aligned} \quad (5.12)$$

where A_θ is now the total longitudinal component of the potential vector \vec{A} minus the stabilizing part given in Eq. (5.1), i.e. $-(c/2)(G_1 x^2 + G_2 z^2)$.

The form of the perturbing Hamiltonian H_1 suggests a further assumption.

Third assumption: The perturbing fields are small enough for us to neglect the square terms Φ^2 , A_x^2 , and A_z^2 with respect to the linear ones. This means

$$H_1 = \frac{1}{c|B\rho|} \left[R^2 \left(\frac{\Phi}{\beta} - A_\theta \right) - R (p_x A_x + p_z A_z) \right]. \quad (5.13)$$

In most cases it is possible to develop H_1 [Eq. (5.13)], which is a function of x , z , p_x , and p_z , in a series of terms which are homogeneous polynomials of degree N in the four canonical variables:

$$H_1 = \sum_N H_1^{(N)} (x, p_x, z, p_z, \theta) = \sum_N \sum_{\substack{J, K, L, M=0 \\ J+K+L+M=N}}^N b_{JKLM}^{(N)}(\theta) x^J p_x^K z^L p_z^M. \quad (5.14)$$

Following Section 3, the next step consists of expressing H_1 -- or every term $H_1^{(N)}$ -- as a function of the constants a_1 , \bar{a}_1 , a_2 , \bar{a}_2 of the unperturbed motion, by using Eqs. (5.10). Changing the name of the perturbing Hamiltonian from H_1 into U , as in Eqs. (3.36), we get

$$U(a_n, \theta) = \sum_N \sum_{\substack{j, k, l, m=0 \\ j+k+l+m=N}}^N h_{jklm}^{(N)}(\theta) a_1^j \bar{a}_1^k a_2^l \bar{a}_2^m \exp \left\{ i \left[(j-k)Q_x + (l-m)Q_z \right] \theta \right\}. \quad (5.15)$$

The perturbing Hamiltonian (5.15) has been obtained by putting the expressions of the canonical variables (5.10) into the second Eq. (5.14). Since these variables are all proportional to the Floquet functions given in Eq. (5.9) or to their derivatives, the coefficients $h_{jklm}^{(N)}$ introduced in Eq. (5.15) are proportional to the following quantity [see also Eq. (8.1)]

$$h_{jklm}^{(N)}(\theta) \sim b_{JKLM}^{(N)} \sqrt{\frac{\beta_x}{2R}}^{(j+k)} \sqrt{\frac{\beta_z}{2R}}^{(l+m)} \exp \left\{ -i[(j-k)Q_x + (l-m)Q_z]\theta \right\}, \quad (5.16)$$

where $j + k = J + K$ and $l + m = L + M$.

Since the perturbing electromagnetic fields have the circumferential periodicity in a circular accelerator, a Fourier development of the function U is possible

$$h_{jklm}^{(N)}(\theta) = \sum_{q=-\infty}^{\infty} h_{jklm q}^{(N)} e^{iq\theta} \quad (5.17)$$

with

$$h_{jklm q}^{(N)} = \frac{1}{2\pi} \int_0^{2\pi} h_{jklm}^{(N)}(\theta) e^{-iq\theta} d\theta.$$

Putting Eq. (5.17) in Eq. (5.15) gives

$$U(a_n, \theta) = \sum_N \sum_{\substack{j, k, l, m=0 \\ j+k+l+m=N}}^N \sum_{q=-\infty}^{\infty} h_{jklm q}^{(N)} a_1^j a_1^k a_2^l a_2^m \exp \left\{ i[(j-k)Q_x + (l-m)Q_z + q]\theta \right\}.$$

(5.18)

Equation (5.18) consists of terms whose explicit dependence on θ is of oscillatory character, the frequencies being

$$(j-k)Q_x + (l-m)Q_z + q. \quad (5.19)$$

The final assumption concerns the frequencies (5.19).

Fourth assumption: For relatively small perturbations, the amplitude and phase of a_1 and a_2 change little within the period of one oscillation or one revolution. This means that significant changes in a_1 and a_2 will only take place at low frequencies.

Consequently, the perturbing Hamiltonian (5.18) may be restricted to its low-frequency part, which thus gives the slow but important variations of the variables a_n .

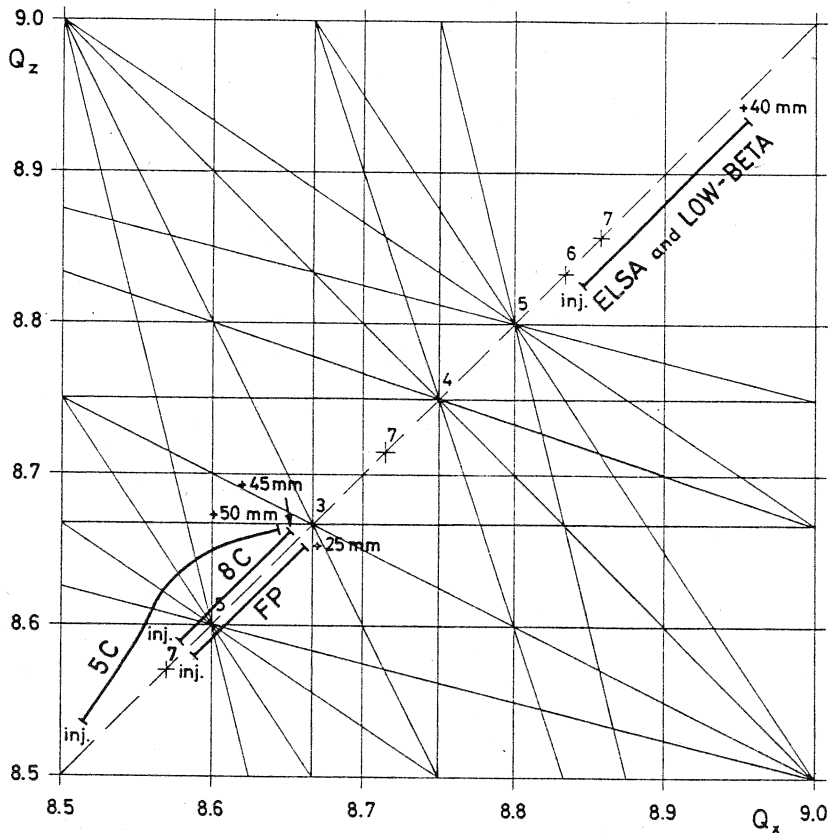


Fig. 3 Region of the tune plane in which the ISR are working

This low-frequency part of U includes, on the one hand, all the terms with zero frequency, i.e.

$$j = k, \quad \ell = m, \quad q = 0 \quad (5.20)$$

and, on the other hand, the terms for which the wave numbers Q_x and Q_z satisfy the condition

$$n_x Q_x + n_z Q_z = p \quad \text{where } n_x, n_z, p \text{ integers} \geq 0 \quad (5.21)$$

i.e.

$$j - k = \pm n_x, \quad \ell - m = \pm n_z, \quad q = \mp p.$$

Equation (5.21) is a generalization of the resonance condition mentioned in the Introduction [Eq. (1.6)]. When the transverse tunes satisfy Eq. (5.21) the amplitude of the motion may grow rapidly. The quantity $N^* = |n_x| + |n_z|$ is called the order of the resonance. In the tune plane (Q_x, Q_z) , the conditions (5.21) are represented by straight lines, which intersect on the diagonal $Q_x = Q_z$ for a given order N^* . Figure 3 shows such resonance lines in the region of the tune plane where the ISR are working.

The low-frequency part of the perturbing Hamiltonian (5.18) may be written as [by virtue of Eqs. (5.20) and (5.21)]

$$U(a_n, \theta) = \sum_v \sum_{q+s=v} h_{qqss}^{(2v)} (a_1 \bar{a}_1)^q (a_2 \bar{a}_2)^s +$$

$$+ \sum_N \sum_{\substack{j,k,\ell,m,p \\ j+k+\ell+m=N \\ j-k=n_x \\ \ell-m=n_z \\ |n_x|+|n_z|=N^* \\ 1 \leq N^* \leq N}} \left\{ h_{jk\ell m-p}^{(N)} a_1^j \bar{a}_1^k a_2^\ell \bar{a}_2^m \exp \left[i(n_x Q_x + n_z Q_z - p) \theta \right] + \right.$$

$$\left. + h_{kjml-p}^{(N)} a_1^k \bar{a}_1^j a_2^m \bar{a}_2^\ell \exp \left[-i(n_x Q_x + n_z Q_z - p) \theta \right] \right\}. \quad (5.22)$$

特定の共鳴に
対する
 m_x, m_z, p
が確定

The second double summation in Eq. (5.22) first sums over the homogeneous polynomials of degree N [Eq. (5.14)] and secondly sums all the resonances of the order N^* which may be excited by the polynomials of degree N .

In Eq. (5.22), the terms associated with resonances are defined by four integers j , k , ℓ , and m (plus the harmonic number p). For each set of these integers, it is worth noting that there is a unique resonance (5.21) concerned, but there are many terms or polynomials of the series (5.14) which can excite this resonance (the only condition is $N \geq N^*$).

Consequently, there are two approaches to the study of resonances:

- i) Assuming that the tunes are almost satisfying a relation of the form (5.21), it is worth considering this single resonance and taking only the strongest term among all the polynomials which excite it, i.e. $N = N^*$.

In this case, the indices j , k , ℓ , and m can only take the following values

$$\begin{aligned} j &= |n_x|, \quad k = 0 && \text{if } n_x \geq 0 \\ j &= 0, \quad k = |n_x| && \text{if } n_x < 0 \\ \ell &= |n_z|, \quad m = 0 && \text{if } n_z \geq 0 \\ \ell &= 0, \quad m = |n_z| && \text{if } n_z < 0. \end{aligned} \quad (5.23)$$

- ii) Assuming there is a family of $2N$ -pole magnetic elements (associated with a homogeneous polynomial of degree N) in a machine, it may be worth determining what are the resonances which are excited by these elements, i.e. $N^* \leq N$, $j - k = n_x$, $\ell - m = n_z$. It is then possible to treat each of these resonances separately depending upon the tune values.

In the two approaches a single resonance excited by elements which are associated with a given polynomial is considered. The only difference appears in the analytical expression of the coefficient $h_{jk\ell m-p}^{(N)}$ which figures in Eq. (5.22) and this means that the following treatment is valid for both the approaches.

From now on, we shall use the following names for the coefficients of Eq. (5.22)

$h_{qqss0}^{(2v)}$ = stabilizing coefficients

$h_{jk\bar{m}-p}^{(N)}$ = κ = excitation coefficients .

While the first terms can stabilize the resonances, the second ones are those which create the instabilities.

Providing the intersection of several resonance lines (Fig. 3) is not considered, the low-frequency part (5.22) of the Hamiltonian associated with a single resonance becomes with these notations .

$$U = \sum_v \sum_{q+s=v} h_{qqss0}^{(2v)} (a_1 \bar{a}_1)^q (a_2 \bar{a}_2)^s +$$

$$+ \kappa a_1^j \bar{a}_1^k a_2^l \bar{a}_2^m e^{ie\theta} + \bar{\kappa} \bar{a}_1^j a_1^k \bar{a}_2^l a_2^m e^{-ie\theta} \quad (5.24)$$

where e stands for the distance from the resonance line,

$$e = n_x Q_x + n_z Q_z - p . \quad (5.25)$$

5.3 Equations of the perturbed motion^{8,11,12)}

Going back to Section 3, the equations of motion for the coefficients a_1 and a_2 are given by Eqs. (3.36) where a_1 , \bar{a}_1 , a_2 , \bar{a}_2 are the coefficients c_k .

The a_n coefficients (5.11) have the convenient properties of [using the definition (3.31)]

$$[a_1, \bar{a}_1] = i, \quad [a_1, \bar{a}_2] = 0, \quad [a_1, a_2] = 0$$

$$[a_2, \bar{a}_1] = 0, \quad [a_2, \bar{a}_2] = i, \quad (5.26)$$

so that the equations of motion can be simplified to

$$\frac{da_1}{d\theta} = i \frac{\partial U}{\partial \bar{a}_1}$$

$$\frac{da_2}{d\theta} = i \frac{\partial U}{\partial \bar{a}_2} \quad (5.27)$$

and the complex conjugates. The function U is given in Eq. (5.24).

As an example, the first equation (5.27) gives

$$\frac{da_1}{d\theta} = i \sum_v \sum_{q+s=v} q h^{(2v)}_{qqss} a_1 (a_1 \bar{a}_1)^{(q-1)} (a_2 \bar{a}_2)^s + \\ + i \kappa k a_1^j \bar{a}_1^{(k-1)} a_2^{\ell} \bar{a}_2^m e^{i\theta} + i \bar{\kappa} j \bar{a}_1^{(j-1)} a_1^k \bar{a}_2^{\ell} a_2^m e^{-i\theta}, \quad (5.28)$$

while the second equation (5.27) gives a similar expression for $da_2/d\theta$.

Since the coefficients a_n are the complex amplitudes of the transverse motions (5.5), i.e. a slowly "oscillating" envelope component, it is interesting to replace the complex variables by real amplitudes and phases

$$a_1 = r_1 e^{i\phi_1}, \quad a_2 = r_2 e^{i\phi_2}. \quad (5.29)$$

The relations (5.9) and (5.10) show that r_1, r_2 are related to the peak amplitudes of the oscillations by

$$r_1^2 = |a_1|^2 = \sqrt{\frac{R}{2\beta_y}} \hat{y}. \quad (5.30)$$

On top of this an emittance E_y can be associated with the peak amplitude

$$\hat{y} = \sqrt{\frac{\beta_y E}{\pi}}. \quad (5.31)$$

Hence

$$r_1^2 = |a_1|^2 = \frac{RE}{2\pi}. \quad (5.32)$$

The coordinates (y, y') of a single particle at a point s of the circumference describe an ellipse during the revolutions⁹⁾. The emittance E_y is the area of this ellipse (Fig. 4).

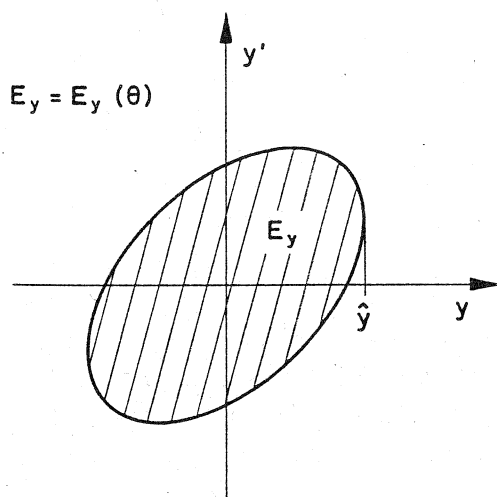


Fig. 4
Trajectory and emittance of a particle in the transverse phase plane

If the motion is not perturbed, this area is a constant. On the contrary, in the presence of a perturbation the emittance may vary with time or θ in agreement with Eqs. (5.28) and (5.32).

Putting Eqs. (5.29) in Eqs. (5.28) and then splitting the equations into real and imaginary parts gives the equations for r_1, ϕ_1 and r_2, ϕ_2 , assuming from now on $N = N^*$ for convenience.

$$\begin{aligned}
 j + h &= |m_x| \\
 l + m &= |m_z|
 \end{aligned}
 \boxed{
 \begin{aligned}
 \frac{dr_1}{d\theta} &= n_x |\kappa| r_1 (|n_x|-1) r_2 |n_z| \sin \psi \\
 \frac{d\phi_1}{d\theta} &= \sum_v \sum_{q+s=v} q h_{qqss}^{(2v)} r_1^{2(q-1)} r_2^{2s} + |n_x| |\kappa| r_1 (|n_x|-2) r_2 |n_z| \cos \psi \\
 \frac{dr_2}{d\theta} &= n_z |\kappa| r_1 |n_x| r_2 (|n_z|-1) \sin \psi \\
 \frac{d\phi_2}{d\theta} &= \sum_v \sum_{q+s=v} s h_{qqss}^{(2v)} r_1^{2q} r_2^{2(s-1)} + |n_z| |\kappa| r_1 |n_x| r_2 (|n_z|-2) \cos \psi,
 \end{aligned}
 }
 \tag{5.33}$$

where

$$\psi = n_x \phi_1 + n_z \phi_2 + \phi_\kappa + \theta e,$$

ϕ_κ being the phase of the complex coefficient κ [Eq. (5.24)] and e the distance from the resonance [Eq. (5.25)]. The equations (5.33) give the solution to our problem.

If the Hamiltonian (5.24) comprises only zero frequency terms, either because the excitation coefficients are zero or because Q_x and Q_z are too far from satisfying Eq. (5.21), the equations (5.33) are simplified to

$$\begin{aligned}
 \frac{dr_1}{d\theta}^2 &= 0 \\
 \frac{d\phi_1}{d\theta} &= \sum_v \sum_{q+s=v} q h_{qqss}^{(2v)} r_1^{2(q-1)} r_2^{2s} \\
 \frac{d\phi_2}{d\theta} &= \sum_v \sum_{q+s=v} s h_{qqss}^{(2v)} r_1^{2q} r_2^{2(s-1)}.
 \end{aligned}
 \tag{5.34}$$

They show that the amplitude is constant, apart from the rapidly oscillating part. This is the case of an oscillation without excitation. Obviously, $d\phi/d\theta$ are corrections to the frequencies due to the perturbation, the effective frequencies being $Q_x + d\phi_1/d\theta$ and $Q_z + d\phi_2/d\theta$. The linear perturbations ($v = 1$) produce a frequency shift independent of amplitude.

If the excitation term κ is different from zero, it causes a change in amplitude. This term is therefore responsible for the excitation of what we called a *resonance*. Suppose that ϕ_1 and ϕ_2 are such that at a given time there is an amplitude growth. How far the growth will continue depends upon the change of phase due to the equations (5.33). In general, the phases will, after some time, have changed enough to cause the amplitude to decrease again. The motion is then a beating oscillation. However, under certain conditions, there may be an unlimited build-up. If the stabilizing coefficients $h_{qqss}^{(2v)}$ are all zero, except $h_{11000}^{(2)}$ and $h_{00110}^{(2)}$, there are no frequency shifts associated with the amplitude except those due to the excitation term κ . The equations of motion then take the more particular form

$$\begin{aligned}\frac{d\phi_1}{d\theta} &= h_{11000}^{(2)} + |n_x| |\kappa| r_1^{|n_x|-2} r_2^{|n_z|} \cos \psi \\ \frac{d\phi_2}{d\theta} &= h_{00110}^{(2)} + |n_z| |\kappa| r_2^{|n_z|-2} r_1^{|n_x|} \cos \psi \\ \frac{dr_1}{d\theta} &= n_x |\kappa| r_1^{|n_x|-1} r_2^{|n_z|} \sin \psi \\ \frac{dr_2}{d\theta} &= n_z |\kappa| r_2^{|n_z|-1} r_1^{|n_x|} \sin \psi.\end{aligned}\tag{5.35}$$

The maximum rate of growth is obtained for $\sin \psi = 1$, i.e. $\cos \psi = 0$. This condition means

$$\begin{aligned}\frac{d\phi_1}{d\theta} &= h_{11000}^{(2)} = \text{const.} \\ \frac{d\phi_2}{d\theta} &= h_{00110}^{(2)} = \text{const.}\end{aligned}\tag{5.36}$$

This may be maintained automatically, since

$$\begin{aligned}\frac{d\psi}{d\theta} &= e + n_x \frac{d\phi_1}{d\theta} + n_z \frac{d\phi_2}{d\theta} = \\ &= e + n_x h_{11000}^{(2)} + n_z h_{00110}^{(2)}\end{aligned}\tag{5.37}$$

and $d\psi/d\theta = 0$ if the effective frequencies $Q_x + d\phi_1/d\theta$ and $Q_z + d\phi_2/d\theta$ satisfy the condition for a resonance.

It is obvious from this that any terms shifting the frequency with amplitude tend to limit the build-up of amplitude, transforming it into a mere beating of the oscillation.

5.4 Invariants of the perturbed motion^{8,11,13)}

For studying the range of amplitudes covered by the oscillations in the course of its beating, it is very useful to establish the invariants of motion, i.e. invariant relations between amplitudes and phases.

Combining the two equations (5.33) for r_1 and r_2 gives

$$\frac{r_1}{n_x} \frac{dr_1}{d\theta} = \frac{r_2}{n_z} \frac{dr_2}{d\theta}. \quad (5.38)$$

Integrating Eq. (5.38) gives the *first invariant*

$$A^* = \frac{r_1^2}{n_x} - \frac{r_2^2}{n_z}. \quad (5.39)$$

It is also possible, starting from Eq. (5.33), to write the Hamiltonian associated with the variables $r_1^2, \phi_1, r_2^2, \phi_2$:

$$G = \sum_v \sum_{q+s=v} h_{qqss}^{(2v)} (r_1^2)^q (r_2^2)^s + 2|\kappa| (r_1^2)^{|n_x|/2} (r_2^2)^{|n_z|/2} \cos \psi. \quad (5.40)$$

This form of G is easily verified via the canonical equations (3.15), which become in the present case

$$\left\{ \begin{array}{l} \frac{d\phi_1}{d\theta} = \frac{\partial G}{\partial r_1^2} \\ \frac{dr_1^2}{d\theta} = -\frac{\partial G}{\partial \phi_1} \end{array} \right. \quad \left\{ \begin{array}{l} \frac{d\phi_2}{d\theta} = \frac{\partial G}{\partial r_2^2} \\ \frac{dr_2^2}{d\theta} = -\frac{\partial G}{\partial \phi_2} \end{array} \right. \quad [\phi_i, r_j^2] = \delta_{ij} \quad (5.41)$$

Putting Eq. (5.40) into Eqs. (5.41) gives Eqs. (5.33).

Since G depends explicitly on θ in ψ , the Hamiltonian G is not directly an invariant. But we can use the relation (3.18) of Section 3.2 which states that

$$\frac{dG}{d\theta} = \frac{\partial G}{\partial \theta}. \quad (5.42)$$

Since $\psi = e\theta + n_x \phi_1 + n_z \phi_2 + \phi_K$, the following relations apply

$$\begin{aligned} \frac{\partial G}{\partial \phi_1} &= n_x \frac{\partial G}{\partial \psi} \\ \frac{\partial G}{\partial \psi} &= \frac{1}{n_x + n_z} \left(\frac{\partial G}{\partial \phi_1} + \frac{\partial G}{\partial \phi_2} \right). \end{aligned} \quad (5.43)$$

Consequently, using Eq. (5.43) and the canonical equations (5.41) we get

$$\begin{aligned}
 \frac{dG}{de} &= \frac{\partial G}{\partial \theta} = \frac{\partial G}{\partial \psi} \frac{\partial \psi}{\partial \theta} = \frac{\partial G}{\partial \psi} (n_x Q_x + n_z Q_z - p) \\
 &= Q_x \frac{\partial G}{\partial \phi_1} + Q_z \frac{\partial G}{\partial \phi_2} - \frac{p}{n_x + n_z} \left(\frac{\partial G}{\partial \phi_1} + \frac{\partial G}{\partial \phi_2} \right) = \\
 &= -Q_x \frac{dr_1^2}{d\theta} - Q_z \frac{dr_2^2}{d\theta} + \frac{p}{n_x + n_z} \frac{d}{d\theta} (r_1^2 + r_2^2) .
 \end{aligned} \tag{5.44}$$

Equating the first and the last terms of this series of equalities and then integrating the obtained relation gives an invariant

$$G + \left(Q_x - \frac{p}{n_x + n_z} \right) r_1^2 + \left(Q_z - \frac{p}{n_x + n_z} \right) r_2^2 = C' . \tag{5.45}$$

Multiplying Eq. (5.45) by either n_x or n_z , and using the first invariant (5.39) gives a simpler form for the *second invariant*

$n_x G + er_1^2 = C_x \quad \text{for } n_x \neq 0$		(5.46)
$n_z G + er_2^2 = C_z \quad \text{for } n_z \neq 0$		

remembering that $e = n_x Q_x + n_z Q_z - p$. G is defined in Eq. (5.40).

The first invariant exhibits interesting properties:

- i) n_x and n_z have the same sign

Equation (5.39) indicates that the difference of the transverse "normalized" amplitudes remains constant. This means that both the amplitudes can grow, provided that this difference is constant. These resonances are thus unstable and harmful.

- ii) n_x and n_z have opposite signs

Equation (5.39) shows that the amplitudes r^2 in the x - and z -direction stay on a certain ellipse during the motion. Thus both amplitudes necessarily remain finite, and the resonance does not cause instability. In such a "stable" resonance one of the amplitudes decreases while the other is increasing. There is a constant periodic exchange of "energy" (amplitude square) between the two transverse planes. However, if the initial unperturbed amplitudes are very different, e.g. $r_{2,0} \ll r_{1,0}$, averaging these slow oscillations over many turns will show an apparent increase of the small amplitude at the expense of the other one. This is the reason why these resonances also need to be discussed.

The resonances of type (i) are called *sum resonances* while the resonances of type (ii) are called *difference resonances*.

6. DISCUSSION OF RESONANCE CHARACTERISTICS^{8,11-13)}

6.1 Detailed discussion of the invariants

In this section, we analyse the invariants (5.39) and (5.46). The second invariant C_y can be written as follows

$$C_y = k_2 r^2 + k_4 r^4 + \dots + k_{2(N/2)} r^{2(\bar{N}/2)} + \cos \psi k_{2N-1} r^{|n|} (E^* \pm r^2)^{|N-n|/2}. \quad (6.1)$$

where

r stands for r_1 or r_2 [the other having been eliminated by using Eq. (5.39)],
 $|n|$ stands for $|n_x|$ or $|n_z|$,

$\bar{N}/2$ is the smallest integer $\geq N/2$ (the series is terminated when the order of the perturbation is reached),

$k_{2N-1} = 2|\kappa| |n| \left| \frac{N-n}{n} \right|^{|N-n|/2}$ (proportional to the excitation coefficient),

$E^* = A \frac{|n|}{|N-n|}$, A being proportional to the first invariant (5.39). A stands for A_1 or A_2 which are defined as follows

$$|N-n| \text{ は } N-|n| \text{ の意味} \quad A_1 = r_2^2 - \frac{n_z}{n_x} r_1^2 \quad (6.2)$$

$$N = |n_x| + |n_z| \quad A_2 = r_1^2 - \frac{n_x}{n_z} r_2^2,$$

$k_2 = e + n_x h_{11000}^{(2)} + n_z h_{00110}^{(2)}$, linearly depending on e ,

k_{2j} are parameters depending on the stabilizing coefficients $h_{qqss0}^{(2v)}$, by virtue of Eqs. (5.46) and (5.40).

The sign (\pm) is associated with the sum and difference resonances, respectively.

It is possible to define the two coordinates r and ψ/N as polar coordinates valid in the vicinity of the resonances and then to consider the phase diagrams $r = r(\psi/N)$ as following from the invariant C_y [Eq. (6.1)]. Such phase plots have been frequently used for discussing linear and non-linear *one-dimensional* oscillations. For two-dimensional oscillations this plot is not convenient.

Thus, the examples given of phase-plane paths are in the vicinity of *one-dimensional resonances* of order 2 and 4 (Figs. 5 and 6).

These paths are either closed or they reach infinity representing, respectively, stable or unstable motions. The case where $k_2 = 0$ and $k_4 = 0$ is unstable. Going from $k_4 = 0$ to $k_4 \neq 0$, the paths are made to close at finite amplitudes and the motion becomes stable.

Note that, in these phase paths, it has been assumed that only the first two stabilizing coefficients k_2 and k_4 are different from zero. The topology of the paths may be affected at large amplitudes by stabilizing coefficients of higher order.

Further, note the appearance of *islands* outside the origin in certain stabilized cases. The centres of these islands are *stable fixed points*, which represent motions with fixed amplitude and phase, i.e. $d\psi/d\theta = 0$ [Eq. (5.37)]. It follows that, at a fixed point, the

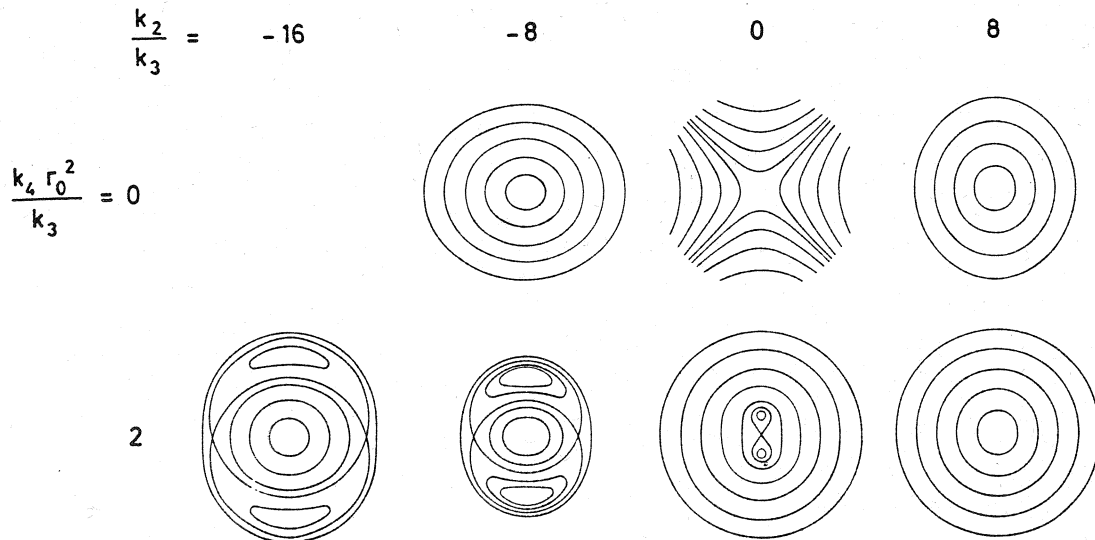


Fig. 5 Phase-plane paths in the vicinity of resonances of order 2

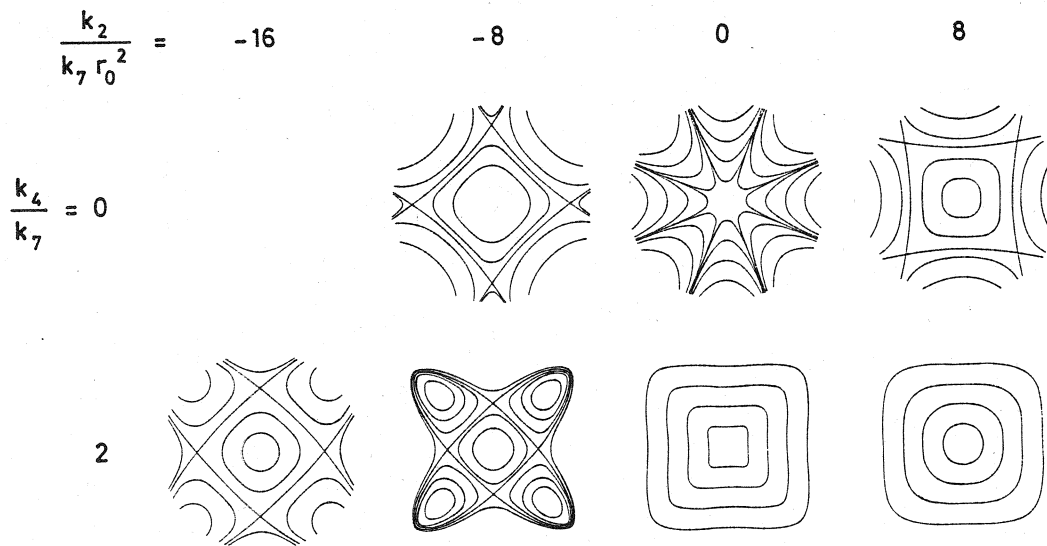


Fig. 6 Phase-plane paths in the vicinity of resonances of order 4

effective frequencies satisfy the resonance condition (5.21), i.e. the orbits close after N revolutions. A particle which lies near a stable fixed point will oscillate around it.

There are also *unstable fixed points* when two paths are crossing. At these points, the condition $d\psi/d\theta = 0$ is also satisfied and the amplitude and the phase remain constant. However, a very small perturbation will cause a particle to move away from such an unstable fixed point. These paths are also called *separatrices* and a particle which follows a separatrix needs an infinite time in order to reach one of the unstable fixed points.

All these characteristics of the paths given in Figs. 5 and 6 can be deduced analytically. As an example, we will discuss below the second invariant (6.1) for the one-dimensional resonances of order 2 and 4, which have been considered in these figures. Assuming that, among the parameters k_{2j} , only k_2 and k_4 may be different from zero, the second invariant becomes

$$C_y = k_2 r^2 + k_4 r^4 + \cos N\phi k_{2N-1} r^N \quad (6.3)$$

with the definition $\phi = \psi/N$.

When all the stabilizing coefficients are zero, the invariant (6.3) for one-dimensional resonances becomes

$$C_y = k_{2N-1} r^N \cos N\phi . \quad (6.4)$$

Equation (6.4) is the equation for families of curves which have asymptotes at $\cos N\phi = 0$ and minima in the amplitude r when $\sin N\phi = 0$, i.e.

$$\left. \begin{array}{l} \text{Asymptotes for } \phi = \frac{\pi}{2N} + m \frac{\pi}{N} \\ \text{Minima in } r \text{ for } \phi = m \frac{\pi}{N} \end{array} \right\} m \text{ being an integer .}$$

These families are represented among others in Figs. 5 and 6, for $N = 2$ and $N = 4$, respectively.

Let us now define the analytical conditions which are associated with the fixed points mentioned above. C_y represents a family of functions of r , the two extreme members of the family being obtained for $\cos \psi = \pm 1$. The existence of fixed points requires that a unique value of r corresponds to a certain value of C_y . This can only be satisfied at a minimum or maximum on the curve $C_y(r)$. If the highest function of the family has a maximum or if the lowest function has a minimum, the amplitude r is strictly limited to a unique value and the fixed point is stable. If the highest function of the family has a minimum or if the lowest function has a maximum, the amplitude may vary on either side, still satisfying a function $C_y(r)$ which is a member of the family, and the fixed point is unstable. This is illustrated in Fig. 7. Hence, to look for fixed points it is necessary to look for the extreme values of the two functions C_y (6.3) which are associated with $\cos N\phi = \pm 1$,

$$\frac{dC_y}{dr} = 2k_2 r + 4k_4 r^3 \pm N r^{N-1} k_{2N-1} = 0 \quad \cos N\phi = \pm 1 . \quad (6.5)$$

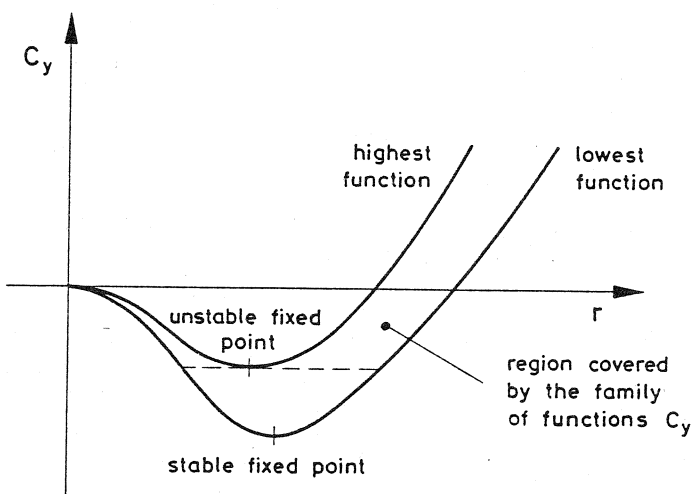


Fig. 7 Second invariant and possible fixed points

The two equations (6.5) give the amplitude r_0 and the phase ϕ_0 of a fixed point. The first equation does not always have solutions (different from the trivial one $r = 0$), which means that fixed points may not exist. If they exist, the phase is necessarily given by $\cos \psi = \pm 1$ and the sign to be considered depends on the sign of the coefficients k_2 , k_4 , and k_{2N-1} . The analysis of Eqs. (6.5) for the orders 2 and 4 and the results are summarized in Table 1. These results give the main features of the paths shown in Figs. 5 and 6.

It is then interesting to look at the motion around fixed points. The equations of the motion (5.33) become for one-dimensional resonances

$$r' = N|\kappa|r^{(N-1)} \sin N\phi \quad (6.6)$$

$$\phi' = \frac{k_2}{N} + 2k_4 r^2 + N|\kappa|r^{(N-2)} \cos N\phi.$$

$h_4 = h_{2,00}^4$

Table 1

List of fixed points for one-dimensional resonances of order 2 and 4 ($k_{2N-1} > 0$)

Order	k_2	k_4	Type of possible fixed points ^{*)}
N = 2	≥ 0	0	No fixed points
	0	≥ 0	Stable fixed points for $\cos \psi = \mp 1$
	$k_2 > k_3$	> 0	No fixed points
	$-k_3 < k_2 < k_3$		Stable fixed points for $\cos \psi = -1$
	$k_2 < -k_3$		Stable fixed points for $\cos \psi = -1$
	$k_2 > k_3$	< 0	Unstable fixed points for $\cos \psi = 1$
	$-k_3 < k_2 < k_3$		Unstable fixed points for $\cos \psi = -1$
	$k_2 < -k_3$		Stable fixed points for $\cos \psi = 1$
N = 4	0	≥ 0	No fixed points
	≥ 0	0	Unstable fixed points for $\cos \psi = \mp 1$
	> 0	$k_4 > k_7$	No fixed points
		$-k_7 < k_4 < k_7$	Unstable fixed points for $\cos \psi = -1$
		$k_4 < -k_7$	Stable fixed points for $\cos \psi = 1$
	< 0	$k_4 > k_7$	Unstable fixed points for $\cos \psi = -1$
		$-k_7 < k_4 < k_7$	Unstable fixed points for $\cos \psi = 1$
		$k_4 < -k_7$	Stable fixed points for $\cos \psi = -1$

^{*)} Note that the coordinates of the fixed points can be calculated in each case by using Eqs. (6.5), with the appropriate sign being given in the table.

Assuming that r_0 and ϕ_0 are the polar coordinates of a fixed point, we can develop Eqs. (6.6) around this point. Keeping only the terms of the first order in $\Delta r = r - r_0$ and $\Delta\phi = \phi - \phi_0$, Eqs. (6.6) become

$$\begin{aligned}\Delta r' &= N^2 |\kappa| r_0^{(N-1)} \cos N\phi_0 \Delta\phi \\ \Delta\phi' &= \left[2k_4 r_0 + N|\kappa|(N-2)r_0^{(N-3)} \cos N\phi_0 \right] \Delta r.\end{aligned}\quad (6.7)$$

The two equations (6.7) can be combined to give a differential equation of the second order in Δr . If the coefficient $|\kappa|$ is small with respect to k_4 , this equation is

$$\Delta r'' = \underbrace{2N^2 |\kappa| r_0^N}_{4} k_4 \cos N\phi_0 \Delta r. \quad (6.8)$$

The solution of Eq. (6.8) is stable if $k_4 \cos N\phi_0 < 0$ (sinusoidal function) and unstable if $k_4 \cos N\phi_0 > 0$ (exponential function). The first solution describes the oscillations around a stable fixed point, while the second solution gives the motion diverging from an unstable fixed point. The conditions we have found for $k_4 \cos N\phi_0$ are in agreement with the contents of Table 1.

The whole analysis of the second invariant associated with one-dimensional resonances has been done by only taking into account the two stabilizing coefficients $h_{1100}^{(2)}$ and $h_{2200}^{(4)}$. However, this analysis can be repeated in the same way when many parameters k_{2j} are different from zero.

As mentioned before, the phase-plane representation is not suitable for discussing *two-dimensional resonances*. Furthermore, the quantity of practical interest, with regard to the confinement of particles by the field of a synchrotron, is the range of amplitudes covered by the oscillation. As illustrated before, it depends upon the parameters k_{2j} and on the value of the invariant C_y . The beating range is thus better investigated by the type of curves given in Fig. 7. As a particular example, these curves are represented in Fig. 8 as a function of the frequency shift k_2 , for resonances of order 3 with $k_4 \neq 0$.

In this figure, the two extreme curves C_y (6.1) associated with $\cos \psi = \pm 1$ are plotted as functions of r^2/r_0^2 . The range of amplitudes covered by the oscillation is that part of the line $C_y = \text{constant}$ which is bounded by the two extreme curves associated with the same value of k_2 . This diagram illustrates the stabilizing effect of k_4 , since all the considered beatings have finite amplitude. Nevertheless, this beating may be large (Fig. 8).

It is now interesting to look for the maximum value r_{\max} that can be reached from the initial value r_0 . In order to do this, we have to go back to the invariant (6.1). The extreme values of the amplitude r are given by the solutions of the two equations

$$F_{\pm}(k_2, r) = k_2 r^2 + \dots \pm k_{2N-1} r^{|n|} (E^* \pm r^2)^{|N-n|/2} = \text{const.}, \quad (6.9)$$

where it is always possible to assume $k_{2N-1} \geq 0$, without restricting the generality of the treatment.

$$\cos \psi = \pm 1 \text{ の 时 } \frac{dr}{d\theta} = 0$$

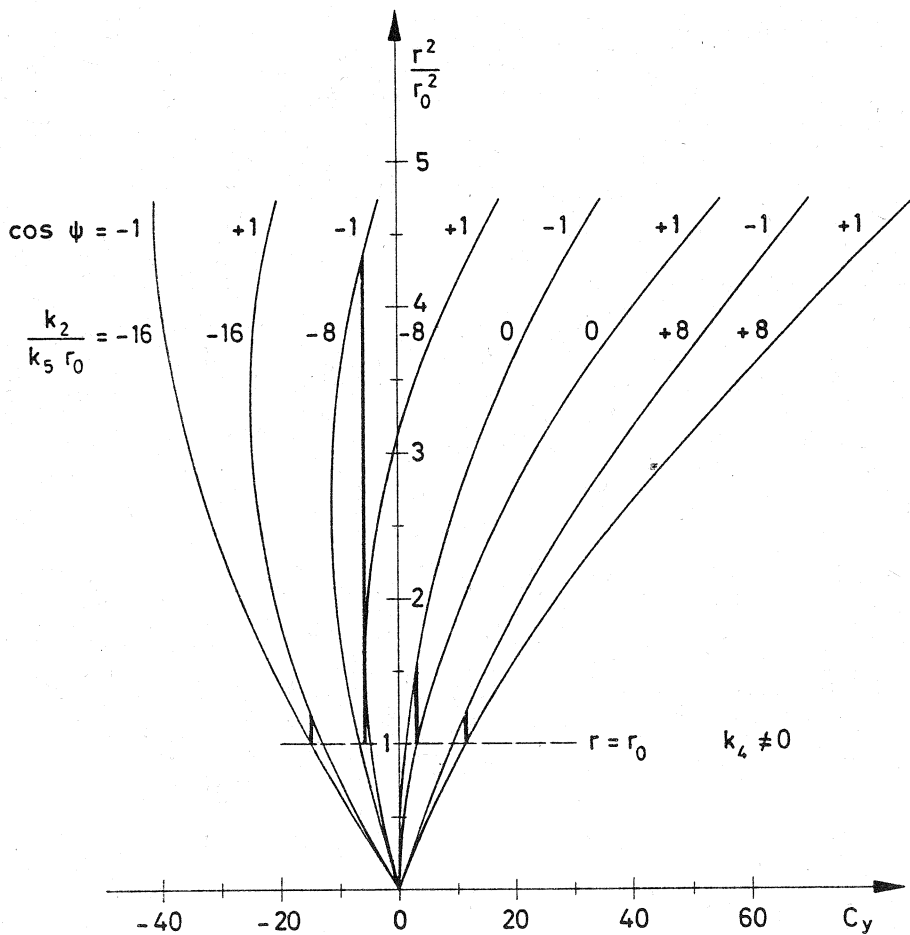


Fig. 8 Beating ranges in a graphical representation of C_y

For given initial conditions, the extreme values of the constant are given by $F_{\pm}(k_2, r_0)$. Thus, for known initial conditions, the extreme values of r are determined by the four equations

$$\begin{array}{ll} F_{++}^I = F_+(k_2, r_0) - F_+(k_2, r) = 0 \\ ++ \quad + \quad - \\ +- \quad - \quad + \\ -- \quad - \quad - \end{array} \quad (6.10)$$

It is obviously useful to normalize the amplitude by introducing a new variable $x = r/r_0$, assuming that $r_0 \neq 0$. It is also advantageous to normalize the stabilizing coefficients with respect to the excitation term, i.e.

$$c_{2j} = \frac{k_{2j}}{k_{2N-1} r_0^{N-2j}}. \quad (6.11)$$

Thus we get an equation of the form

$$F_{++}^{II} = c_2(1-x^2) + c_4(1-x^4) + \dots + (E_1^* - x^N E_2^*) = 0 .$$

++	+	+
--	-	+
-+	-	-
--	-	-

(6.12)

The definitions of E_1^* and E_2^* are

$$E_1^* = \left(\frac{E^*}{r_0^2} \pm 1 \right)^{|N-n|/2}$$

$$E_2^* = \left(\frac{E^*}{r_0^2 x^2} \pm 1 \right)^{|N-n|/2} ,$$
(6.13)

where E^* is the coefficient introduced and defined in Eq. (6.1) and is proportional to either A_1 or A_2 [Eqs. (6.2)]. The sign (\pm) is associated with sum and difference resonances, respectively.

We have seen that k_2 is proportional to the distance e from the resonance. Hence, c_2 in Eq. (6.11) is also proportional to e and it is interesting to solve Eqs. (6.12) with respect to c_2 , which gives four relations:

$$c_2^{++} = -c_4(1+x^2) - \dots - c_2(\bar{N}/2) \left[1+x^2+\dots+x^{2(\bar{N}/2-1)} \right] + (-E_1^* + x^N E_2^*)/(1-x^2)$$

c_2^{+-} =	-	-
c_2^{-+} =	+	+
c_2^{--} =	+	-

(6.14)

where only the two signs inside the last but one bracket change with the top indices of c_2 .

Equations (6.14) define four curves $c_2 = c_2(x)$, which are so-called *resonance curves* and which restrict the transverse amplitudes of the oscillation. The characteristics of these curves are different for sum and difference resonances and will be discussed in the next two sections.

6.2 Resonance curves and bandwidths for sum resonances

The resonance curves $c_2 = c_2(x)$ are defined in Eqs. (6.14), where c_2 is proportional to the distance e from the resonance and x is the relative amplitude r/r_0 in either transverse direction.

For sum resonances, the positive sign has to be used in E_1^* and E_2^* [Eqs. (6.13)]. In order to get the shapes of the four curves c_2^{++} , c_2^{+-} , c_2^{-+} and c_2^{--} , in the physical range $x \geq 1$, it is sufficient to calculate the limits of these functions when x tends to one from higher values and when x tends to infinity from lower values.

First case: the coefficients $c_4, c_6, \dots, c_{2(N/2)}$ are all zero. The above-mentioned limits (for $N > 2$) and the asymptotic behaviours are given in Table 2.

Table 2

Limits for $N > 2$ and asymptotes of the sum resonance curves

Top indices of c_2	Value of c_2 when $x \rightarrow 1$ $x \rightarrow +\infty$		Asymptotic behaviour
++	D_1	$-\infty$	$-x^{N-2}$
+-	$+\infty$	$+\infty$	x^{N-2}
-+	$-\infty$	$-\infty$	$* -x^{N-2}$
--	D_2	$+\infty$	x^{N-2}

According to Table 2 the resonance curves have the shapes illustrated in Fig. 9 for $N = 3$ and $N = 5$. Inside the interval $[D_1, D_2]$, there is obviously no limitation of the amplitude. This interval corresponds to the stopband of a sum resonance and the *bandwidth* is defined as the increment in the distance ϵ from the resonance, which corresponds to the difference $D_2 - D_1$, i.e. by virtue of Eq. (6.11)

$$\Delta\epsilon = k_{2N-1} r_0^{N-2} \left[c_2^{--}(x=1) - c_2^{++}(x=1) \right] \quad (6.15)$$

Remark: This definition is general and is quite convenient in the estimation of the effects of a resonance. Nevertheless, there are three particular cases where the bandwidth calculated in this way [Eq. (6.15)] is not the width of an actual stopband but the width of a virtual stopband.

These exceptions are

$$\begin{aligned} Q_x = p, Q_z = p, & \quad \text{for } N = 1 \\ Q_x + Q_z = p, & \quad \text{for } N = 2. \end{aligned} \quad (6.16)$$

For the two dipole resonances, the asymptotes vary as $1/x$ (Table 2). Hence, there is no finite interval where the amplitude is without limitation, but $\Delta\epsilon$ can still be defined on the straight line $x = 1$ (Fig. 10).

For the quadrupole sum resonance, the asymptotes are constants (Table 2), but the interval where the amplitude is not limited is smaller than $\Delta\epsilon$, which is defined on the line $x = 1$ (Fig. 10).

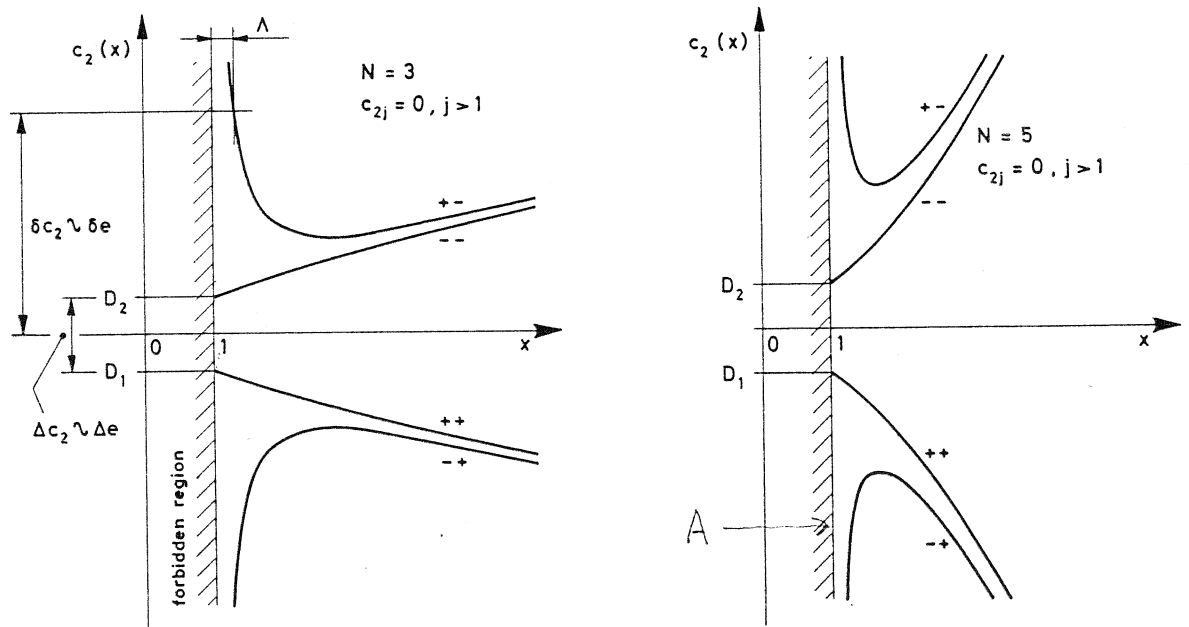


Fig. 9 Resonance curves and stopbands for sum resonances of order 3 and 5

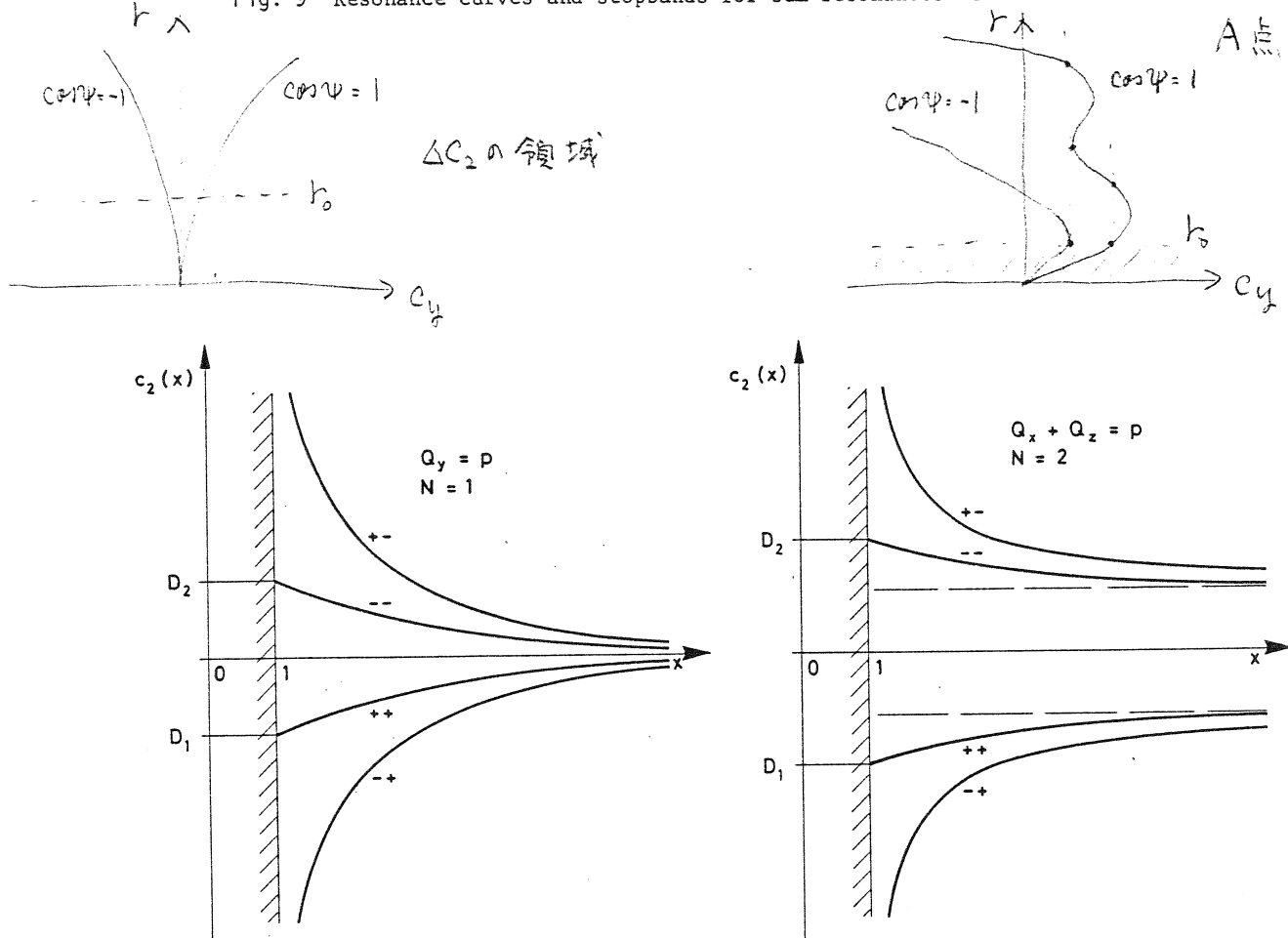


Fig. 10 Virtual stopbands associated with particular resonance curves

Calculating explicitly the limits in Eq. (6.15) and introducing the emittances [Eq. (5.32)], the expression for the bandwidth becomes

$$m_x \geq 0, m_z \geq 0$$

$$\Delta e = 2|\kappa| \left(\frac{R}{2\pi} \right)^{(N-2)/2} E_{x,0}^{(n_x-2)/2} E_{z,0}^{(n_z-2)/2} \left(n_x^2 E_{z,0} + n_z^2 E_{x,0} \right). \quad (6.17)$$

Second case: the coefficients $c_4, c_6, \dots, c_{2(\bar{N}/2)}$ are all different from zero. The limits of the functions c_2 when x tends to one from higher values and when x tends to infinity from lower values depend on the value of $c_{2(\bar{N}/2)}$ and on the parity of N , and the asymptotes are given by

$$\text{For } N \text{ even: } -[c_{2(\bar{N}/2)}^{+1}]^{N-2} \quad \text{for } c_2^{++} \text{ and } c_2^{-+}$$

$$-[c_{2(\bar{N}/2)}^{-1}]^{N-2} \quad \text{for } c_2^{+-} \text{ and } c_2^{--}$$

$$\text{For } N \text{ odd: } -c_{2(\bar{N}/2)} x^{N-1} \quad \text{for all the } c_2 \text{'s}.$$

The consequence is that, for N odd, the amplitude is always restricted if $c_{2(\bar{N}/2)} \neq 0$, and that, for N even, the amplitude is restricted everywhere only if $c_{2(\bar{N}/2)} > 1$ or $c_{2(\bar{N}/2)} < -1$. The resonance curves of such a stabilized resonance of order 4 are given in Fig. 11.

Intermediate cases may appear when only a few coefficients c_{2j} of lower order are different from zero. In such cases, the amplitude may not always be restricted, even if the resonance curves are asymmetrical with respect to the axis $c_2 = 0$. An example is given in Fig. 12 for a resonance of order 5, assuming $c_4 \neq 0$ and $c_{2j} = 0$ for $j > 2$.

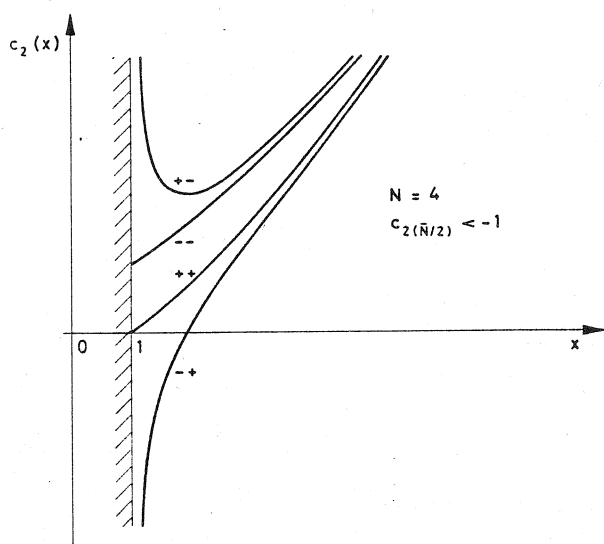


Fig. 11 Curves $c_2(x)$ for a stabilized sum resonance of order 4

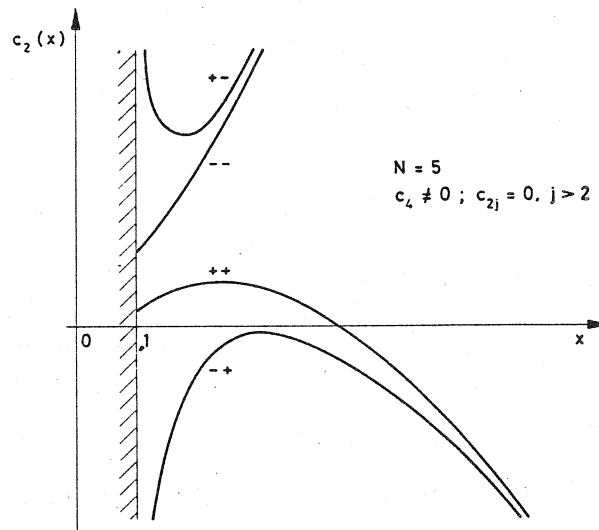


Fig. 12 Curves $c_2(x)$ for a sum resonance of order 5 when only c_4 is different from zero

Remarks: $\kappa = h_{jk\ell m-p}^{(N)} \sim k_{2N-1} \sim c_{2N-1}$ was called the excitation coefficient, since it is the source of the instability and it is taken as a separate factor in the expression of the bandwidth (6.17).

$h_{qqss 0}^{(2v)} \sim k_{2j} \sim c_{2j}$ were called stabilizing coefficients, since they may limit the amplitude growth for the same value of κ .

6.3 Resonance curves and bandwidths for difference resonances

For difference resonances, the negative sign has to be used in E_1^* and E_2^* [Eqs. (6.13)]. As has already been done for sum resonances, the shapes of the resonance curves are deduced from the limits of the functions $c_2(x)$ at the extreme values of x and at $x = 1$. The extreme values of x are given by the first invariant (5.39) and/or Eqs. (6.2)

$$0 \leq x_1 \leq \sqrt{1 + \left| \frac{n_x}{n_z} \right| \frac{E_{z,0}}{E_{x,0}}} = x_{1,\max} \quad (6.18)$$

$$0 \leq x_2 \leq \sqrt{1 + \left| \frac{n_z}{n_x} \right| \frac{E_{x,0}}{E_{z,0}}} = x_{2,\max}.$$

Equations (6.18) give the physical range of the values of x_1 and x_2 for difference resonances.

First case: the coefficients c_{2j} are zero. The above-mentioned limits are given in Table 3.

Table 3
Limits of the difference resonance curves

Top indices of c_2	Values of c_2 when			
	$x \geq 0$	$x \leq 1$	$x \geq 1$	$x \leq x_{\max}$
++	D_{11}	D_{10}	D_{10}	D_{22}
--	D_{11}	$-\infty$	$+\infty$	D_{22}
-+	D_{21}	$+\infty$	$-\infty$	D_{12}
--	D_{21}	D_{20}	D_{20}	D_{12}

The curves have the shapes given in Fig. 13 as following from Table 3.

In order to define a resonance characteristic similar to the one which has been introduced for the sum resonances, we will define a virtual bandwidth for difference resonances. Since the transverse amplitude is always limited, there is no actual stopband and this

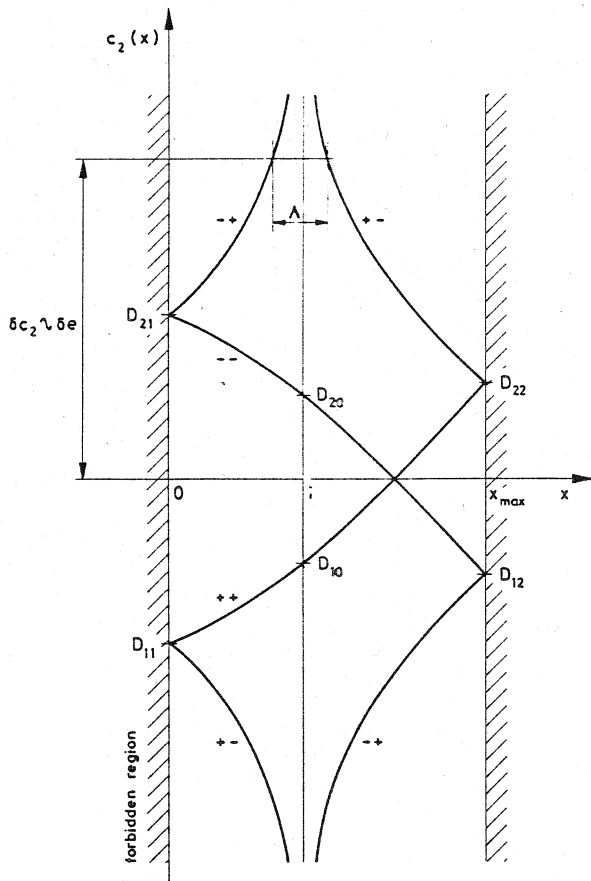


Fig. 13 Resonance curves for difference resonances

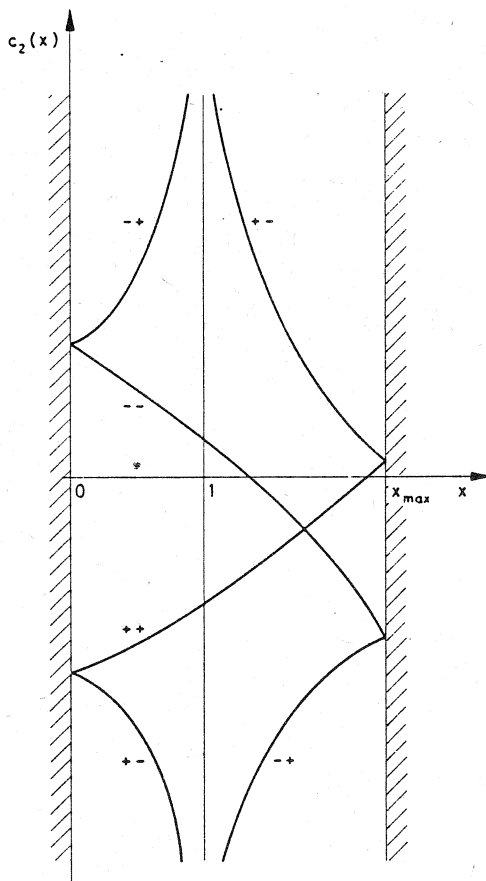


Fig. 14 Curves $c_2(x)$ for a difference resonance with $c_{2j} \neq 0$

virtual bandwidth defines a region where the extreme amplitudes $x = 0$ or $x = x_{\max}$ may be reached. By definition, the bandwidth will be the increment of e which corresponds to the average of the differences $D_{21} - D_{11}$ and $D_{22} - D_{12}$. By virtue of Eq. (6.11),

$$\Delta e = \frac{1}{2} k_{2N-1} r_0^{N-2} [c_2^{--}(0) - c_2^{++}(0) + c_2^{++}(x_{\max}) - c_2^{--}(x_{\max})]. \quad (6.19)$$

Calculating explicitly the limits in Eq. (6.19), i.e. the coefficients D_{lm} , and introducing the emittances (5.32), the expression for the bandwidth becomes

$$\Delta e = 2|\kappa| \left(\frac{R}{2\pi}\right)^{(N-2)/2} E_x^{(|n_x|-2)/2} E_z^{(|n_z|-2)/2} (|n_x|E_{z,0} + |n_z|E_{x,0}). \quad (6.20)$$

Second case: the coefficients c_4, c_6, \dots are different from zero. The finite values D_{lm} change and the resonance curves are bent up or down, but the shapes remain similar. An example of such resonance curves is given in Fig. 14.

6.4 Criterion concerning the distance of the working point from the resonance line⁸⁾

For all the sum and difference resonances, the bandwidth Δe gives a measure of their importance and thus makes it possible to compare different resonances.

This parameter also gives the possibility to formulate a criterion giving the distance of the working point (Q_x, Q_z) from the resonance line, which has to be maintained in order to prevent serious amplitude growth or beating of a single particle.

The resonance curves (Figs. 9 and 13) indeed show that the amplitude variation x is strictly limited by the curves c_2^{+-} and c_2^{-+} , if the distance δc_2 from the resonance is large enough. Having the analytical expressions for c_2^{+-} and c_2^{-+} [Eqs. (6.14)], it is not difficult to calculate the necessary distance δc_2 (i.e. δe) to limit either the relative amplitude growth or the relative amplitude beating in an interval Λ above or around one.

This criterion is for a sum resonance

$$\boxed{\delta e \geq \frac{\Delta e}{2} \left(1 + \frac{1}{\Lambda} \frac{n_x^2 E_{z,0} + n_z^2 E_{x,0}}{n_x^2 E_{z,0} + n_z^2 E_{x,0}} \right)}, \quad \begin{array}{l} n_x > 0 \\ n_z > 0 \end{array} \quad (6.21)$$

and for a difference resonance

$$\boxed{\delta e \geq \frac{\Delta e}{2} \frac{1}{\Lambda}}. \quad (6.22)$$

Note: In the preceding analysis, we assumed that c_2 had a given constant value and we determined via the resonance curves if the amplitudes were limited or not. It may now be interesting to study what happens when c_2 varies with time. On top of this, it may happen that the excitation of the resonance (κ) varies explicitly with time (not only via the azimuth θ). This will be considered in the next section.

7. AMPLITUDE VARIATIONS IN SYSTEMS WITH CHANGING PARAMETERS

So far, the parameters characterizing the system and the perturbation have been assumed to be constant in time. In reality, there will be variations due to the energy oscillations of the particles connected with the acceleration mechanism, the changes in the guiding field, and momentum diffusion processes. With these energy oscillations are associated *tune variations* and we can now imagine that particles are moving along the vertical coordinate c_2 ($\sim e$) of the resonance curves (Figs. 9 and 13). These changes of c_2 (of the tunes) mean that the particles may cross the stopbands of *sum resonances*. Let us try to see what are the effects of these crossings.

These effects depend on the speed of the tune variations. If the rate of change of the distance from the resonance e is small with respect to the period a particle takes to complete its phase-plane cycle [Eqs. (5.33)], the change is quasi-static or adiabatic and the particles remain "trapped" in the resonance¹⁴⁾, i.e. $d\psi/d\theta = 0$ with $\sin \psi = 1$. On the contrary, a sudden jump of e , within a time which is small compared to the cycle period, is non-adiabatic and the particles are not "trapped", i.e. their amplitude changes are not very large.

The limiting speed for a resonance traversal is defined as the speed of the tune variation, below which the particles are locked in the resonance. Analytical expressions of this limiting speed for two-dimensional resonances exist¹⁴⁾, and give the limit between adiabatic and non-adiabatic tune changes.

7.1 Non-adiabatic change of the parameters^{8,11,14)}

In the case of a single rapid (*i.e.* non-adiabatic) crossing of a sum resonance, the blow-up in amplitude can be calculated from the equations of motion (5.33). Looking, for instance, at the horizontal motion, we obtain from Eqs. (5.33)

$$\frac{dr_1}{d\theta} = n_x |\kappa| r_1^{(|n_x|-1)} r_2^{|n_z|} \sin \psi, \quad n_x \neq 0. \quad (7.1)$$

The first invariant is used in order to eliminate r_2 , the bandwidth Δe [Eq. (6.17)] is introduced to replace κ and x_1 is used to represent the relative horizontal amplitude $x_1 = r_1/r_{1,0}$. Hence, the equation (7.1) becomes

$$\left(\frac{n_x E_{z,0}}{n_z E_{x,0}} \right)^{n_z/2} \frac{dx_1}{\left(\frac{n_x E_{z,0}}{n_z E_{x,0}} - 1 + x_1^2 \right)^{n_z/2} x_1^{(n_x-1)}} = \frac{\Delta e}{\left(n_x + \frac{n_z^2 E_{x,0}}{n_x E_{z,0}} \right) \times 2} \sin \psi d\theta. \quad (7.2)$$

The left-hand side of Eq. (7.2) can always be integrated. Explicit expressions of these integrals and recurrence relations are given in Ref. 11.

Assuming that the variation of ψ with θ is due to the tune changes, the integral of the right-hand side of Eq. (7.2) can be estimated. Because of the oscillating character of the integrand the main contribution to this integral comes from the neighbourhood of the point where $\psi' = 0$. In this neighbourhood, ψ may be approximated by

$$\psi \approx \psi_1 + \frac{1}{2} \psi''_1 (\theta - \theta_1)^2. \quad (7.3)$$

Putting expression (7.3) into Eq. (7.2) gives Fresnel's integrals. These integrals approach their asymptotic values as the limits are infinite, that is as θ passes from a point a long way from the resonance on one side to a far-distant point on the other side. Assuming that these conditions are satisfied, the integral of $\sin \psi$ is

$$\int_{-\infty}^{+\infty} \sin \psi d\theta = \sqrt{\frac{2\pi}{|\psi''_1|}} \sin \left(\psi_1 \pm \frac{\pi}{4} \right) \leq \sqrt{\frac{2\pi}{\left| \frac{d\psi}{d\theta} \right|} \times 2}. \quad (7.4)$$

複号 : $\psi''_1 > 0$ +
 $\psi''_1 < 0$ -

The extreme right-hand side of Eqs. (7.4) has been obtained by using the inequality $\sin(\psi_1 \pm \pi/4) \leq 1$ and the definition of ψ given below the equation (5.33).

Taking into account the expressions (7.2) and (7.4) and using de/dt instead of $de/d\theta$, the maximum horizontal amplitude growth due to one rapid traversal of a sum resonance is

$$\left(\frac{n_x E_{z,0}}{n_z E_{x,0}} \right)^{n_z/2} \int_1^{x_1} \frac{dx_1}{\left(\frac{n_x E_{z,0}}{n_z E_{x,0}} - 1 + x_1^2 \right)^{n_z/2} x_1^{(n_x-1)}} = \frac{\Delta e}{n_x + \frac{n_z^2 E_{x,0}}{n_x E_{z,0}} \sqrt{2R}} \frac{\sqrt{\pi \beta c}}{\sqrt{|de/dt|}} \quad (7.5)$$

$n_x \neq 0$

The maximum vertical amplitude growth is obtained by exchanging the indices x and z in Eq. (7.5) and by replacing x_1 with x_2 (assuming $n_z \neq 0$).

For one-dimensional resonances, Eq. (7.5) can be explicitly integrated in a simple way ($n_z = 0$, $n_x = N$, $x_1 = x$),

$$\left. \begin{array}{l} N = 1 \quad x - 1 \\ N = 2 \quad \ln x \\ N > 2 \quad \frac{1 - x^{(2-N)}}{N - 2} \end{array} \right\} = \frac{\Delta e}{N} \frac{\sqrt{\pi \beta c}}{\sqrt{2R}} \frac{1}{\left| \frac{de}{dt} \right|^{\frac{1}{2}}} \quad (7.6)$$

Equations (7.6) give simple expressions for the amplitude growth, which have frequently been used¹²⁾.

This treatment applies, for instance, to the particles which are accelerated in a synchrotron. The particles are indeed grouped in bunches and have energy oscillations inside these bunches, while the average energy of all the particles increases slowly during the acceleration. The bunches may traverse the region of a sum resonance because of this slow drift in momentum, and the individual particles then quickly cross the resonance many times because of the energy oscillations. Thus we can have many traversals and Eq. (7.5) gives the maximum possible blow-up for each of them. Since the phase ψ_1 [Eq. (7.3)] is random for each single crossing, the average of the amplitude growth will be $\sqrt{n_R/2}$ times the value given by Eq. (7.5), in the case of n_R crossings. $\sqrt{n_R}$ simply comes from the fact that each contribution adds quadratically, while $1/\sqrt{2}$ is the square root of the average of $\sin^2(\psi_1 \pm \pi/4)$, which comes from Eqs. (7.4).

7.2 Adiabatic change of the parameters^{15,16)}

For an adiabatic change of the parameters, it is useful to consider the phase-plane topology in the vicinity of a resonance (e.g. the resonance of order 4 with $k_4 \neq 0$ of Fig. 6). If the passage through the resonance is in the appropriate direction, stable islands will

appear and begin to move outwards to regions of larger amplitude as the tunes (and hence k_2) change. As these islands move outwards, they also grow in phase-space area. Under adiabatic conditions, particles can stream into these islands through the regions around the unstable fixed points, since these are intrinsically non-adiabatic regions. Hence, the moving islands can trap particles in their migration. Since they are growing, the particles are transported towards larger amplitudes until they are deposited on the boundary walls and are lost.

This mechanism is also apparent when looking at the resonance curves, for example the curves which are associated with a similar resonance of order 4 (Fig. 11). If c_2 goes adiabatically from negative values to positive values, the particles cross the resonance region until they reach the minimum of the curve c_2^{+-} . At this point, particles with a small amplitude will remain stable, x being restricted by the curve c_2^{+-} , while other particles with larger amplitudes will start to diffuse inside the interval defined by the curves c_2^{--} and c_2^{++} until they reach the boundary walls. This mechanism shows that *particles can reach large amplitudes even if their amplitudes appear to be always limited in a static system*.

If we cross the resonance in the other direction, particles can never reach large amplitudes and in fact their amplitudes are even decreasing when we move off the resonance (Fig. 11).

This migration process involves a population of particles (not a single particle any more) and can be formally described by a trapping efficiency, which is simply the fraction of particles trapped during a single resonance passage.

The evaluation of the trapping efficiency has been considered for one-dimensional resonances¹⁵⁾ (e.g. $n_x = N$, $n_z = 0$). It will depend on the rate of change of the tune, on the distribution of the particle amplitude r_1 , and on the resonance characteristic, i.e. the bandwidth. Three points are relevant in this evaluation:

- i) Since the unstable fixed points move outwards and their radial position grows (Fig. 6), the amplitude of the particles which may be trapped in the islands has to be large enough for growing at least with the same rate. This minimum amplitude can be estimated for a resonance of order N

$$r_{1,\min} = r_{1,\text{rms}} \sqrt{2} \left[\frac{2\pi \left| \frac{de}{dt} \right|}{\beta c \Delta e h_{2200}^{(4)} E_{x,\text{rms}}} \right]^{1/N} \quad (7.7)$$

where $h_{2200}^{(4)}$ is the first non-linear detuning term which appears in the second Eq. (5.34), $E_{x,\text{rms}}$ is the r.m.s. horizontal beam emittance (5.32) and Δe is the bandwidth of the resonance (6.17). de/dt depends on the rate of change of the tune [Eq. (5.25)].

- ii) The distribution of particle amplitude is not far from a Gaussian. Taking a Gaussian, the number of particles, which have an amplitude larger than the necessary minimum $r_{1,\min}$ (7.7), is proportional to

$$e^{-\gamma}, \quad \text{with } \gamma = \frac{1}{2} \left(\frac{r_{1,\min}}{r_{1,\text{rms}}} \right)^2. \quad (7.8)$$

- iii) The trapping efficiency for those particles which have large enough amplitude can be approximated by the area of the moving islands (relative to the beam area) at the time when these islands are emerging from the beam. If the island area is taken at the amplitude corresponding to one r.m.s. beam emittance this ratio is proportional to

$$\alpha = \sqrt{\frac{\pi \Delta e}{h_{2200}^{(4)} N R E_{x,rms}}} . \quad (7.9)$$

Putting these three results together with the correct factor of proportionality gives the trapping probability in a one-dimensional resonance of order N

$$P_T = \frac{\sqrt{2}\pi}{\sqrt{N}} \alpha e^{-\gamma} \quad (7.10)$$

α and γ being defined by Eqs. (7.7), (7.8) and (7.9).

To produce beam loss from the trapping mechanism, there must be a process which causes the tune to vary with time. Since this variation has to be adiabatic, we will consider momentum diffusion, with a diffusion constant D_p

$$D_p = \frac{d}{dt} \left(\frac{\Delta p}{p} \right)_{rms}^2 . \quad (7.11)$$

Through the machine chromaticity Q' , this momentum diffusion translates into tune diffusion. The tune diffusion constant arising from this is described by

$$D_Q = (Q')^2 D_p . \quad (7.12)$$

The trapped particles moving outwards inside the stable islands will be lost against the aperture at a certain tune distance δQ from the resonance. δQ is the tune change which causes the island centre to reach the aperture limit and it can be approximated by the non-linear detuning at the aperture

$$\delta Q = h_{2200}^{(4)} \frac{R}{2\pi} E_{x,ap} \quad (7.13)$$

where $E_{x,ap}$ is the horizontal emittance [Eq. (5.32)] corresponding to the aperture amplitude.

For a Gaussian amplitude distribution, but a uniform tune density, the fractional loss rate at time T is¹⁶⁾

$$\frac{\dot{N}_p}{N_p} = - \frac{2P_T}{\Delta Q} \sqrt{\frac{D_Q}{\pi T}} e^{-\delta Q^2/4D_Q T} , \quad (7.14)$$

where N_p is the total number of particles in the beam and ΔQ is the total tune spread in the beam.

The function (7.14) has a maximum so that the *maximum percentage loss rate* can be estimated to be

$$\left(\frac{\dot{N}_p}{N_p} \right)_{\max} \approx - \frac{P_T D_Q}{\Delta Q \delta Q} . \quad (7.15)$$

The four parameters, which are necessary for estimating the loss rate, are all expressed in terms of bandwidth, stabilizing coefficient, emittance, chromaticity and rate of tune change [see the relations (7.7) to (7.13)].

This treatment applies, for instance, to the particles which are stacked in storage rings. Basically, the particles have a constant momentum and the problem is static. But, there are momentum diffusion processes, which are due to the intra-beam scattering and to the beam-residual gas scattering. Hence, the particle tunes may diffuse ($Q' \neq 0$) and particles on each side of a non-linear resonance may be brought into the resonance. Their amplitude then grows slowly and they are finally lost on the walls.

7.3 Change of the parameters and of the perturbation

The perturbation, i.e. the potentials \vec{A} and ϕ of Eq. (5.13) can vary explicitly with time. In this case, the perturbing Hamiltonian of order N , i.e. $H_1^{(N)}$ [Eq. (5.14)], depends on time. It is interesting to study the situation where $H_1^{(N)}$ has the following form

$$H_1^{(N)} = f(t) \sum_{\substack{J,K,L,M=0 \\ J+K+L+M=N}}^N b_{JKLM}^{(N)} x^J p_x^K z^L p_z^M . \quad (7.16)$$

Following Section 5.2, the Hamiltonian H_1 takes the form

$$U(a_n, \theta, t) = f(t) \sum_N \sum_{j,k,\ell,m} \sum_{q=-\infty}^{\infty} h_{jk\ell m q}^{(N)} a_1^j \bar{a}_1^k a_2^\ell \bar{a}_2^m \exp \left\{ i \left[(j-k)Q_x + (\ell-m)Q_z + q \right] \theta \right\} . \quad (7.17)$$

Before restricting the Hamiltonian to its low-frequency part, it is now necessary to analyse the function $f(t)$ in a Fourier series and this is done below

$$f(t) = \sum_{b=-\infty}^{+\infty} f_b e^{-ib(2\pi/T)t} , \quad (7.18)$$

with

$$f_b = \frac{1}{T} \int_0^T f(t) e^{ib(2\pi/T)t} dt .$$

T is the period of the variation of the perturbation and f_b are the Fourier coefficients of the function $f(t)$.

In the expression (7.17) of the Hamiltonian, there are two independent variables t and θ . In order to keep only one of them, we can use θ instead of t in the relations (7.18). The ratio θ/t is equal to the angular revolution frequency Ω_{rev} , so that

$$t = \frac{\theta}{\Omega_{\text{rev}}} = \frac{R\theta}{\beta c} . \quad (7.19)$$

Introducing the angular frequency of the perturbation $\Omega_{\text{per}} = 2\pi/T$ instead of the period T and using Eqs. (7.19) gives for Eq. (7.18)

$$f(t) = \sum_{b=-\infty}^{+\infty} f_b \exp \left[-ib \frac{\Omega_{\text{per}}}{\Omega_{\text{rev}}} \theta \right] \quad (7.20)$$

with

$$f_b = \frac{1}{2\pi} \int_0^{2\pi} f(\zeta) e^{+ib\zeta} d\zeta ,$$

where ζ is a variable of integration such that $\zeta = \Omega_{\text{per}} t$.

Combining Eqs. (7.17) and (7.20) gives for the Hamiltonian

$$U(a_n, \theta) = \sum_N \sum_{j,k,\ell,m} \sum_{b,q=-\infty}^{+\infty} h_{jk\ell m q}^{(N)} f_b a_1^j \bar{a}_1^k a_2^\ell \bar{a}_2^m \exp \left\{ i \left[(j-k)Q_x + (\ell-m)Q_z + q - b \frac{\Omega_{\text{per}}}{\Omega_{\text{rev}}} \right] \theta \right\} . \quad (7.21)$$

Equation (7.21) shows that the low-frequency part of U , associated with a time-varying perturbation, includes the terms with

$$\boxed{j = k, \quad \ell = m, \quad q = 0, \quad b = 0} , \quad (7.22)$$

and the terms describing resonances

$$\boxed{n_x Q_x + n_z Q_z - p - b \frac{\Omega_{\text{per}}}{\Omega_{\text{rev}}} = 0} . \quad (7.23)$$

This is the resonance condition in the presence of a variable perturbation. The corresponding excitation coefficient, κ , comes directly from the expression of U (7.21)

$$\kappa = f_b h_{jk\ell m q}^{(N)} , \quad (7.24)$$

and the stabilizing coefficients are

$$h_{qqss}^{(2v)} f_0 , \quad (7.25)$$

f_0 and f_b being defined by Eqs. (7.20).

The bandwidth of the resonances characterized by Eq. (7.23) arises from Eqs. (6.17) and (6.20) in which the expression (7.24) for κ is introduced. Once the bandwidth is defined, all the relations which have been established in Sections 7.1 and 7.2 apply. Hence, if the parameters of the system change either abruptly or adiabatically in the presence of a time-varying perturbation, the relations (7.5) (for amplitude growth) and (7.15) (for percentage loss rate) apply respectively, provided that the sum resonance bandwidth be taken equal to

$$\Delta\omega = 2 f_b h_{jk\ell m}^{(N)} \left(\frac{R}{2\pi}\right)^{(N-2)/2} E_{x,0}^{(n_x-2)/2} E_{z,0}^{(n_z-2)/2} \left(n_x^2 E_{z,0} + n_z^2 E_{x,0}\right) . \quad (7.26)$$

8. APPLICATIONS TO DIFFERENT SOURCES OF PERTURBATION

In all the following applications, the excitation coefficient κ and the bandwidth $\Delta\omega$ are calculated. Therefore, an explicit expression of the coefficients $h_{jk\ell m-p}^{(N)}$ is necessary. The way to get this is given in Section 5.2. When the perturbing Hamiltonian has the form given in Eq. (5.14), these coefficients become, in agreement with Eq. (5.16):

$$\begin{aligned} h_{jk\ell m-p}^{(N)} &= \sum_{J,K,L,M} \sum_{k'=0}^J \binom{J}{k'} \sum_{m'=0}^L \binom{L}{m'} \sum_{k''=0}^K \sum_{m''=0}^M \binom{K}{k''} \binom{M}{m''} \times \\ &\times \frac{1}{2\pi} \int_0^{2\pi} \left[\left(-\frac{R\alpha_x}{\beta_x} + i \frac{R}{\beta_x} \right)^{(K-k'')} \left(-\frac{R\alpha_x}{\beta_x} - i \frac{R}{\beta_x} \right)^{k''} \left(-\frac{R\alpha_z}{\beta_z} + i \frac{R}{\beta_z} \right)^{(M-m'')} \left(-\frac{R\alpha_z}{\beta_z} - i \frac{R}{\beta_z} \right)^{m''} \right] \times \\ &\times \sqrt{\frac{\beta_x}{2R}}^{-(j+k)} \sqrt{\frac{\beta_z}{2R}}^{-(\ell+m)} b_{JKLM}^{(N)} e^{i(\mu_x - Q_x \theta)(j-k)} e^{i(\mu_z - Q_z \theta)(\ell-m)} e^{ip\theta} d\theta , \end{aligned} \quad (8.1)$$

with the complementary relations

$$\begin{aligned} k' + k'' &= k, & m' + m'' &= m , \\ j + k &= J + K, & \ell + m &= L + M , \end{aligned}$$

and with the definition

$$\binom{J}{k'} = \frac{J!}{(J-k')!k'!} .$$

Equation (8.1) gives the stabilizing coefficients if the indices of h satisfy the relations (5.20), and the excitation coefficient which is predominant for a single resonance if the indices of h satisfy the relations (5.23).

8.1 Magnetic defects in the machine hardware

We have seen in the Introduction that transverse dipole and quadrupole magnetic fields are necessary in order to maintain a stable circulating beam. These fields may not be perfect and the components of the imperfections are mainly transverse ($B_\theta = 0$). These imperfections are described by a potential vector \vec{A} which has only the longitudinal component A_θ different from zero. Since A_θ can be written in a polynomial series, we obtain for the potential vector \vec{A} :

$$A_x = A_z = 0$$

$$A_\theta = - \frac{cB\varrho}{R^2} \sum_{\substack{k_1, k_2 \\ k_1+k_2=N}} \frac{1}{N!} \binom{N}{k_2} x^{k_1} z^{k_2} \begin{cases} (-1)^{k_2/2} K_z^{(N-1)} & \text{if } k_2 \text{ even} \\ (-1)^{(k_2+1)/2} K_x^{(N-1)} & \text{if } k_2 \text{ odd} \end{cases} \quad (8.2)$$

Equation (8.2) gives the well-known multipole analysis and the field components are given by Maxwell's equation $\vec{B} = \nabla \times \vec{A}$. Consequently, the parameters $K_z^{(N-1)}$ and $K_x^{(N-1)}$ are related to the field derivatives

$$K_z^{(N-1)} = \frac{R^2}{|B\varrho|} \frac{\partial^{(N-1)} B_z}{\partial x^{(N-1)}} \quad (8.3)$$

$$K_x^{(N-1)} = \frac{R^2}{|B\varrho|} \frac{\partial^{(N-1)} B_x}{\partial x^{(N-1)}}.$$

On the one hand, the coefficient $K_z^{(N-1)}$ is associated with right 2N-pole elements, where the angle between one pole axis and the horizontal axis is equal to $\pi/2N$. On the other hand, the coefficient $K_x^{(N-1)}$ is associated with skewed 2N-pole elements, where the above-defined angle is equal to zero. Illustrations of such elements are given in Fig. 15.

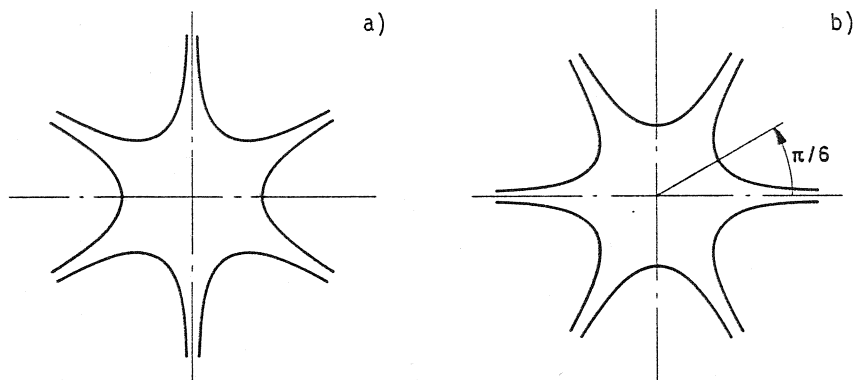


Fig. 15 Examples of skew (a) and right (b) multipoles

Putting the potential vector (8.2) in the expression (5.13), the perturbing Hamiltonian H_1 may be written

$$H_1 = \sum_{N} \sum_{\substack{J, L=0 \\ J+L=N}}^N b_{JOL0}^{(N)} x^J z^L \quad (8.4)$$

with

$$b_{JOL0}^{(N)} = \frac{1}{N!} \binom{N}{L} \begin{cases} (-1)^{(L+2)/2} K_z^{(N-1)} & \text{if } L \text{ even} \\ (-1)^{(L-1)/2} K_x^{(N-1)} & \text{if } L \text{ odd} \end{cases}$$

The next step consists of introducing the appropriate coefficients $b_{JOL0}^{(N)}$ [Eq. (8.4)] in the expression (8.1). Assuming at first that the indices j, k, l, m , and p of Eq. (8.1) satisfy the relations (5.20), we get the stabilizing coefficients

$$h_{qqss 0}^{(2v)} = \frac{(-1)^{s+1}}{2\pi(2R)^v (q!s!)^2} \int_0^{2\pi} \beta_x^q \beta_z^s K_z^{(2v-1)} d\theta, \quad (8.5)$$

where $q + s = v$, $v \leq N/2$. Assuming then that the indices j, k, l, m , and p of Eq. (8.1) satisfy the relations (5.23), we get the excitation coefficient of the resonance (5.21)

$$\kappa = \frac{1}{2\pi(2R)^{(N/2)} |n_x|! |n_z|!} \int_0^{2\pi} d\theta \beta_x^{|n_x|/2} \beta_z^{|n_z|/2} \times$$

$$\times \exp \left\{ i \left[n_x u_x + n_z u_z - (n_x Q_x + n_z Q_z - p) \theta \right] \right\} \begin{cases} (-1)^{(|n_z|+2)/2} K_z^{(N-1)} & \text{for } n_z \text{ even} \\ (-1)^{(|n_z|-1)/2} K_x^{(N-1)} & \text{for } n_z \text{ odd} \end{cases} \quad (8.6)$$

Having these coefficients, we can apply the whole treatment which has been carried out in the preceding sections: invariant analysis, bandwidth calculation, estimation of the amplitude variations.

The most important coefficient κ , which is the driving term of the resonance, gives indications on how to compensate a resonance due to magnetic defects:

- i) Use $2N$ -pole elements; right ones if n_z is even and skew ones if n_z is odd.
- ii) Choose the positions of the elements in such a way that $\beta_x^{|n_x|/2} \beta_z^{|n_z|/2}$ is large, in order to minimize the necessary field.

- iii) One type of multipole excites all the corresponding resonances with the same parity in n_z . Hence, it is useful to use a few identical elements placed in a way that the phase difference between them is π for one resonance and 2π for the next one (the phase difference is $n_x \Delta \mu_x + n_z \Delta \mu_z$). Consequently, the effects will be self-compensating on one resonance, while they will be accumulative on the other.

Such schemes have been studied in the ISR¹⁷⁾, where four sextupoles and four octupoles have been installed for the compensation of third- and fourth-order resonances. These lenses are orientable around their axis to provide both right and skew elements. The main characteristics of these lenses and their disposition in the rings are shown in Fig. 16. Looking at the phase shifts, the advantages of using them in pairs are obvious: no detuning, a minimum of α_y and β_y distortion, a complete decoupling between the compensations of third- and fourth-order resonances (the two opposite sextupole components which are encountered by off-centred particles in an octupole pair are dephased by 26π in θ , which means that they have no effect on the third-order resonances).

These elements have been used for measuring the strength of the resonances in the ISR. The influence of the machine hardware is studied using small bunched beams which are displaced slowly across the aperture by the RF system. Crossing a resonance produces a blow-up and an intensity loss if the aperture is sufficiently limited. This loss generally depends upon the direction of the beam displacement, because of the stabilizing terms which create an asymmetry in the resonance curves (Fig. 11). The loss disappears when the resonance is compensated by means of multipole elements. Knowing the positions and the strengths of the lenses when the compensation is achieved, Eqs. (8.3) and (8.6) give K_x , K_z , and κ , from which the bandwidth (6.17) is deduced. For example, the losses resulting from aperture

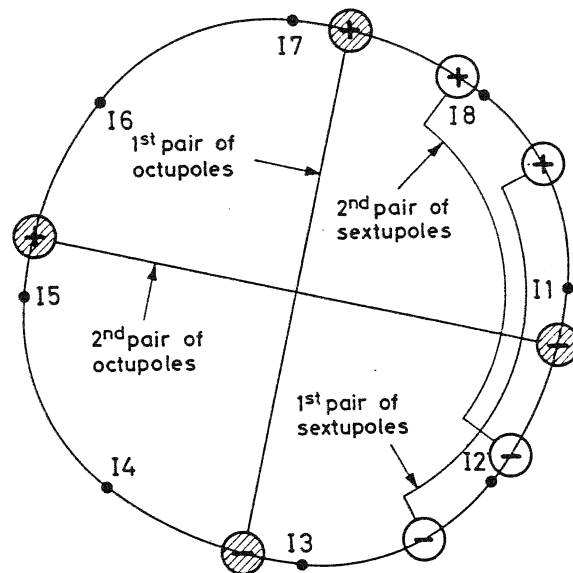


Fig. 16 Sextupoles ($G'L_{\max} = 22.8 \text{ Tm}^{-1}$) and octupoles ($G''L_{\max} = 522 \text{ Tm}^{-2}$) for the compensation of third- and fourth-order resonances in the ISR

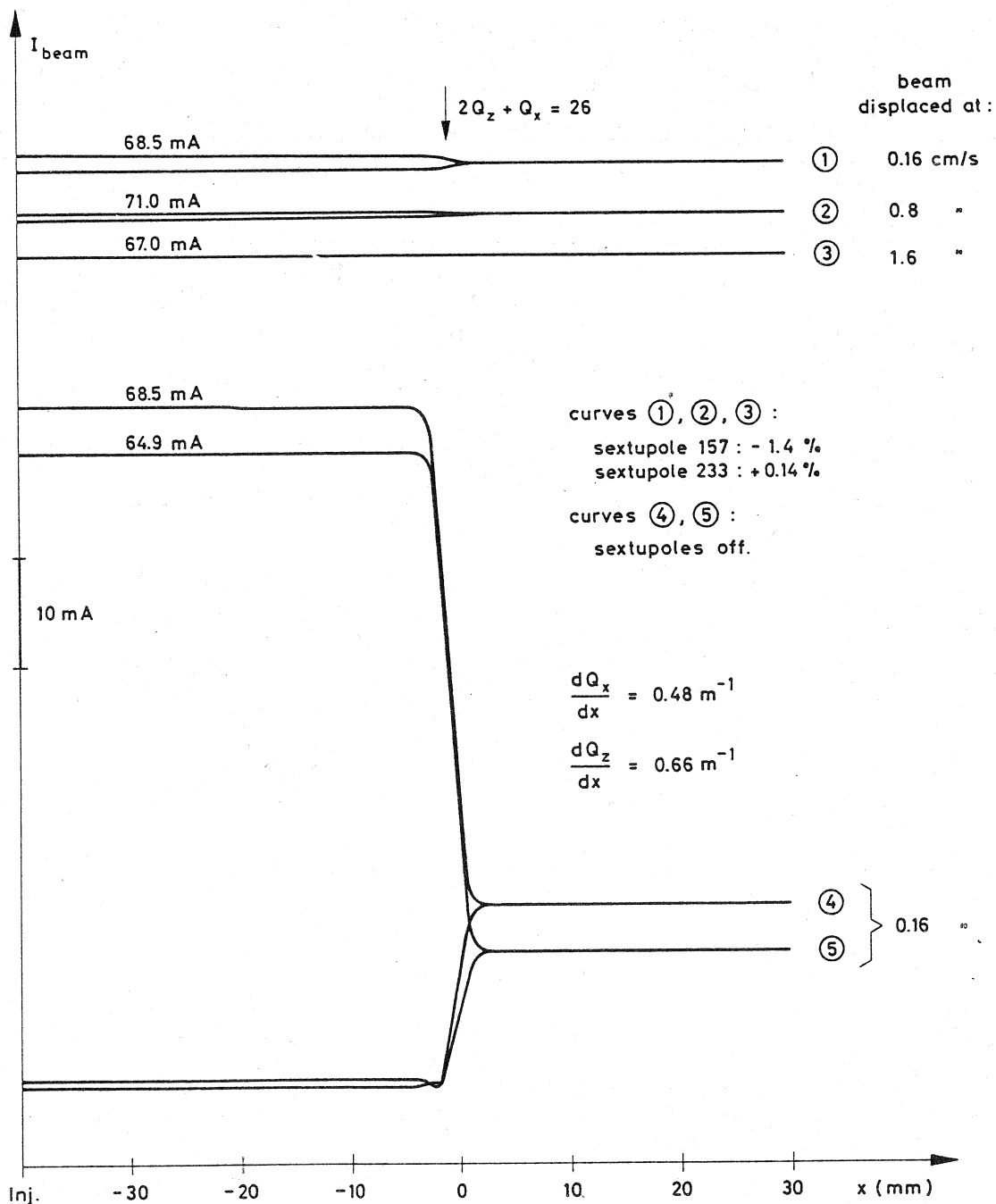


Fig. 17 Losses measured in the ISR for the resonance $2Q_z + Q_x = 26$, excited by hardware magnetic defects

scans done in the presence and the absence of compensation of the resonance $2Q_z + Q_x = 26$ are represented in Fig. 17. The compensation reduces the beam loss, when crossing the resonance at the speed of 0.16 cm/s, by a factor 90 (curves 1 and 4 of Fig. 17).

The results obtained by this method in the ISR¹⁷⁾ are summarized in Table 4 for defects in the machine hardware.

Table 4

Resonance excitation produced by the machine hardware
for different beam momenta p , in the ISR

p (GeV/c)	Resonances	Bandwidths $\Delta\epsilon$	Magnetic defects
11	$2Q_z + Q_x = 26$	450×10^{-6}	$\left\langle \frac{\partial^2 B_z}{\partial x^2} \right\rangle = 0.021 \text{ Tm}^{-2}$
	$3Q_z = 26$	60×10^{-6}	$\left\langle \frac{\partial^2 B_x}{\partial x^2} \right\rangle = 0.0076 \text{ Tm}^{-2}$
15	$4Q_x = 35$	24 35×10^{-6}	$\left\langle \frac{\partial^3 B_z}{\partial x^3} \right\rangle = 1.9$ to 2.7 Tm^{-3}
	$3Q_x + Q_z = 35$	6.5×10^{-6}	$\left\langle \frac{\partial^3 B_x}{\partial x^3} \right\rangle = 0.3 \text{ Tm}^{-3}$
22	$4Q_x = 35$	6.3×10^{-6}	$\left\langle \frac{\partial^3 B_z}{\partial x^3} \right\rangle = 1.0 \text{ Tm}^{-3}$
26	$4Q_x = 35$	4.5×10^{-6}	$\left\langle \frac{\partial^3 B_z}{\partial x^3} \right\rangle = 1.0 \text{ Tm}^{-3}$

These values of $\Delta\epsilon$ (Table 4) are small as will be shown in the next section when comparing them with the bandwidths due to beam-beam effects. In other words, the resonance excitation produced by the machine hardware is not really harmful in the ISR, compared with the beam-beam resonance excitation.

8.2 Electromagnetic fields due to coasting beams crossing horizontally

When two coasting beams are crossing horizontally with an angle χ , a particle of beam 1 sees the electric field due to the charges sitting in beam 2 and the magnetic field associated with the motion of these charges¹⁸⁾. The electric and magnetic forces are proportional and this may easily be shown for a cylindrical beam. In that case, the field components are

$$\epsilon_a = \frac{\rho_a}{2\epsilon_0} a, \quad B_\phi = \frac{\mu_0 \rho_a}{2} v_s a, \quad (8.7)$$

where a and ϕ are local cylindrical coordinates. ρ_a is the radial charge distribution.

Using the identity $\epsilon_0 \mu_0 c^2 = 1$, the radial components of the forces can be written

$$F_a(\text{electr}) = \frac{e\beta}{2\epsilon_0} a$$

$$F_a(\text{magn}) = \frac{e\beta v_s^2}{2\epsilon_0 c^2} a = \beta^2 F_a(\text{electr}) \quad (8.8)$$

and the second equation (8.8) shows that the magnetic force seen by a particle is β^2 times the electric force. This final result holds for other beam sections and thus the total force is

$$F_{\text{tot}} = (1 + \beta^2) F(\text{electr}) \quad (8.9)$$

By virtue of Eq. (8.9), the perturbation of beam 2 may be described by a virtual electric potential equal to $(1 + \beta^2)\Phi$, where Φ is the actual electric potential. Hence, the perturbing Hamiltonian (5.13) for beam-beam interactions may be written

$$H_1 = (1 + \beta^2) \frac{R^2 \Phi}{\beta c |B\beta|} \quad (8.10)$$

The electric potential Φ can be developed into a power series as follows

$$\Phi = \sum_N \sum_{\substack{J, L=0 \\ J+L=N}}^N b_{J0L0}^{(N)} x^J z^L, \quad (8.11)$$

with

$$b_{J0L0}^{(N)} = \frac{1}{N!} \binom{N}{L} \frac{\partial^N \Phi}{\partial x^J \partial z^L}.$$

The introduction of the coefficients $b_{J0L0}^{(N)}$ in the expression (8.1) gives either the stabilizing coefficients or the excitation coefficient, depending on the choice of the indices j, k, l, m and p , as in Section 8.1,

$$h_{qqss0}^{(2v)} = \frac{(1 + \beta^2) R^2}{2\pi (2R)^v \beta c |B\beta| (q! s!)^2} \int_0^{2\pi} \beta_x^q \beta_z^s \frac{\partial^{(2v)} \Phi}{\partial x^{2q} \partial z^{2s}} d\theta$$

$$\kappa = \frac{(1 + \beta^2) R^2}{2\pi (2R)^{N/2} \beta c |B\beta| |n_x|! |n_z|!} \int_0^{2\pi} \beta_x^{|n_x|/2} \beta_z^{|n_z|/2} \frac{\partial^N \Phi}{\partial x^{|n_x|} \partial z^{|n_z|}} \times$$

$$\times \exp \left\{ i \left[n_x \mu_x + n_z \mu_z - (n_x Q_x + n_z Q_z - p) \theta \right] \right\} d\theta, \quad (8.12)$$

where $q + s = v$, $v \leq N/2$, and where the coefficient κ is associated with the resonance $n_x Q_x + n_z Q_z - p = 0$.

Since the particles of beam 1 see beam 2 at the crossing points only, the integrals (8.12) can be replaced by sums over the intersections. The functions u_y and β_y take then the values $u_{y,c.p.}$ and $\beta_{y,c.p.}$ of the crossing points (c.p.) and the interval of integration is taken equal to

$$\Delta\theta = \frac{\Delta s}{R} = \frac{w}{R \sin \chi}, \quad (8.13)$$

where w is the beam width.

The most important parameter κ [second Eq. (8.12)] is proportional to the partial derivative of order N of the electric potential Φ . This potential corresponds to a stack which is assumed to be a flat ribbon of width w , whose vertical distribution of charge is Gaussian

$$\rho_z = \rho_0 \exp\left(-\frac{z^2}{2\sigma_z^2}\right), \quad (8.14)$$

with

$$\rho_0 = \frac{1}{\sqrt{2\pi}\sigma_z w} \frac{I}{\beta c}.$$

σ_z is the r.m.s. vertical beam size and I is the total beam current.

In such a *one-dimensional model*, Poisson's equation

$$\operatorname{div} \vec{\epsilon} = \frac{\partial \epsilon_z}{\partial z} = \frac{\rho_z}{\epsilon_0} \quad (8.15)$$

gives the electric field at a distance z from the beam centre

$$\epsilon_z = \frac{\partial \Phi}{\partial z} = \frac{1}{2\epsilon_0 w} \frac{I}{\beta c} \operatorname{erf}\left(\frac{z}{\sqrt{2}\sigma_z}\right) \quad (8.16)$$

as well as the partial derivatives of the potential Φ for $N \geq 2$

$$\frac{\partial^N \Phi}{\partial z^N} = \frac{\partial^{N-1} \epsilon_z}{\partial z^{(N-1)}} = \frac{1}{\sqrt{2\pi}} \frac{\mu_0 c I}{\beta \sigma_z w} \frac{\partial^{(N-2)}}{\partial z^{(N-2)}} \exp\left(-\frac{z^2}{2\sigma_z^2}\right) \quad (8.17)$$

From this beam model, it turns out that only vertical resonances $NQ_z = p$ are excited by beam-beam interactions, when the beams are crossing horizontally with a finite angle χ . Using Eqs. (8.16) and (8.17) in the second expression (8.12) and then putting Eq. (8.12) in the relation (6.17) gives the *bandwidths of these one-dimensional resonances*

$$\Delta e (N = 1) = \left| \sum_{c.p.} \frac{\mu_0(1+\beta^2)}{4\pi\beta^2} \frac{I\beta_{z,c.p.}}{|B_0|\sigma_z \sin \chi} \operatorname{erf}\left(\frac{z}{\sqrt{2}\sigma_z}\right) \exp\left\{i[\mu_z - (Q_z - p)\theta]\right\} \right|$$

$$\Delta e (N \geq 2) = \left| \sum_{c.p.} \frac{\mu_0(1+\beta^2)N^2}{2\pi\sqrt{2\pi}\beta^2 N!} \frac{I\beta_{z,c.p.}}{|B_0|\sigma_z \sin \chi} \sigma_z^{(N-2)} \frac{\partial^{(N-2)}}{\partial z^{(N-2)}} \exp\left(-\frac{z^2}{2\sigma_z^2}\right) \exp\left\{i[N\mu_z - (NQ_z - p)\theta]\right\} \right|. \quad (8.18)$$

The sums of Eqs. (8.18) have to be done over the crossing points (c.p.) of the two beams and z is the distance of one particle in beam 1 from the centre of beam 2. The definition of Hermite polynomials opens up the possibility of simplifying the second expression (8.18)

$$\Delta e (N \geq 2) = \left| \sum_{c.p.} \frac{\mu_0(1+\beta^2)N^2}{\pi^{3/2}\sqrt{2}(N+1)\beta^2 N!} \frac{I\beta_{z,c.p.}}{|B_0|\sigma_z \sin \chi} \exp\left(-\frac{z^2}{2\sigma_z^2}\right) H_{N-2}\left(\frac{z}{\sqrt{2}\sigma_z}\right) \exp\left\{i[N\mu_z - (NQ_z - p)\theta]\right\} \right|. \quad (8.19)$$

The symbol $H_n(x)$ represents the Hermite polynomial of order n . These polynomials satisfy the following recursion formula

$$H_{n+1}(x) = 2xH_n(x) - 2nH_{n-1}(x) \quad (8.20)$$

with

$$H_0(x) = 1 \quad \text{and} \quad H_1(x) = 2x.$$

Equation (8.20) gives the possibility of numerical evaluations of the bandwidths (8.19).

For example, let us calculate the bandwidths of the vertical resonances which are excited in the ISR by only one crossing point (assuming large vertical beam separations in the other intersections). For this calculation, the following parameter values are used

$$I = 30 \text{ A}, \quad z = 0.2 \text{ mm},$$

$$\beta_{z,c.p.} = 14 \text{ m}, \quad \sigma_z = 1 \text{ mm}, \quad (8.21)$$

$$\chi = 14.77^\circ, \quad |B_0| = 88.7 \text{ Tm},$$

and the results are summarized in Table 5.

Table 5

Resonance excitation produced by beam-beam interactions
at one crossing point of the ISR

Resonance order N	1	2	3	4
Bandwidth $\Delta\epsilon$	5.9×10^{-4}	5.8×10^{-3}	8.7×10^{-4}	1.9×10^{-3}
Resonance order N	5	6	7	8
Bandwidth $\Delta\epsilon$	3.6×10^{-4}	4.0×10^{-4}	8.2×10^{-5}	6.1×10^{-5}

Comparing the bandwidths $\Delta\epsilon$ for $N = 4$ at the same energy, it can be seen that, in the ISR, beam-beam interactions at high current (Table 5) produce a resonance excitation 500 times larger than the hardware defects (Table 4).

These analytical results have been confirmed by the experiments in the ISR¹⁷⁾: only vertical resonances are actually excited by beam-beam effects and, in the aperture scans, beam losses appear on $5Q_z = 43$, $7Q_z = 60$ and $8Q_z = 69$ exclusively when a strong beam is present in the other ring. Examples of aperture scans are given in Fig. 18.

None of the working lines, which have been used in the ISR for beam stacking, crosses resonances of an order lower than 5. Consequently, the most harmful beam-beam resonance, which we have to look at, is the $5Q_z = 43$, as it is visible in Fig. 18. Let us try to apply the results of Section 7 to this specific resonance of the ISR, whose estimated bandwidth is given in Table 5.

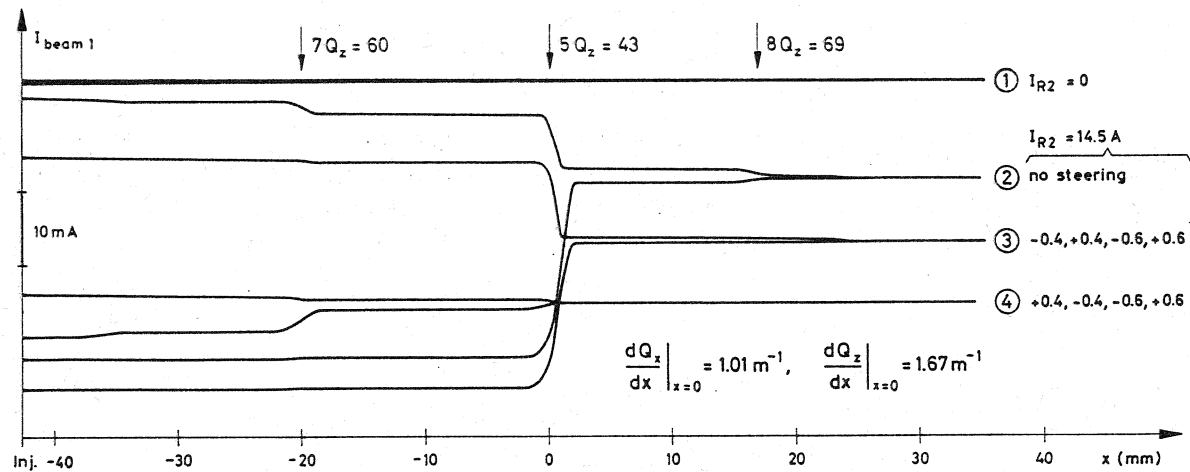


Fig. 18 Aperture scan with small 75 mA beams using the 5C26 working line. Vertical resonances are visible only when a beam of 14.5 A is present in the other ring (scans 2, 3, 4). The resonance $5Q_z = 43$ has been compensated by varying the beam separation by $+0.4$, -0.4 , -0.6 , $+0.6$ in intersections I4, I8, I2, I6, respectively (the values are indicated in this order in the figure).

When crossing this resonance with a bunched pulse, there is a blow-up of the type described in Section 7.1. With the accelerating system of the ISR, the rate of change of the distance ϵ from the resonance is of the order of 1 s^{-1} , for $N = 5$ and $R = 150 \text{ m}$, and none of the particles in the pulse crosses the resonance more than once. The maximum vertical amplitude growth (7.6) associated with the bandwidth given in Table 5 is thus

$$x_2 = 1.174 . \quad (8.22)$$

If we now assume that a stacked beam lies on a fifth-order resonance excited by the other beam, we can try to apply the theory for adiabatic changes of the parameters (Section 7.2). We have the following data for the ISR

$$h_{2200}^{(4)} E_{x,\text{rms}} \approx 2.3 \times 10^{-5} \text{ m}^{-1}, \quad N = 5$$

$$\Delta\epsilon = 3.6 \times 10^{-4}, \quad R = 150 \text{ m} .$$

The diffusion process, which causes the tune to vary, is the intra-beam scattering, since the residual gas scattering is negligible at the ISR pressure. This tune variation is so slow, that γ [Eq. (7.8)] will be small and thus $e^{-\gamma}$ close to one. Equations (7.9) and (7.10) give the trapping probability

$$P_T \approx 0.5 .$$

The diffusion constant (7.11) comes from the intra-beam scattering theory¹⁹⁾ and, for a 30 A beam at 26.59 GeV/c, its value is

$$D_p = 6.7 \times 10^{-11} \text{ s}^{-1} ,$$

which gives for the tune diffusion constant (7.12)

$$D_Q = 5.2 \times 10^{-10} \text{ s}^{-1}$$

when assuming $Q' \approx 2.8$ (which corresponds to the 5C line of Fig. 3).

The total tune spread measured inside an ISR beam is approximately 0.08 and the tune distance δQ as defined by Eq. (7.13) is 5.6×10^{-3} if $E_{x,\text{ap}}$ is assumed to be ten times larger than $E_{x,\text{rms}}$. Putting all these values into the expression (7.15) gives the maximum loss rate to be expected for a stack on a fifth-order resonance

$$\left(\frac{\dot{N}_p}{N_p}\right)_{\text{max}} \approx 5.8 \times 10^{-7} \text{ s}^{-1} \approx 35 \text{ ppm/min} . \quad (8.23)$$

Repeating the same calculation for a stack sitting on an eighth-order resonance, whose bandwidth is given in Table 5, we obtain a maximum loss rate equal to 6 ppm/min. These two loss rate figures show that the beam losses of a stack built on fifth-order resonances should be approximately six times higher than the losses of a stack built on eighth-order resonances.

It is interesting to compare these estimates with the loss rates actually observed in the ISR. Since the relation (7.15) is in fact independent of the beam current, the actual current can differ from the one used in the preceding calculation, whereas the vertical beam size and the energy have to be equal to the values of (8.21). Looking back at the loss rates recorded during an early stage of ISR operation, we found two runs satisfying these conditions. During the run 353, the stacks were built on the 5C working line (Fig. 3), which crosses fifth- and higher-order resonances, and the observed loss rates are shown in Fig. 19. The stacks of the run 418 were built on the more recent 8C working line (Fig. 3), which crosses only eighth- and higher-order resonances, and the observed loss rates are given in Fig. 20. In the case of each working line the best runs have been chosen for the comparison, since the assumptions taken for the numerical calculations are based on a relatively small perturbation corresponding to optimum conditions. In these cases, calculated and measured loss rates are in fairly good agreement.

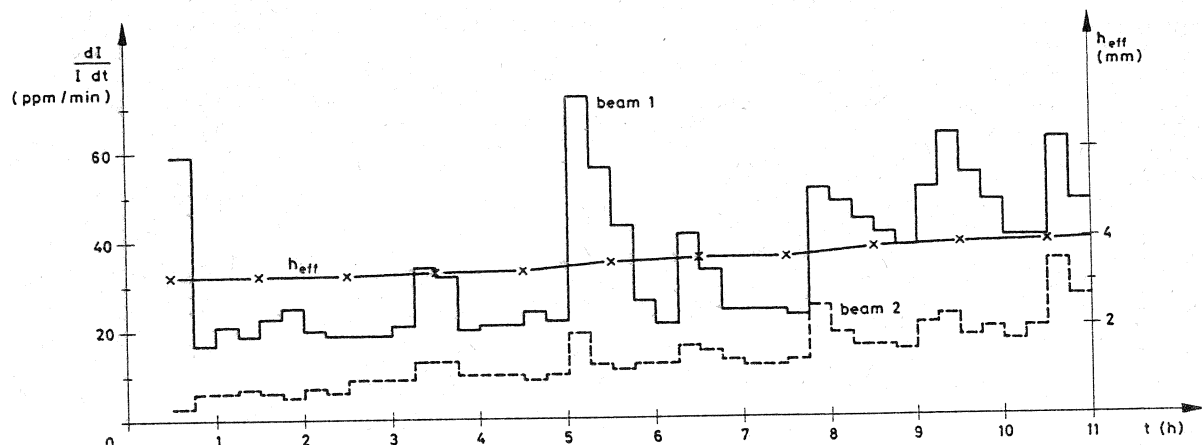


Fig. 19 Loss rates observed in the ISR run 353 with 8 A and 9 A stacks at 26 GeV/c (on the 5C line). The initial effective height ($h_{eff} = 2\sqrt{\pi}\sigma_z$) was 3.2 mm, and the vacuum pressure was between 2.5 and 3×10^{-11} Torr.

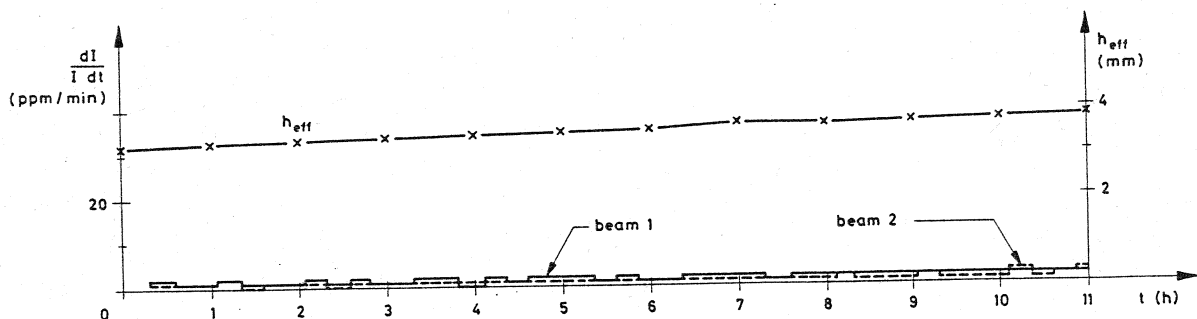


Fig. 20 Loss rates observed in the ISR run 418 with 10 A stacks at 26 GeV/c (on the 8C line). The initial effective height ($h_{eff} = 2\sqrt{\pi}\sigma_z$) was 3.2 mm, and the vacuum pressure was between 2 and 3.5×10^{-11} Torr.

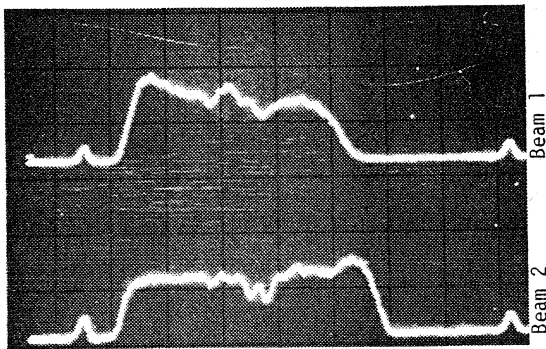


Fig. 21 Longitudinal Schottky scans of the ISR stacks of run 353 (on the 5C line)

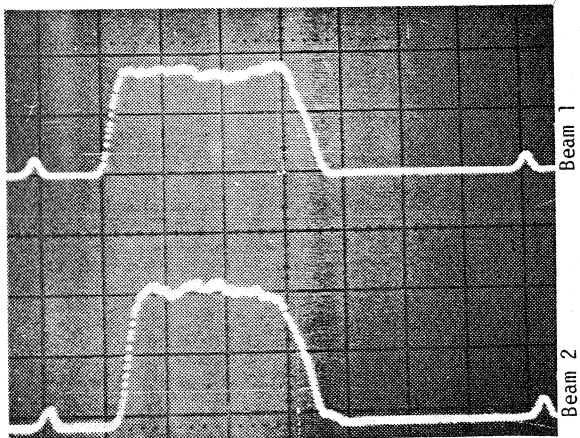


Fig. 22 Longitudinal Schottky scans of the ISR stacks of run 418 (on the 8C line)

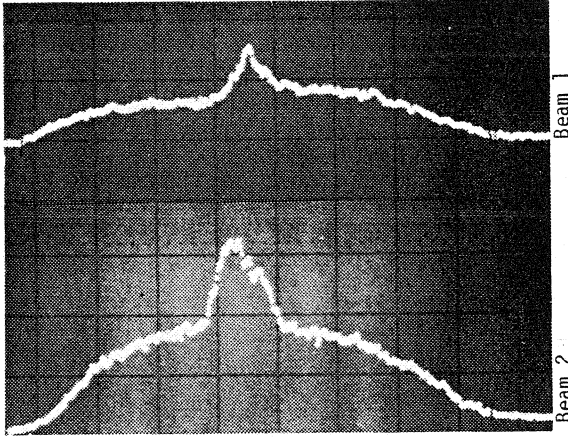


Fig. 23 Vertical Schottky scans of the ISR stacks of run 418, which are sitting on eighth-order resonances

This diffusion of the particles into resonances followed by beam losses may be revealed by Schottky scans. Figure 21 shows a longitudinal scan of the two beams of run 353. Holes due to particle losses appear at the place of the resonances. However, the longitudinal scans (Fig. 22) of run 418 do not show any significant holes since the eighth-order resonances are much weaker. Nevertheless, the transverse scans (Fig. 23) of this run show the growth of vertical amplitudes due to resonances.

High backgrounds in the physics experiments may appear with loss rates of the order of 35 ppm/min [Eq. (8.23)]. This is the reason why, in the more recent ISR runs, the 5C line has been disregarded for physics and only working lines whose stacking regions cross resonances of an order higher or equal to eight have been used (e.g. 8C and ELSA lines of Fig. 3).

8.3 Two-beam overlap knock-out

Two-beam overlap knock-out arises from an overlap between synchrotron frequencies in a bunched beam and the betatron frequencies in a coasting beam. This effect may appear in storage rings, when a bunched beam in one ring interacts with a stack in the other ring. The coupling forces are non-linear, since they are produced by the beam-beam interaction.

We will treat neither the effect of bunches acting on a particle travelling in the same ring, nor the effect of empty buckets in one ring acting on a particle travelling in the other ring. We will only consider the effect of bunches in ring 1 acting on a particle travelling in ring 2. As mentioned in Section 8.2, the particle sees the electromagnetic fields of the bunched beam at the crossing points. Hence, the electric potential Φ [Eq. (8.11)] can be used again and estimated for the one-dimensional beam model described in Section 8.2. In agreement with Eqs. (8.16) and (8.17), the perturbing terms are proportional to the current I of the bunched beam. Since this current is distributed inside the bunches and since the revolution frequency of the bunches may differ from the revolution frequency of the perturbed beam, the particle will see an "effective" current which varies with the time. Therefore, we are exactly in the situation which is described in Section 7.3, where the perturbation varies with time, i.e.

$$I(t) = f(t) I_0 \quad (8.24)$$

where I_0 is the average current in one bunch.

This means that the results of Section 7.3 apply directly to the overlap knock-out. The resonance condition is thus given by Eq. (7.23), while the excitation coefficient is given by Eq. (7.24). In this equation, $h_{jklm}^{(N)}$ has to be equal to the coefficient κ defined in Eqs. (8.12) for two coasting beams, and f_b are the harmonic coefficients of the bunches.

The geometry for two-beam overlap knock-out is sketched in Fig. 24, where θ as before is the independent variable for the perturbed particle, and ζ is a variable associated with the bunches, which is identical to the ζ that was introduced in Eq. (7.20) of Section 7.3. The f_b 's are simply given by Eqs. (7.20), in which the function $f(\zeta)$ becomes the current distribution inside the bunches. Assuming parabolic bunches, the distribution $f(\zeta)$ inside one bunch is

$$f(\zeta) = \frac{3}{2} \left[1 - \left(\frac{2R}{\ell} \right)^2 \zeta^2 \right], \quad (8.25)$$

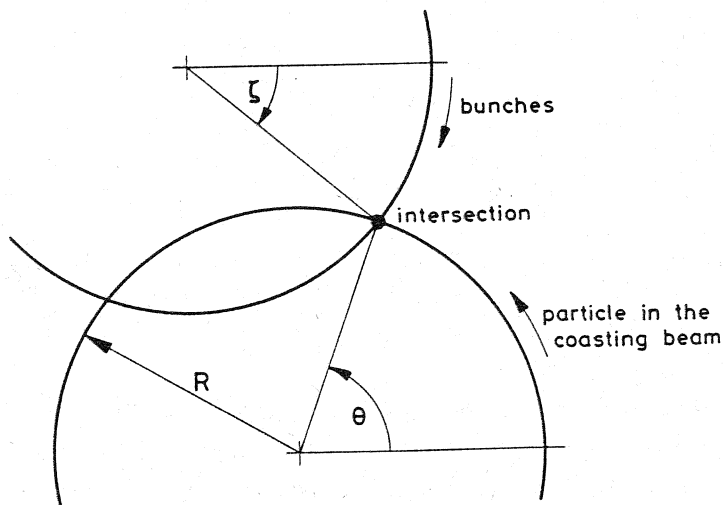


Fig. 24 Angle definition for two-beam overlap knock-out

where ℓ is the bunch length. For M equidistant bunches, the coefficients f_b are

$$\begin{cases} f_b = 0 & \text{if } b \neq nM \\ f_{nM} = \frac{4R}{\pi n^2 M \ell} \left[\frac{2R}{nM\ell} \sin \frac{nM\ell}{2R} - \cos \frac{nM\ell}{2R} \right] & \text{if } b = nM, \end{cases} \quad (8.26)$$

n being an integer. Equations (8.26) mean that only the harmonics which are a multiple of the number of bunches are different from zero. Considering this and remembering that only the vertical resonances are excited for two beams crossing at a finite horizontal angle, the resonance condition (7.23) becomes

$$NQ_z - p - nM \frac{\Omega_{\text{per}}}{\Omega_{\text{rev}}} = 0 \quad (8.27)$$

and the excitation coefficient (7.24) is

$$\kappa = \frac{(1+\beta^2)R^2 f_{nM}}{2\pi c \beta (2R)^{N/2} N! |B_0|} \int_0^{2\pi} \sqrt{\beta_z}^N \frac{\partial^N \Phi}{\partial z^N} \exp \left\{ i \left[N\mu_z - \left(NQ_z - p - nM \frac{\Omega_{\text{per}}}{\Omega_{\text{rev}}} \right) \theta \right] \right\} d\theta. \quad (8.28)$$

In this case, Ω_{per} is the angular frequency of the bunches. Equations (8.16) and (8.17) give the derivatives of the potential Φ in the one-dimensional model. Using these derivatives and integrating Eq. (8.28) over the interaction regions only, gives for the bandwidths $\Delta\theta$ the same expressions as Eqs. (8.18) and (8.19), except for being multiplied by f_{nM} [Eq. (8.26)] and having a phase term equal to that of Eq. (8.28).

The effects of the overlap knock-out have been observed in the ISR. With the bunch length associated with an RF voltage of 16 kV, the coefficients f_{nM} [Eqs. (8.26)] can be neglected for $n \geq 8$. Since the range of the n values is thus limited and since Ω_{per} is very close to Ω_{rev} , first-order effects predominate for tune values close to integers. The ELSA line (Fig. 3), which is frequently used in the ISR, is close to nine, and the dipole overlap knock-out resonances, for $n \leq 7$ and for bunches at the injection in the other ring, are sitting in the stack region. Their positions are given by Eq. (8.27) and are represented in Fig. 25.

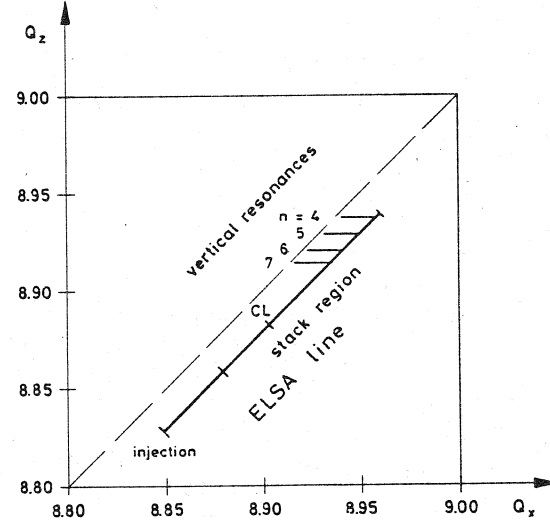


Fig. 25 Dipole overlap knock-out resonances on the ELSA line

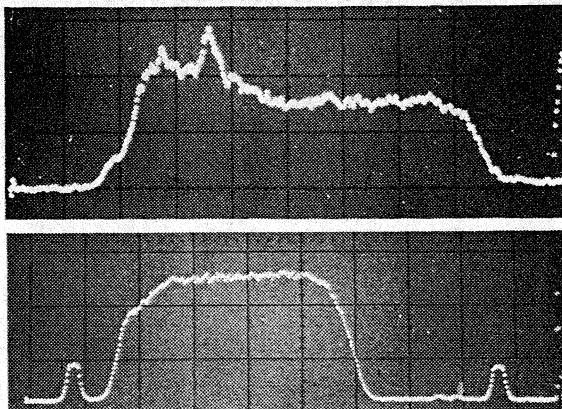


Fig. 26 Schottky scans of a beam crossing overlap knock-out resonances (ISR run 568): the upper scan shows the growth of vertical amplitudes at the top of the stack; the lower, longitudinal scan shows a decrease of stack density, due to beam losses, at the positions of the resonances.

Beam losses and vertical blow-up of the top of the stack have been observed in the ISR, in the presence of overlap knock-out resonances (Fig. 26). Various parameters have an influence on these resonances. The effects may be substantially reduced by increasing the bunch length which reduces the high-frequency components in the bunch spectrum (8.26). The blow-up is smaller when the Q-values are decreased, since the most dangerous resonances with a low n are eliminated from the stack. Since the bandwidths $\Delta\omega$ depend on the vertical separation between the bunches and the coasting beam at the intersections, the losses can be diminished by putting large beam separations with the same sign in all the intersections.

In the ISR, the elimination of the dipole resonances due to two-beam overlap knock-out (Fig. 25) has been done by using the influence of the first two parameters only, in order not to depend on the beam positions at the intersections²⁰:

- i) A slight reduction of the tunes, by 0.015, during stacking eliminates the effects of the resonances $n = 4$ and $n = 5$ (Fig. 25).
- ii) A reduction of the cavity voltage from 16 kV to 4 kV as soon as the bunches are trapped creates a bunch lengthening. Hence, the coefficients f_{nM} (8.26) are smaller and become negligible for $n \geq 6$.

In this way, the vertical beam blow-up has been eliminated at 26 GeV/c and the ELSA line may be used without any harmful effects. However, overlap knock-out still remains a severe limitation when deuterons and protons are stacked together. For the same momentum, the ratio Ω_d/Ω_p is such that the bunch frequency $n = 1$ excites a resonance when using the ELSA line which, therefore, must be replaced by the 8C line (Fig. 3).

The influence of the two-beam overlap knock-out has been studied using a small beam left circulating at the top of ELSA within a limited vertical aperture, while moving bunches in the other ring. Figure 27 shows localized enhancements of current loss when overlap knock-out resonances are crossed. According to Eq. (8.27), Nth-order resonances must be

visible for tune values close to $NQ_z = \text{integer}$. In Fig. 27, the intermediate losses do indeed correspond to crossing second-order resonances. A similar experiment has been made²⁰⁾ to investigate third-order resonances near $3Q_z = 26$. Current losses corresponding to $n = 1$, $n = 2$, and $n = 3$ are visible on the curve in Fig. 28. Such high-order effects can also cause serious difficulties when different particles or momenta are considered.

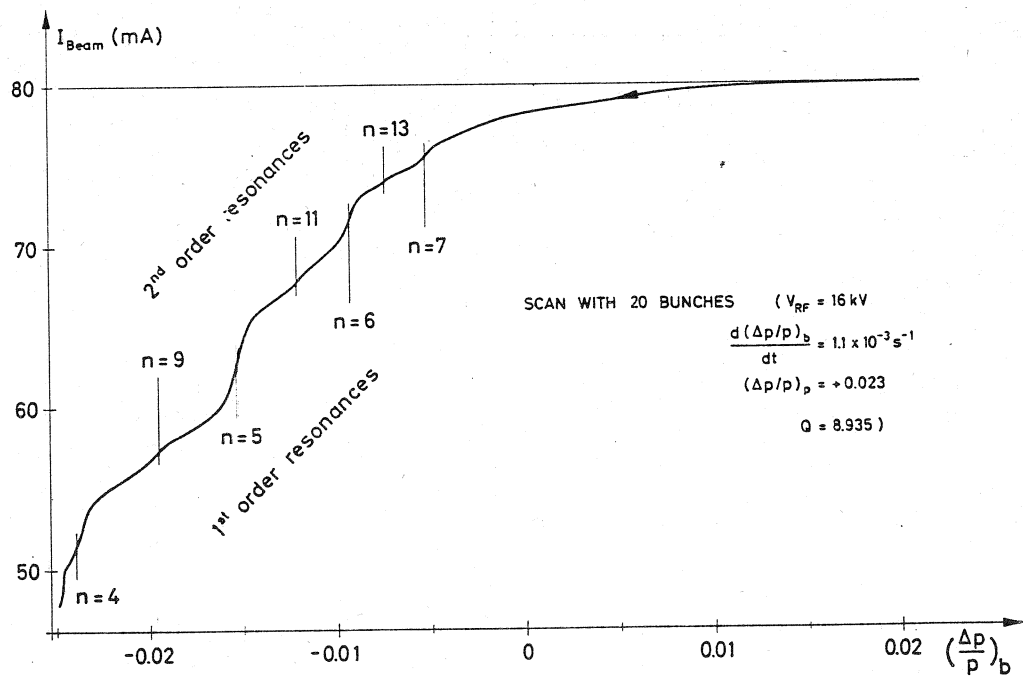


Fig. 27 Overlap knock-out resonances of order 1 and 2 in the ISR (ELSA line)

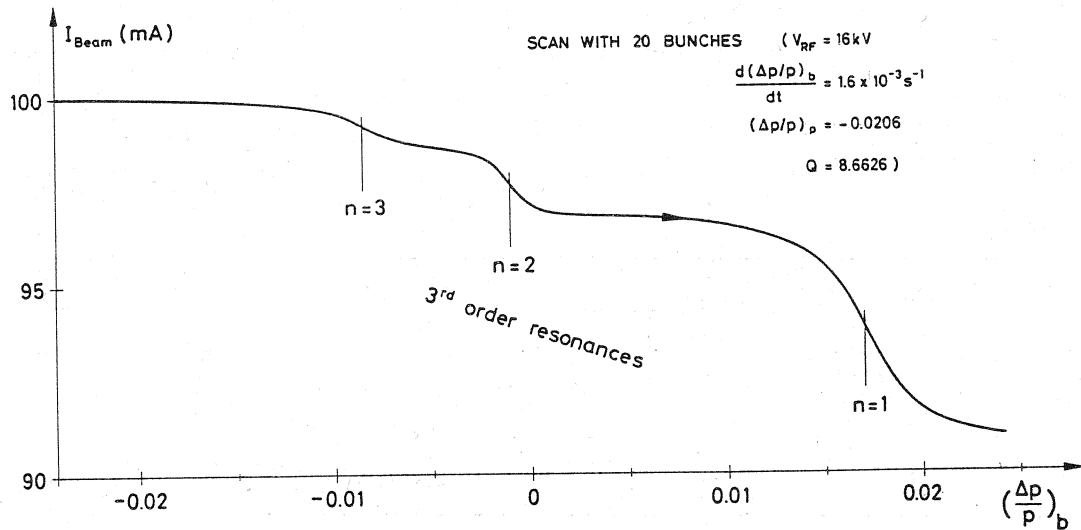


Fig. 28 Overlap knock-out resonances of order 3 in the ISR (8C line)

8.4 Linear coupling in three-dimensional fields⁸⁾

In Section 8.1, *transverse* magnetic defects have been considered. It may, however, happen that an important *longitudinal* field is present in a synchrotron. This is the case, for instance, when a solenoid is installed at one intersection of storage rings for the analysis of secondary particles. Such a longitudinal field couples the two transverse motions. Since the field due to multipole elements (Section 8.1) may also couple the transverse motions, a complete treatment of the coupling has to consider three-dimensional fields. The non-linear theory with three-dimensional fields exists⁹⁾, but here we will restrict ourselves to the linear coupling, i.e. to the coupling terms in the quadratic part of the Hamiltonian. Looking at the expression of H_1 [Eq. (5.13)], this condition implies that A_θ is quadratic in x and z , while A_x and A_z depend linearly on x and z . Using Maxwell's relations in a region where the current density is zero ($\text{div } \vec{B} = 0$ and $\overrightarrow{\text{rot}} \vec{B} = 0$), we get for the potential vector

$$\begin{aligned} A_x &= cB_\theta z \\ A_z &= -cB_\theta x \\ A_\theta &= -\frac{c}{2} \left[\frac{\partial B_x}{\partial x} - \frac{\partial B_z}{\partial z} \right]_{x=z=0} xz . \end{aligned} \quad (8.29)$$

Putting Eqs. (8.29) in Eq. (5.13) gives the perturbing Hamiltonian H_1 and the function U (5.22), which simply becomes

$$\begin{aligned} U(a_n, \theta) &= h_{11000}^{(2)} a_1 \bar{a}_1 + h_{00110}^{(2)} a_2 \bar{a}_2 + h_{jklm-p}^{(2)} a_1^j \bar{a}_1^k a_2^l \bar{a}_2^m \exp(i\epsilon\theta) + \\ &+ h_{kjml-p}^{(2)} \bar{a}_1^j a_1^k \bar{a}_2^l a_2^m \exp(-i\epsilon\theta) . \end{aligned} \quad (8.30)$$

The field satisfying Eqs. (8.29) excites two different quadrupole resonances, i.e. $Q_x + Q_z = p$ and $Q_x - Q_z = p$. Since the working line of a storage ring often lies very close to the diagonal $Q_x = Q_z$ or close to any parallel $Q_x = Q_z \pm$ integer with the diagonal, it is particularly interesting to study the resonance $Q_x - Q_z = p$. This means that $j = 1$, $k = 0$, $l = 0$, and $m = 1$ in Eq. (8.30) and that the excitation coefficient (8.1) becomes

$$\begin{aligned} \kappa &= h_{1001-p}^{(2)} = \frac{1}{8\pi} \frac{R}{|B_\theta|} \int_0^{2\pi} \sqrt{\beta_X \beta_Z} \left[\left(\frac{\partial B_x}{\partial x} - \frac{\partial B_z}{\partial z} \right) + \right. \\ &\quad \left. + B_\theta \left(\frac{\alpha_x}{\beta_x} - \frac{\alpha_z}{\beta_z} \right) - iB_\theta \left(\frac{1}{\beta_x} + \frac{1}{\beta_z} \right) \right] \exp \left[i(\mu_x - \mu_z - e\theta) \right] d\theta , \end{aligned} \quad (8.31)$$

where $e = Q_x - Q_z - p$.

The effect of a solenoid clearly appears in Eq. (8.31) via B_θ . The effect of skew quadrupoles appears in the term $(\partial B_x / \partial x - \partial B_z / \partial z)$ and the following relation applies

$$\frac{\partial B_x}{\partial x} = - \frac{\partial B_z}{\partial z} . \quad (8.32)$$

The end effect of a solenoid also appears in the term $(\partial B_x / \partial x - \partial B_z / \partial z)$ but the following relation becomes true

$$\frac{\partial B_x}{\partial x} + \frac{\partial B_z}{\partial z} = - \frac{\partial B_\theta}{\partial \theta} . \quad (8.33)$$

In the expression (8.31), the two terms $B_\theta(1/\beta_x + 1/\beta_z)$ and $(\partial B_x / \partial x - \partial B_z / \partial z)$ are orthogonal in the complex plane when the phase of the exponential is not considered and this may give the impression that the effect of a solenoid cannot be compensated with skew quadrupoles. However, this is generally *not true*. The phase difference $(\mu_x - \mu_z)$ is indeed very important and it is possible to find skew-quadrupole positions in a given machine where this difference is large enough that the two terms mentioned above are no longer orthogonal.

In fact, it was easy to find a skew-quadrupole scheme²¹⁾ for the ISR which compensates the effect either of one solenoid or of tilted main units, without introducing a vertical dispersion in the intersection.

An interesting application of the resonance theory comes from the use of the invariants (5.39) and (5.46). In the specific case of linear coupling, the use of the extreme values ± 1 for $\cos \psi$ in these invariants gives

$$r_1^2 + r_2^2 = \tau_1 \quad (8.34)$$

$$r_2^2 e^{\mp 2|\kappa|r_1 r_2} = \tau_2 ,$$

where τ_1 and τ_2 are constants.

Let us apply these relations (8.34) to the case where the coherent oscillation of a kicked pulse is measured⁸⁾. By kicking in the horizontal plane, the signal of Fig. 29 can be observed.

Initially, when the kick is given, the horizontal amplitude is maximum and the vertical one is zero. Later, the two envelopes of the amplitudes oscillate, and the horizontal amplitude reaches a minimum where the vertical is maximum. This is an illustration of the exchange of energy previously mentioned (Section 5.4) for difference resonances.

The initial conditions define the constants τ_1 and τ_2 of Eqs. (8.34)

$$\tau_1 = r_{1,\max}^2, \quad \tau_2 = 0 . \quad (8.35)$$

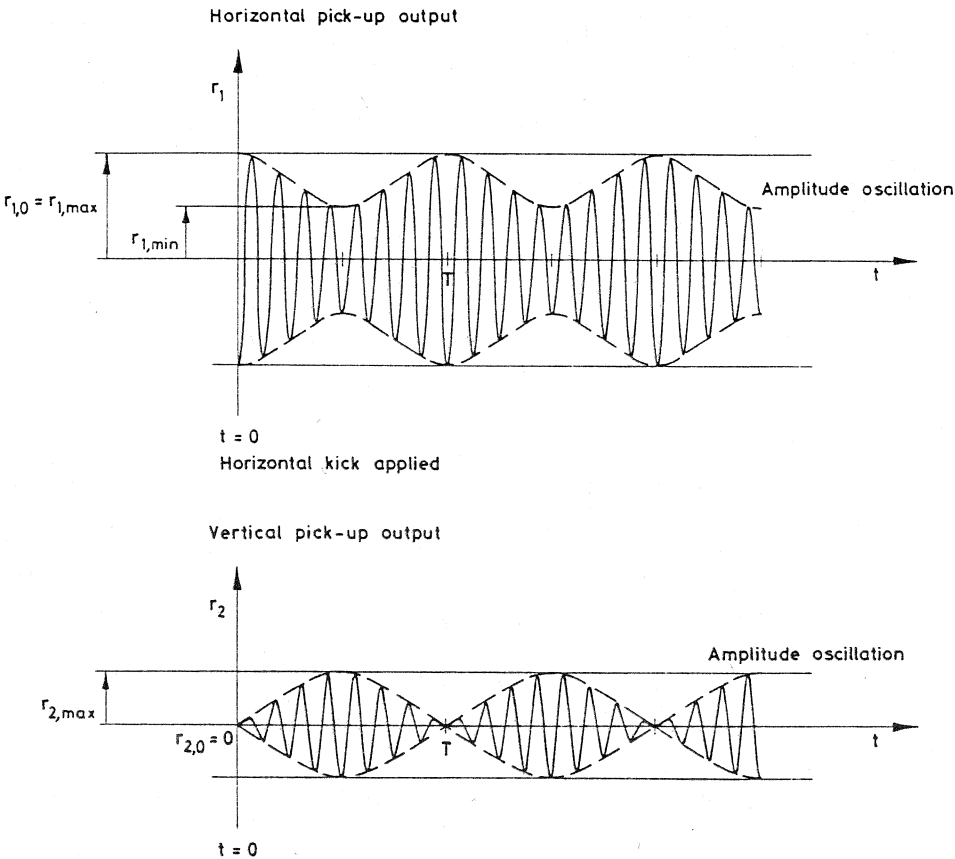


Fig. 29 Pick-up outputs for linear coupling measurement

Eliminating r_2 from the two equations (8.34) and replacing r_1 by $r_{1,\min}$, since the extreme values of $\cos \psi$ were taken, gives

$$\sqrt{r_{1,\max}^2 - r_{1,\min}^2} e \mp 2|\kappa|r_{1,\min} = 0, \quad (8.36)$$

which can be rewritten as follows

$$\frac{r_{1,\min}}{r_{1,\max}} = \frac{e}{\sqrt{e^2 + 4|\kappa|^2}}. \quad (8.37)$$

Thus, the relation (8.37) gives a method for measuring the excitation coefficient $|\kappa|$, provided that the distance e from the resonance is known. This distance can be obtained by calibration of one set of quadrupoles, but a more elegant way of solving the problem consists of measuring the period T (Fig. 29) of the amplitude oscillations. It will be shown later that this period is

$$T = \frac{1}{f_{\text{rev}} \sqrt{e^2 + 4|\kappa|^2}}. \quad (8.38)$$

From the two equations (8.37) and (8.38) it is possible to eliminate either $|e|$ or $|\kappa|$, which gives expressions for these two parameters

$$\boxed{\begin{aligned} |e| &= \frac{r_{1,\min}}{r_{1,\max} T f_{\text{rev}}} \\ |\kappa| &= \frac{1}{2 T f_{\text{rev}}} \sqrt{1 - \left(\frac{r_{1,\min}}{r_{1,\max}} \right)^2}. \end{aligned}} \quad (8.39)$$

Since $r_{1,\min}/r_{1,\max}$ and T may be measured on the pick-up outputs (Fig. 29), Eqs. (8.39) give a method for calculating²²⁾ $|e|$ and $|\kappa|$.

It has been mentioned in Section 5.4 that a periodic exchange of "energy" between the two transverse planes takes place for difference resonances and that the averaging of these slow oscillations on many turns will show an apparent increase of the small dimension of the beam at the expense of the other dimension. This clearly applies to the linear coupling.

In this specific case, the equations (5.27) and (5.28) of the perturbed motion are linear since the low-frequency part U [Eq. (8.30)] of the Hamiltonian is quadratic. These equations are⁸⁾

$$\begin{aligned} a'_1 &= i\kappa a_2 e^{-ie\theta} \\ a'_2 &= i\kappa a_1 e^{ie\theta}. \end{aligned} \quad (8.40)$$

They can be solved by defining the new variable $a_2 e^{-ie\theta}$ and then differentiating the second equation (8.40). The solutions of Eqs. (8.40) are⁸⁾

$$\begin{aligned} a_1 &= \frac{i}{\kappa} \left(\frac{A_+}{\omega_+} e^{i\omega_+ \theta} + \frac{A_-}{\omega_-} e^{i\omega_- \theta} \right) \\ a_2 &= \left(A_+ e^{i\omega_+ \theta} + A_- e^{i\omega_- \theta} \right) e^{ie\theta}, \end{aligned} \quad (8.41)$$

where A_+ and A_- are complex constants of the motion and ω_{\pm} are the frequencies given by

$$\omega_{\pm} = -\frac{e}{2} \pm \sqrt{\left(\frac{e}{2}\right)^2 + |\kappa|^2}. \quad (8.42)$$

The complete solutions of the perturbed motion are given by the Eqs. (5.10a) in which the expressions (8.41) are introduced and the characteristic frequencies of these solutions are $\omega_y' \pm \omega_{\pm}$. Hence, the single particle motions contain fast and slow oscillations associated with the phases ω_y and $\omega_{\pm}\theta$, respectively. It is thus interesting to factorize the signal into a slowly oscillating envelope component and a fast oscillating component²³⁾. Doing this, we find that the angular frequency of the envelope oscillations is equal to $\omega_+ - \omega_-$,

i.e. $\sqrt{e^2 + 4|\kappa|^2}$ by virtue of Eq. (8.42). This factorization of the signal is illustrated in Fig. 29 and the angular frequency we obtained agrees with the expression (8.38) of the period T.

Averaging the complete solutions of the perturbed motion over time and over the particle distribution inside the beam, gives the apparent variations in the beam dimensions²³⁾

$$\boxed{\frac{\sigma_x}{\sigma_{x,0}} = \sqrt{1 + \frac{1}{2} \left(\frac{1}{\lambda} - 1 \right) \frac{4|\kappa|^2}{e^2 + 4|\kappa|^2}}$$

$$\frac{\sigma_z}{\sigma_{z,0}} = \sqrt{1 + \frac{1}{2} (\lambda - 1) \frac{4|\kappa|^2}{e^2 + 4|\kappa|^2}}, \quad (8.43)}$$

where λ is the ratio of the initial emittances, i.e.

$$\lambda = \frac{E_{x,0}}{E_{z,0}}. \quad (8.44)$$

Since $2|\kappa|$ appears in the most important relations (8.37), (8.38) and (8.43) associated with the linear coupling, it is convenient to define the linear coupling coefficient⁸⁾ as

$$C = 2\kappa. \quad (8.45)$$

Coupling measurements have been made in the ISR by using the Q-filter outputs and the relations (8.39). Figure 30 shows the signals given by the Q-filter outputs and Fig. 31 shows the relative sizes and positions of the vectors excited by the basic ISR and a superconducting solenoid installed in one intersection for particle detection. The coupling

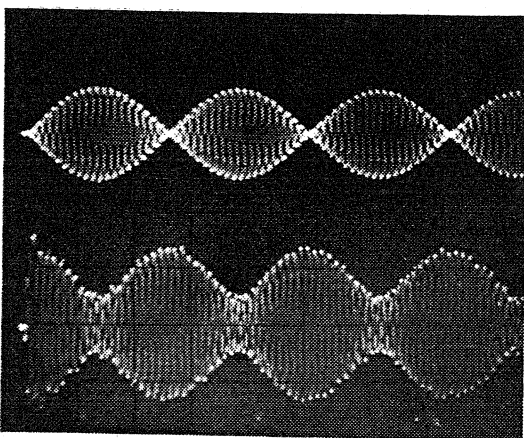


Fig. 30 Filter output signals of the Q-meter. The upper and lower traces show the vertical and horizontal coherent oscillations, respectively.

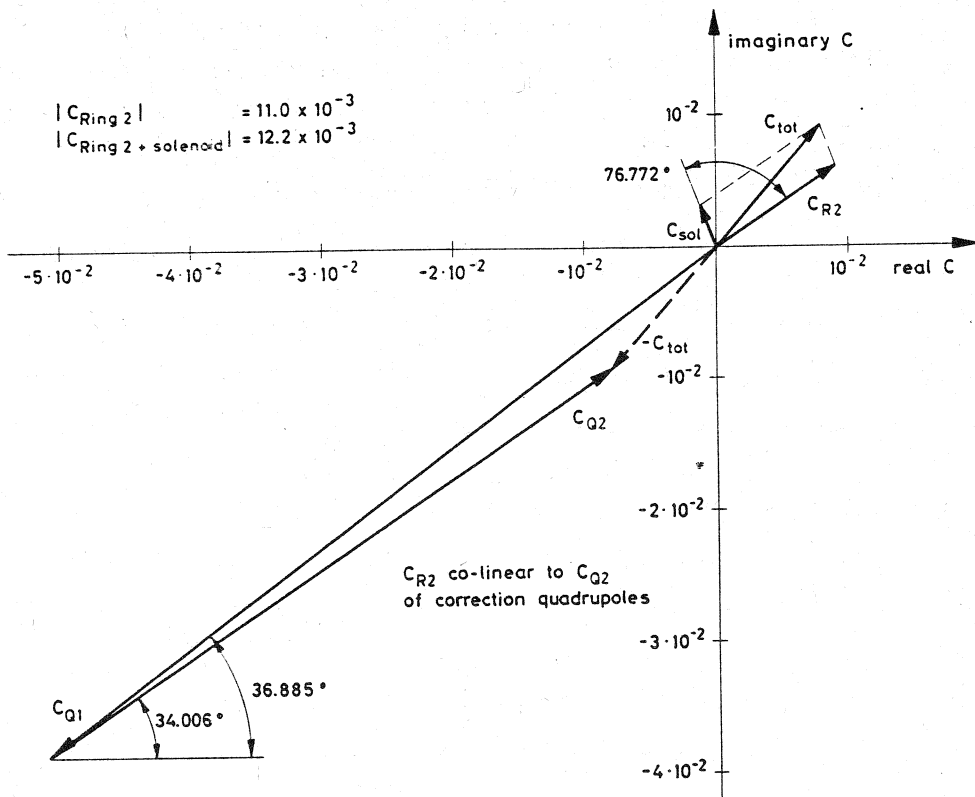


Fig. 31 Coupling vectors in the ISR

effect of the solenoid is small since it has end-plate slots which partially compensate the main field. By using the theoretical phase angle, C_{solenoid} was calculated to be 2.6×10^{-3} , which is within 20% of the theoretical value of 3.3×10^{-3} . The solenoid was corrected by means of the skew-quadrupole scheme which existed at the time of the experiment (Fig. 31). The measured values were

$$|C_{\text{ring } 2}| = 11.0 \times 10^{-3} \quad (8.46)$$

$$|C_{\text{ring } 2 + \text{solenoid}}| = 12.2 \times 10^{-3} .$$

It is now interesting to estimate the beam-size variations which could result from the coupling measured in ring 2 [Eqs. (8.46)], in the absence of compensation. The emittance ratio in the ISR is $\lambda \approx 2$ and Eqs. (8.43) give for $e = 0.01$

$$\frac{\sigma_x}{\sigma_{x,0}} = 0.92 \quad (8.47)$$

$$\frac{\sigma_z}{\sigma_{z,0}} = 1.14 .$$

A decrease of luminosity of 14% corresponds to the vertical beam blow-up given in Eqs. (8.47). This is not negligible and shows that the compensation of the solenoid, of the main unit tilts, and of non-zero vertical orbit distortions in the sextupoles is necessary. Therefore, a new skew-quadrupole scheme, which may easily produce a vector for correcting the solenoid (Fig. 31), has recently been installed in the ISR.

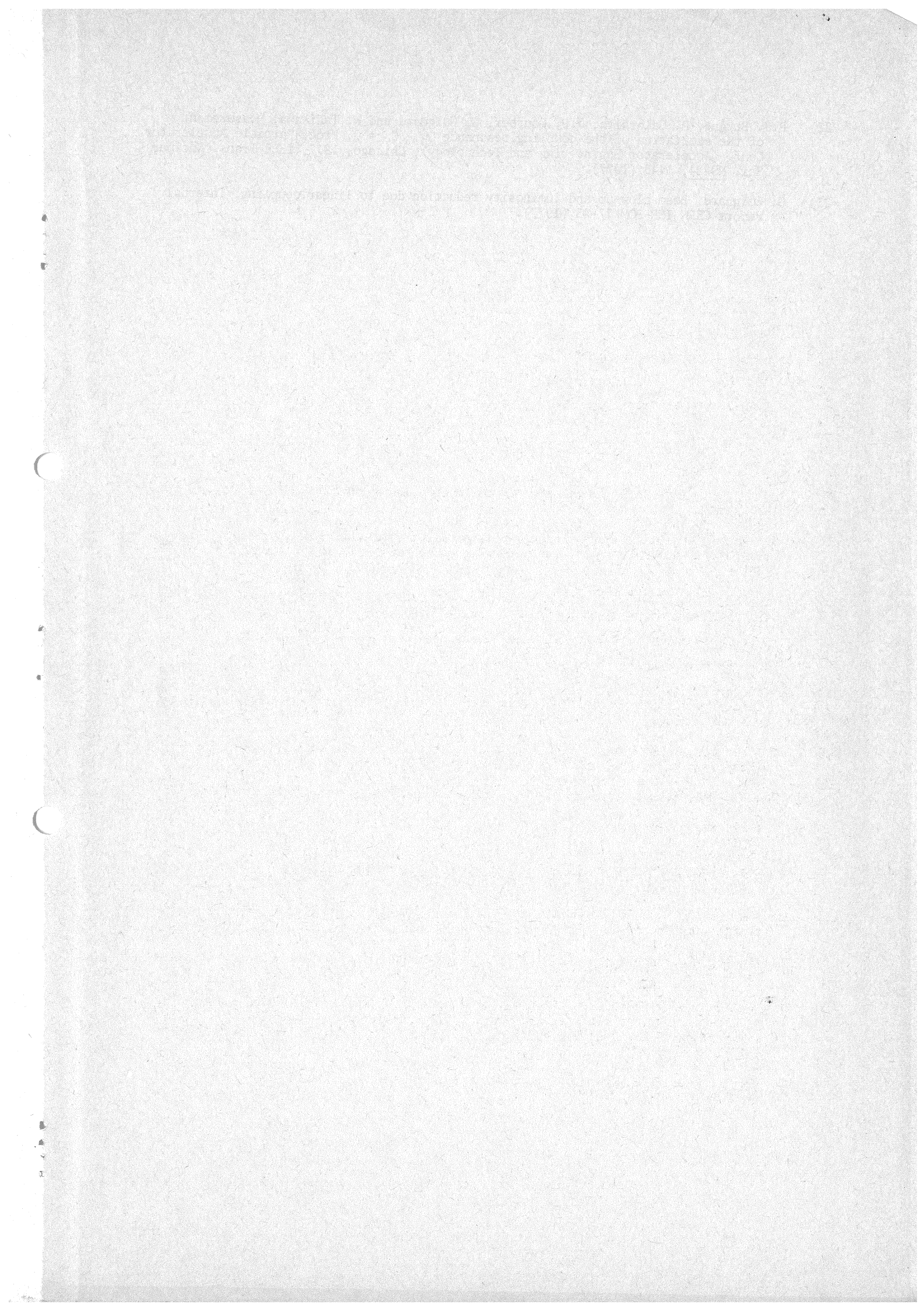
9. CONCLUSION

These lectures describe a general treatment of the resonances due to perturbing electromagnetic fields in particle accelerators. The treatment is based on the perturbation theory in the Hamiltonian formalism. This basic theory is reviewed (Section 3) and then applied to the transverse motions of the particles (Section 4). From the part of the Hamiltonian which is associated with a single resonance, the equations and the invariants of the perturbed motion around this resonance, are deduced (Section 5 and 6). Important parameters which characterize the perturbing resonance, such as the excitation coefficient κ , the stabilizing coefficients $h_{qss}^{(2v)}$ and the bandwidth $\Delta\omega$, are given for sum and difference resonances. There is a detailed discussion on the possible limitations of the amplitude growth or beating, under static conditions. In order to be as complete as possible, dynamic conditions associated with adiabatic and non-adiabatic variations of the parameters are also considered (Section 7).

This classical theory of non-linear resonances is then applied to different sources of perturbation (Section 8) which may in some cases only be observed in storage rings, where two beams are crossing and where the particles are accelerated before circulating for several hours. For this reason it is convenient to use the CERN ISR for illustrating these applications. It is shown how the theory explains both qualitatively and quantitatively the effects measured in the ISR and indicates the way of compensating these effects. It is perhaps interesting to note that the theory presented here can satisfactorily account for all the resonance effects observed in the ISR without using the non-classical concepts of Arnold diffusion and stochasticity limit.

REFERENCES

- 1) L. Landau and E. Lifshitz, Physique théorique, t. 1: Mécanique (Ed. de la Paix, Moscow, 1967).
- 2) C.L. Siegel, Symplectic geometry (Academic Press, New York, 1964).
- 3) H. Goldstein, Classical mechanics (Addison-Wesley, Reading, Mass., 1953).
- 4) J.B. Marion, Classical dynamics (Academic Press, New York, 1965).
- 5) J.W. Leech, Eléments de mécanique analytique, Monographie 32 (Dunod, Paris, 1961).
- 6) S. Flügge (ed.), Handbuch der Physik, Vol. III/1 (Springer, Berlin, 1960).
- 7) L. Landau and E. Lifshitz, Physique théorique, t. 2: Théorie du champ (Ed. de la Paix, Moscow, 1967).
- 8) G. Guignard, The general theory of all sum and difference resonances in a three-dimensional magnetic field in a synchrotron, CERN 76-06 (1976).
- 9) H. Bruck, Accélérateurs circulaires de particules; Introduction à la théorie (Presses universitaires de France, Paris, 1966).
- 10) E.D. Courant and H.S. Snyder, Theory of the alternating-gradient synchrotron, Ann. Phys. (USA) 3, 1 (1958).
- 11) G. Guignard, Effets des champs magnétiques perturbateurs d'un synchrotron sur l'orbite fermée et les oscillations bétatroniques, ainsi que leur compensation, CERN 70-24 (1970).
- 12) A. Schoch, Theory of linear and non-linear perturbations of betatron oscillations in alternating-gradient synchrotrons, CERN 57-21 (1957).
- 13) R. Hagedorn, Stability and amplitude ranges of two-dimensional non-linear oscillations with periodical Hamiltonian, CERN 57-1 (1957).
- 14) G. Guignard, Vitesse limite de traversée d'une résonance quelconque; Application aux petites perturbations et conséquence pour les accroissements maximaux d'amplitude, Internal report CERN/SI/Int.DL/72-2 (1972).
- 15) A.W. Chao and M. Month, Particle trapping during passage through a high-order non-linear resonance, Brookhaven report BNL 18860, CRISP 74-9 (1974).
- 16) M. Month, Beam loss in a coasting beam from a high-order isolated resonance, Proc. 9th Internat. Conf. on High-Energy Accelerators, Stanford, 1974 (CONF 740522, USAEC, Washington, 1974), p. 402.
- 17) J.P. Gourber, Control of betatron frequencies and of resonance excitation in the ISR, Proc. 4th All-Union Nat. Conf. on Particle Accelerators, Moscow, 1974 (Nauka, Moscow, 1975), Vol. 2, p. 73.
- 18) P.M. Hanney and E. Keil, The width of non-linear resonances excited by beams crossing at small angles in low- β sections, Internal report CERN ISR-TH/73-55 (1973).
- 19) A. Piwinski, Intra-beam scattering, Proc. 9th Internat. Conf. on High-Energy Accelerators, Stanford, 1974 (CONF 740522, USAEC, Washington, 1974), p. 405.
- 20) J.P. Gourber, H.C. Hereward and S. Myers, Overlap knock-out effects in the CERN Intersecting Storage Rings (ISR), Proc. Particle Accelerator Conf. (Accelerator Engineering and Technology), Chicago, 1977, IEEE Trans. Nuclear Sci. NS-24, 1405 (1977).
- 21) P.J. Bryant, Possible skew quadrupole schemes for the ISR, Internal report CERN ISR-MA/75-51 (1975).



- 22) P.J. Bryant, P. Galbraith, J.P. Gourber, G. Guignard and K. Takikawa, Measurement of the excitation of the coupling resonance $Q_h - Q_v = 0$, Proc. Particle Accelerator Conf. (Accelerator Engineering and Technology), Chicago, 1977, IEEE Trans. Nuclear Sci. NS-24, 1440 (1977).
- 23) G. Guignard, Beam blow-up and luminosity reduction due to linear coupling, Internal report CERN ISR-BOM/77-43 (1977).